

INAUGURAL-DISSERTATION

zur
Erlangung der Doktorwürde der
Naturwissenschaftlich-Mathematischen Gesamtfakultät
der
Ruprecht-Karls-Universität Heidelberg

vorgelegt von:
Muriel Rakotomalala MSc.
aus Germigny-L'évêque, Frankreich

Tag der mündlichen Prüfung:
15 Juli 2011

Synthesis and Investigation of
Heterocyclic Organophosphorus
Compounds as Flame Retardants for
Epoxy Resins

Gutachter:

Prof. Dr. Manfred Döring

Prof. Dr. A. Stephen K. Hashmi

To my husband,

ACKNOWLEDGEMENTS

First and foremost I would like to thank my doctoral supervisor Prof. Dr. Manfred Doering, for his support and for giving me the opportunity to learn about the field of flame retardants. I also wish to thank all the members of the AK Doering past and present for their help throughout my research.

I am grateful to Sebastian Wagner, my partner in crime, for synthesising compounds 7 and 9, for his contribution and patience during the manuscript-writing process, for his willingness to share his knowledge of organic chemistry and his help writing my Kurzzusammenfassung.

I also wish to thank Dr Michael Ciesielski for the many interesting discussions and for ensuring that I did not poison myself while carrying out the thionation reactions.

I would like to thank my past and present lab-mates, Kai Stoess and Patrick Mueller for providing compound 10.

My thanks also go to Dr Thomas Zevaco and Dr Olaf Walter for carrying out the 2D NMR and X-Ray measurements as well as Dr Wiebke Lohstroh for taking care of the TD-MS apparatus.

In the technical team, I would especially like to show my appreciation to Marion Lenzner, Sigrid Silbernagel-Donath and Gilbert Zwick.

I wish to express my gratitude to Prof. Giovanni Camino and Matteo Lavaselli in the Polytechnical University of Torino, at the Alessandria campus in Italy, for giving me the opportunity to carry out the oxygen index test on the sulphur containing compounds and for carrying out the thermal stability tests on the nanocomposite materials.

I especially would like to thank Johannes Schroeder and Philipp Becker for the many interesting discussions on our way to and from work and their precious help with my knowledge of the German language.

Last but not least, I cannot thank enough my parents, bother and husband, as none of this would have been possible without their constant support.

ABSTRACT:

In the course of this doctoral work, a series of organophosphorus derivatives were synthesised in order to deepen our understanding of the influence of the environment around the phosphorus on the flame retardant mechanism. The Friedel-Crafts reaction of PCl_3 with 2-hydroxybiphenyl, 2,2-dimethylpropane-1,3-diol and 2-aminobiphenyl yielded the phosphorus chloride precursor of 9,10-dihydro-9-oxa-10-phosphaphenanthrene-10-oxide (DOPO), 5,5-dimethyl-[1,3,2]-dioxaphosphorinane-2-oxide (DDPO) and 9,10-dihydro-9-aza-10-phosphaphenanthrene 10-oxide(DAPO) respectively. The phosphorus chloride derivatives were then either hydrolysed, oxidised, or thionised to yield a series of molecules where the environment around the phosphorus atom varied. The synthesized molecules were chemically incorporated (preformulation) in phenol epoxy novolac (DEN 438) with different phosphorus concentrations. According to standard EE processes, the modified resins were then cured using DICY as hardener and Fenuron as accelerator.

The influence of the chemical modification of the epoxy phenol novolac resin, on the glass transition temperature (T_g) of the cured material, was investigated using DSC. As a result of the decreasing number of epoxy functional group available for cross-linking, the T_g decreased with increasing phosphorus loading. This effect was enhanced when sulphur containing molecules were used. However, chemical modification with DAPO only resulted in a negligible impact on T_g as the amine functionality could contribute to the cross-linking.

The flame retardant efficiency of the modified resin with different phosphorus loading was evaluated using the UL-94 test, in accordance with the DIN IEC 60695-11-10. All phosphorus derivatives improved the flame retardancy of phenol epoxy novolac resin with comparable phosphorus loading to DOPO. However, 9,10-dihydro-9-oxa-10-phosphaphenanthrene-10-sulfide (DOPS) imparted UL-94 V0 rating with only 1.0 % phosphorus loading.

In order to further understand the role of the PO and PS radicals in the mode of flame retardancy of DOPS, Limiting Oxygen Test (LOI) and thermal desorption mass spectrometry (TD-MS) were carried out. TD-MS experiments revealed that PS and PO

radicals are released sequentially in the gas which can rationalise the better efficiency of DOPS in comparison to DOPO. LOI experiments showed that the intumescent mechanism of DDPO was reduced when sulphur replaced oxygen in 5,5-dimethyl-[1,3,2]-dioxaphosphorinane-2-sulfide (DDPS).

Finally, a part of a cooperation with Prof. G. Camino (Politecnico di Torino, Italy), a DOPO modified resin was cured in the presence of an organically modified montmorillonite nanoclay (Cloisite 30B), in an effort to understand the interactions between DOPO and nanoclays and their impact on the flame retardancy of epoxy phenol novolac. The flammability of cured materials was tested using UL-94 test, LOI and cone calorimetry. The cone calorimeter enables to measure the heat released by the polymeric material under controlled conditions, as well as the gases evolving from the combustion process.

KURZFASSUNG:

Im Zuge der vorliegenden Promotionsarbeit wurde eine Serie verschiedener phosphororganischer Heterozyklen synthetisiert. Ziel war es, den Einfluss der chemischen Umgebung des Phosphoratoms, sowohl auf die Flammsechutzeigenschaften als auch auf den Flammsechutzmechanismus des Moleküls zu untersuchen. Durch eine Friedel-Crafts Reaktion mit PCl_3 und 2-Hydroxybiphenyl, 2,2-Dimethylpropan-1,3-diol sowie 2-Aminobiphenyl wurden die entsprechenden Phosphorchlorid-Vorstufen von 9,10-dihydro-9-oxa-10-phosphaphenanthren-10-oxid (DOPO), 5,5-dimethyl-[1,3,2]-dioxaphosphin-2-oxid (DDPO) sowie 9,10-dihydro-9-aza-10-phosphaphenanthren 10-oxid (DAPO) in guten Ausbeuten erhalten werden. Durch Hydrolyse, Oxidation bzw. Thionierung dieser Vorstufen wurde eine Serie unterschiedlicher Derivate mit verschiedenen chemischen Umgebungen dargestellt. Die so erhaltenen phosphororganischen Verbindungen wurden durch an den Oxiranring mit dem Novolak Epoxid Harz DEN 438 verbunden (Präformulierung). Auf diesem Wege wurde eine Reihe von Präformulierungen mit unterschiedlichen Flammsechutzmittelbeladungen (ausgedrückt durch den prozentualen Phosphorgehalt) dargestellt.

Im Einklang mit der gängigen Praxis in der Herstellung elektronischer Bauteile wurden die so modifizierten Epoxidharze mit DICY als Härter und Fenuron als Beschleuniger ausgehärtet. Die Glasübergangstemperatur (T_g) der fertigen Prüfkörper wurden mittels DSC Analyse untersucht. Durch die chemische Modifizierung des Harzsystems stehen nicht mehr alle Oxiranfunktionen für den Aushärtungsprozess zur Verfügung. Mit steigendem Phosphorgehalt hat dies einen sinkenden T_g zur Folge. Dieser Effekt wird durch die Anwesenheit von Schwefel im Molekül verstärkt, was auf das im Vergleich zu Sauerstoff weichere Schwefelatom zurückzuführen ist (Weichmachereffekt). Im Gegensatz dazu zeigt das bifunktionelle DAPO Molekül nur einen minimalen Einfluss auf dem T_g woraus sich schließen lässt, dass DAPO eine verbrückende Eigenschaft besitzt.

Die Flammsechutzeigenschaften der Epoxidharzprüfkörper mit unterschiedlichen Phosphorbeladungen wurden mittels des UL94-V Tests nach DIN Norm 60695-11-10 bewertet. Alle dargestellten Verbindungen zeigten mit DOPO als Referenz vergleichbare

flammhemmende Eigenschaften in DEN 438. Besonders 9,10-dihydro-9-oxa-10-phosphaphenanthren-10-sulfid (DOPS) besteht die geforderte Klassifikation V0 mit nur 1.0% Phosphorbeladung.

Um die Bedeutung von PO und PS Radikalen während eines Brandszenarios näher zu untersuchen wurde DOPS mechanistischen Studien unterzogen. Zum einen wurde der Limiting Oxygen Test (LOI) und zum anderen eine Thermodesorptions-Massenspektroskopie (TD-MS) durchgeführt. Speziell die TD-MS Untersuchungen belegen die essentielle Bedeutung eben dieser reaktiven Intermediate in der Gasphase und helfen somit den ausgezeichneten Flammenschutz durch DOPS besser zu verstehen. LOI Experimente konnten den Festphasenmechanismus von DDPO und seinen Derivaten näher aufklären. Der Intumeszenz-Charakter von DDPO sinkt, wenn Sauerstoff durch Schwefel ersetzt wird. 5,5-Dimethyl-[1,3,2]-dioxaphosphin-2-sulfid DDPS zeigt daher geringere Festphasenaktivität und partielle Gasphasenaktivität.

Zusätzlich wurde im Rahmen einer Kooperation mit Prof. Dr. G. Camino (Politecnico di Torino, Italien), die Wechselwirkung zwischen DOPO und Nanoclay (Montmorillonit Cloisite 30B) genauer untersucht. DOPO wurde hierfür mit einem Novolak Harz präformuliert. Anschließend wurde Cloisite 30B eingearbeitet und das Harz wie oben beschrieben ausgehärtet. Die Flammsechutzeigenschaften dieser Prüfkörper wurden mittels LOI, UL94-V und einem Cone-Calorimeter untersucht. Das Cone-Calorimeter liefert wertvolle Informationen über z.B. den Wärmestrom und die entstehenden Gase.

TABLE OF CONTENTS

Acknowledgements	iv
Abstract:	v
Kurzfassung:	vii
Table of contents	ix
List of abbreviations	xii
CHAPTER 1: Introduction	1
1.1 Flame retardants in electronic applications.....	4
1.2 Combustion of polymer	7
1.3 Mechanism of flame retardancy.....	8
1.4 Alternative to halogen flame retardants	10
1.4.1 Inorganic flame retardants	10
1.4.2 Nitrogen-based flame retardants.....	11
1.4.3 Phosphorus-based flame retardants	11
1.5 Objectives	12
CHAPTER 2: Evaluation of Flame Retardancy	14
2.1 Thermal Gravimetry Analysis (TGA)	14
2.2 Differential Scanning Calorimetry (DSC)	14
2.3 UL 94 test.....	14
2.4 Oxygen Index Test.....	15
2.5 Cone Calorimetry	16
2.6 Thermal desorption Mass Spectroscopy (TD-MS).....	17
CHAPTER 3: Synthesis of Organophosphorus Compounds	18
3.1 Introduction	18
3.2 6 <i>H</i> -dibenzo[<i>c,e</i>][1,2]oxaphosphinine 6-sulfide (DOPS) derivatives	19
3.2.1 Synthesis of 6 <i>H</i> -dibenzo[<i>c,e</i>][1,2]oxaphosphinine 6-sulfide.....	19
3.2.2 Pudovik reaction of 6 <i>H</i> -dibenzo[<i>c,e</i>][1,2]oxaphosphinine 6-sulfide.....	22
3.2.3 Atherton-Todd reaction of 6 <i>H</i> -dibenzo[<i>c,e</i>][1,2]oxaphosphinine 6-sulfide.....	22
3.3 5,5-Dimethyl-[1,3,2]-dioxaphosphirane-2-sulfide (DDPS) derivatives.....	25
3.3.1 Synthesis of 5,5-dimethyl-[1,3,2]dioxophosphorinane 2-thionic acid.....	25
3.3.2 Synthesis of 5,5-dimethyl-[1,3,2]dioxophosphorinane 2-sulfide.....	26
3.3.3 Pudovik reaction of 5,5-dimethyl-[1,3,2]dioxophosphorinane 2-sulfide.....	26
3.4 9,10-dihydro-9-azaphosphaphenanthrene-10- oxide (DAPO) derivatives	27

3.4.1	Abramov reaction of 9,10-dihydro-9-azaphosphaphenanthrene-10- oxide	31
3.4.2	Oxidation of 9,10-dihydro-9-azaphosphaphenanthrene-10- oxide	33
3.4.3	Synthesis of 9,10-dihydro-9-azaphosphaphenanthrene-10-thionic acid	36
3.4.4	9,10-dihydro-9-azaphosphaphenanthrene-10- sulfide	37
3.5	Summary	38
CHAPTER 4: Investigation of thermal stability of epoxy phenol novolac resin modified with organophosphorus flame retardants		40
4.1	Formulation and curing	40
4.2	Influence of the fusion process on glass transition temperature (T _g) of the cured epoxy phenol novolac resin	42
4.2.1	Influence of phosphaphenanthrene derivatives	43
4.2.2	Influence of dimethyldioxophosphorinane derivatives	44
4.3	Influence of phosphacyclic flame retardants on decomposition temperature (T _d)	45
4.4	UL 94 measurements of cured epoxy phenol novolac resin	46
4.5	Oxygen index measurements	48
4.5.1	Oxa-phosphaphenanthrene derivatives	49
4.5.2	Dioxophosphorinane derivatives	50
4.5.3	Self-quenching time (SQT) measurements	53
4.5.4	Burning rate measurements	56
4.6	Thermal degradation mechanism of organophosphorous derivatives	57
4.7	Summary	60
CHAPTER 5: Synergism of DOPO with exfoliated nanoclay in epoxy resin		62
5.1	Introduction	62
5.2	Influence of Cloisite 30B	62
5.2.1	Formulation	63
5.2.2	Thermal stability investigation	63
5.2.3	Oxygen index test (OIT)	66
5.2.4	Cone calorimetry measurements	67
5.3	Summary	69
CHAPTER 6: Conclusion		70
CHAPTER 7: Experimental section		74
7.1	General experimental	74
7.2	Synthesis	74
7.3	Preformulation:	91
7.4	Formulation and Curing:	92
7.5	Cone calorimetry	92
7.6	Thermal desorption mass spectroscopy	92
Scientific contributions		93
7.7	Publications	93
7.8	Oral Presentations	93

Reference List	94
List of Figures	99
List of Tables	102

LIST OF ABBREVIATIONS

DAPO	9,10-Dihydro-9-aza-10-phosphaphenanthrene 10-oxide
DAPS	9,10-Dihydro-9-aza-10-phosphaphenanthrene 10-sulfide
DAPS-OH	9,10-Dihydro-9-aza-10-phosphaphenanthrene-10-thionic acid
DDM	4,4'-Diaminodiphenylmethane
DDP-Cl	5,5'-Dimethyl-[1,3,2]dioxophosphorinane 2-chloride
DDPO	5,5'-Dimethyl-[1,3,2]dioxophosphorinane 2-oxide
DDPS	5,5'-Dimethyl-[1,3,2]dioxophosphorinane 2-sulfide
DDPS-OH	5,5'-Dimethyl-[1,3,2]dioxophosphorinane 2-thionic acid
DDS	4,4'-Diaminodiphenylsulfone
DFT	Density functional theory
DGEBA	Diglycidylether of Bisphenol A
DMSO	Dimethylsulfoxide
DOPO	9,10-Dihydro-9-oxa-10-phosphaphenanthrene10-oxide
DSC	Differential scanning calorimetry
ESI	Electronensprayionisation
<i>et al.</i>	et altera
Et	Ethyl
FR	Flame retardant
GC	Gas chromatography
h	Hour
HRMS	High resolution mass spectrometry
HRR	Heat release rate
IR	Infrared
LNI	Limiting nitrogen protoxide index
LOI	Limiting oxygen index
Me	Methyl
min	Minute
MS	Mass spectrometry
NMR	Nuclear magnetic resonance
ppm	Parts per million
pHRR	Peak of heat release rate
RT	Room temperature
SQT	Self quenching time
T _d	Temperature of decomposition
TD-MS	Thermal desorption mass spectrometry
TEA	Triethylamine
THF	Tetrahydrofuran
T _g	Glass transition temperature
TGA	Thermogravimetric analysis
THR	Total heat release
TTI	Time to ignition

CHAPTER 1: INTRODUCTION

This chapter constitutes part of the published review in Materials, 2010, 3, 4300-4327.

Since the first commercialisation of synthetic rubber, synthetic polymers have been the subject of an ever-growing interest from both academia and industry. The reinforcement of a large variety of polymer matrices (thermoset or thermoplast) with fibres (glass, carbon, aramide and natural fibres) led to the gradual replacement of steel and metal alloys by composite materials in a wide range of application such as construction, transportation, aerospace, appliances and electrical and electronics.^{1,2} Such composite materials combine good chemical and physical properties with low density, fatigue endurance, good thermal insulation and low thermal expansion.³ However, the organic nature of the base polymer renders composite materials highly prone to fire.⁴ The poor fire resistance of polymeric materials has caused 10 - 20 death per million inhabitants in industrialised countries.⁵ The increase of polymeric based materials in our household has had a direct impact on our safety. A study carried out by the underwriter lab reported that the escape time during a fire event has been reduced from 17 min to 3 min between 1977 and 2007.⁶

The term “epoxy resin” generally refers to uncured polymers containing one or multiple oxiranes or epoxy groups. Even though the synthesis of epoxy compounds were first reported in the 1890s, it is not until the 1940s that the first commercial application of the reaction product of bisphenol A with epichlorohydrin in the presence of anhydride was reported.³ Since the first patent from Ciba AG, the range of epoxy resins was considerably broadened while coatings still remain the main application of epoxy resins.

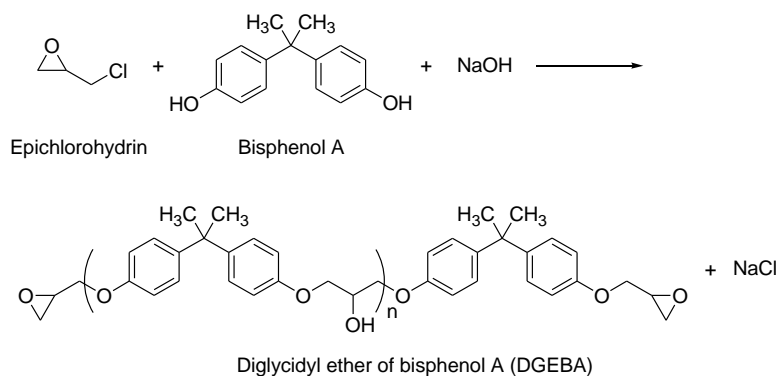


Figure 1-1: Synthesis of diglycidyl ether of bisphenol A from epichlorohydrin.³

Nowadays, the versatility of epoxy resin enables their use in a many applications ranging from coatings, casting resins and adhesives to fibre reinforced composites.²

A large portion of the epoxy composite material in electrical and electronic applications can be found in printed wiring boards (PWB), also known as printed circuit boards. However, as a result of the miniaturisation of portable devices, PWB are more prone to overheating, self-ignition and in turn fire hazard. Without the addition of chemicals that improve their resistance to fire, known as flame retardants, most composite materials and PWB would fail to comply with fire safety regulations. Thus, PWB are composed of 80 % flame retarded resin graded as FR-4 by the National Electrical Manufactures Association (NEMA).⁷ Such FR-4 composite materials are glass-fibre reinforced epoxy resins that meet flame retardancy standards (i.e. UL 94 –V0, LOI, GWT, etc...).⁴ During the first step of the fabrication of **PWB**, the glass is pre-treated with coupling agents such as organosilanes to improve adhesion between the inorganic glass and the organic resin.⁷ In a separate container, the epoxy resin is mixed with additives such as curing agents, accelerators, fillers and flame retardants. The woven glass is then impregnated with the partially cured resin. The resulting partially cured reinforced material is known as pre-peg. Multiple pre-pegs are then thermally pressed to obtain a core. After assembly of several pre-pegs and cores, a layer of copper is electrodispersed on the surface to form a copper-clad laminate. Then holes are drilled and the laminate undergoes the soldering process (Scheme1-1).

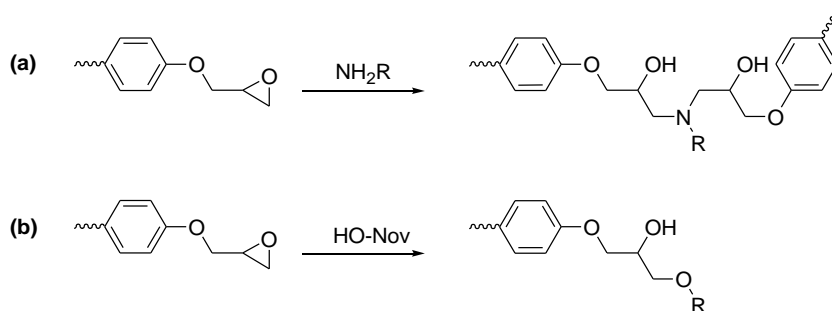


Figure 1-3: Newly formed bonds during curing of epoxy resins using: (a) amine or (b) phenol-novolac.

Different hardeners are used depending on the requirements of the application. In FR-4 laminates, dicyandiamide (**DICY**) and phenol novolac (**PN**) are mostly used (Figure 1-4).¹¹

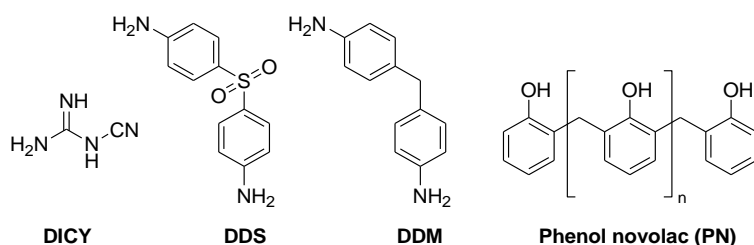


Figure 1-4: Regularly used hardeners for epoxy resins.

1.1 Flame retardants in electronic applications

Epoxy resins used in electronic application are rendered flame retardant by replacement of a part of the polymer by a flame-retardant bromine containing monomer.¹² Until recently, the majority of the flame retardants used for electrical and electronic applications were halogen based and tetrabromobisphenol A (TBBPA) (Figure 1-5) remains the most commonly used flame retardant. Like most halogen based flame retardants, under thermal stress, TBBPA decomposes to yield volatile halogenated radicals. The latter will scavenge the hydrogen radicals present in the flame to form non-flammable gas that will dilute the flame oxidants and in turn lead to the interruption of the flame cycle.¹² Despite their beneficial impact on the fire resistance of polymers, the production of halogenated gas during the fire scenario has been subject to concerns as they increase the amount of toxic gases (CO , or HBr).¹³ The addition of TBBPA in the list of persistent, bio-accumulating toxins (PBT) has stimulated the gradual phasing-out and replacement of halogenated flame retardants.^{14,15}

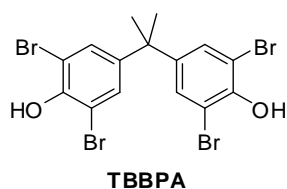


Figure 1-5: Structure of tetrabromobisphenol A.

In February 2003, the Waste Electrical and Electronic Equipment (WEEE) directive and the Restriction of the use of certain Hazardous Substances (RoHS) guideline were introduced.^{16,17} The WEEE directive deals with the recycling and further processing of electronic waste and stipulates the separation of bromine containing plastics from other plastic waste while the RoHS guideline restricts the use of hazardous compounds including polybrominated biphenyl and polybrominated diphenyl ether.^{18,19} Heavy metals such as cadmium, chromium, mercury and lead were later added to the list of restricted compounds.¹⁷ The addition of lead to the list of restricted compound had a direct impact on the development of flame retardants alternatives. The introduction of lead-free soldering techniques was accompanied by an increase of processing temperature ($\sim 40^{\circ}\text{C}$) which in turn required the additives used to have a higher thermal stability. The Registration, Evaluation and Authorization of Chemicals (REACH) directive introduced in 2006, states that only registered flame retardant chemicals that underwent various tests concerning emissions and possible end-of-life issues can be used. In order to comply with WEEE, RoHS, and REACH directives, an increasing number of companies introduced alternative flame retardants to their portfolio.

The emergence of developing countries such as China and India has led to a rising demand of electrical and electronic products. The ever-growing market of portable devices such as cell-phones and computers resulted in a significant increase in the production of plastic for electrical and electronic applications, which represents one of the main applications of epoxy resin composite. A market study carried out by the Freedomia Group, Inc. announced that the global demand for flame retardant additives will grow to 2.2 million metric tons in 2014.²⁰

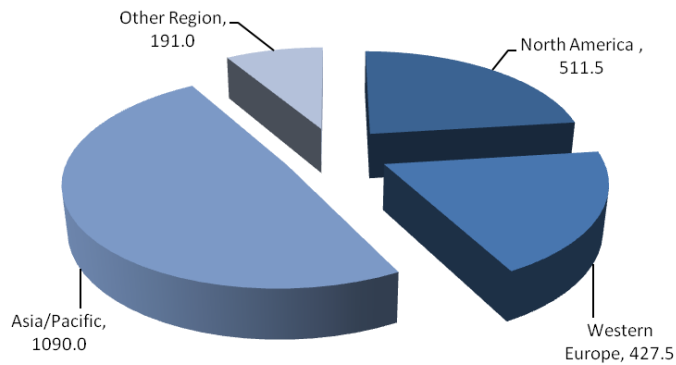


Figure 1-6: Predicted world flame retardant demand (in 1000 metric tonnes) for 2014 by The Freedomia Group Inc.

Hence, in the last decade, there has been considerable effort invested towards the development of new environmentally friendlier flame retardants used in electronic and electrical applications. Figure 1-7 shows a survey of the literature with SciFinder dealing with flame retardant research. Since the beginning of the century, the number of publications has more than doubled. This is indicative of the cumulative effort from the scientific community to answer the flame retardant demand.

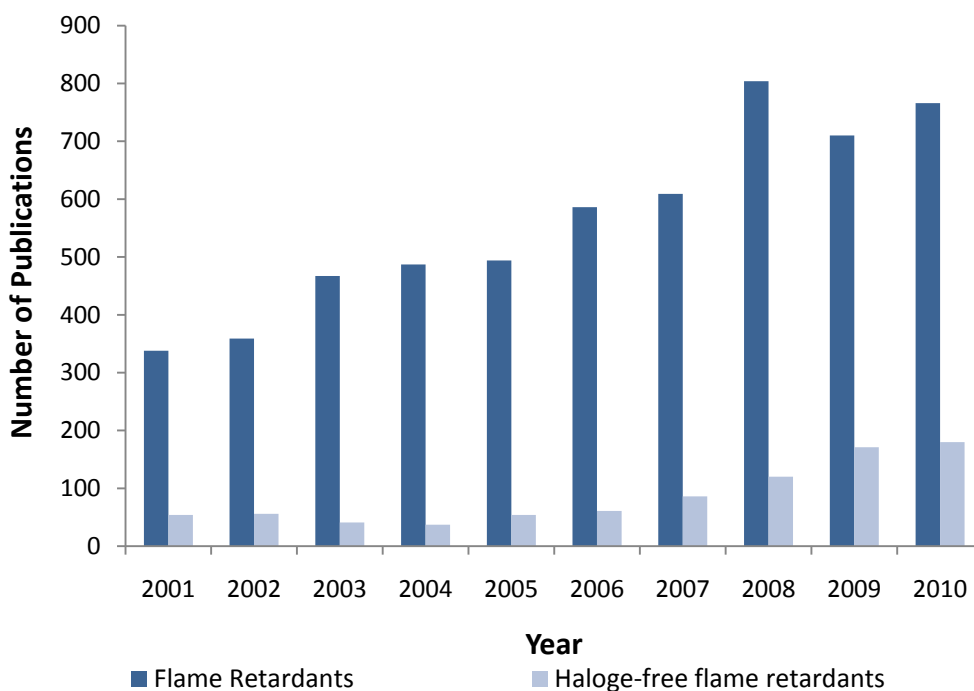
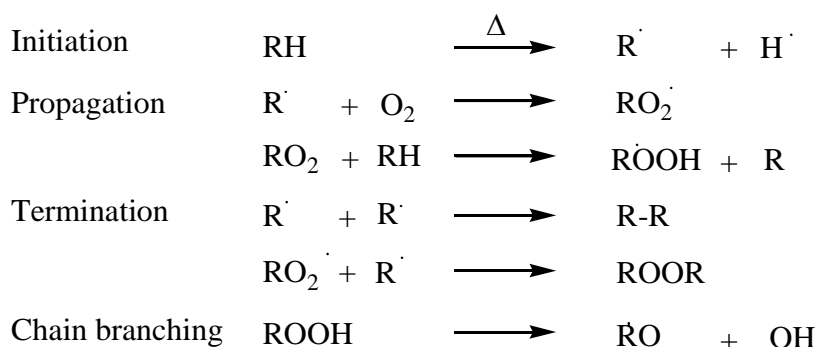


Figure 1-7: Overview of the publications dealing with flame retardancy (Sci Finder).

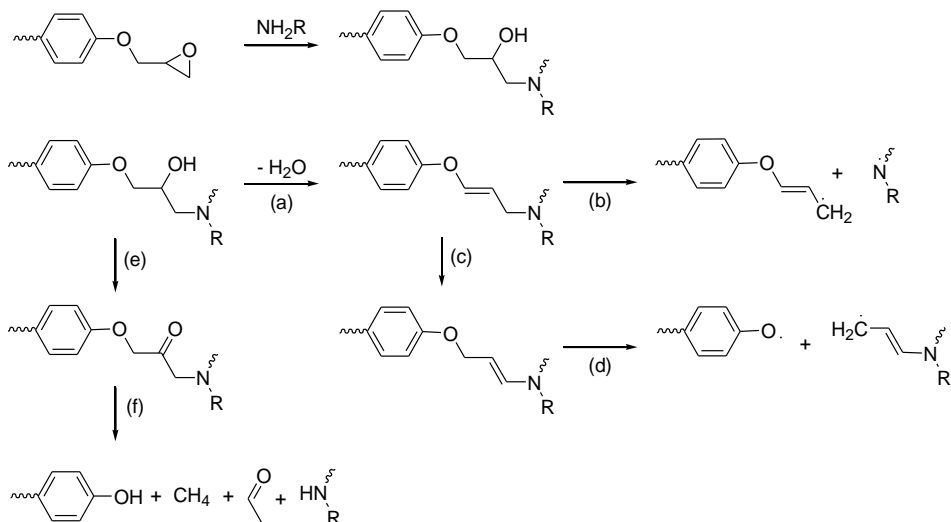
1.2 Combustion of polymer

Before discussing the different flame retardants and their mode of action in further detail, the mechanism of fire spreading and thermal degradation of a polymer must be understood. Three components are required for a flame to spread on a polymer surface: a heat source (flame), fuel (combustible pyrolysis product) and an oxidant (oxygen).²¹ Under thermal stress, polymers form radical species that in turn lead to the formation of volatile combustibles and oxygen feeding the flame in the gas phase (Scheme 1-1).²¹ Further reaction of the non-volatile species in the condensed phase then lead to the formation of a thermally cross-linked char-like material that is much less flammable than the original polymer.²²



Scheme 1-2: Decomposition of polymer matrix.

In the case of epoxy resin materials, the first step is the dehydration or the dehydrogenation of the secondary alcohol functionality formed during the curing process (Scheme 1-3). The newly formed unsaturated amine either undergoes isomerisation followed by an allylic-oxygen bond scission or a direct allylic-nitrogen bond scission depending on the curing agent used.^{10,23-25} The volatile particles formed can then contribute to further polymer degradation (propagation) or charring (termination).²³

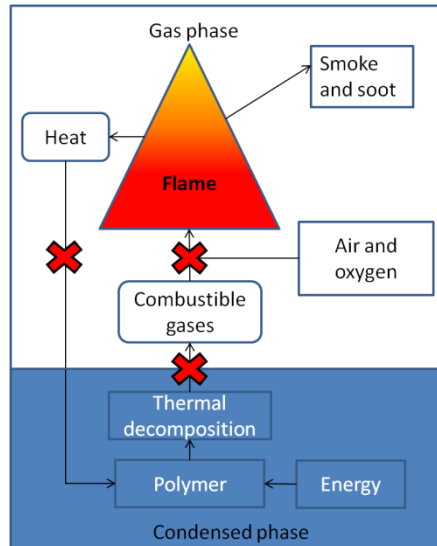


Scheme 1-3 Thermal degradation paths of an amine cured epoxy resin.²⁶

Both the nature of the resin and the hardener determine the thermal stability of the cured resin. When a sample of DGEBA cured with DICY is exposed to fire, significant dripping is observed which prevents it from passing UL 94-V0 rating. However, when epoxy novolac resins are cured using the same hardener, no dripping is observed. Under thermal stress, DGEBA polymer will undergo main chain scission resulting in the formation of smaller polymer chains. The shorter polymer chains formed have lower T_g and will therefore melt and drip off the burning polymer. In contrast, when the highly cross-linked cured epoxy novolac resin undergoes chain scission, the polymer chain length does not endure such a drastic shortening. Hence, no dripping is observed.²⁷

1.3 Mechanism of flame retardancy

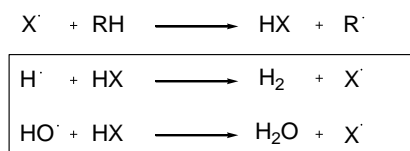
The fire resistance of the cured resin can however be improved by the addition of a flame retardant. Thus, it is important to know that every application demands a different formulation (using different resins, hardeners and fire retardants). As shown in the flame cycle (Scheme 1-4) there are different steps where a fire scenario can be stopped. The flame retardant can either interact with the combustible substance, the oxidising gas or the heat.



Scheme 1-4. Combustion cycle of a polymer fire. Red marks represent the main approaches to extinguish a fire scenario.

The mode of action of flame retardants can be separated in different mechanism:^{21,22}

- Dilution: Non-flammable inorganic material is introduced in the formulation such that the total quantity of combustible material is reduced which improves the flame retardation of the material.²⁵
- Generation of non-combustible gases: the added flame retardants decompose under thermal exposure to yield non-combustible gases that decrease the concentration of oxygen at the front of the flame. The lack of oxygen results in a reduction of the flame and is followed by extinction.²⁸
- Free-radical scavenging: the combustion of the flame retarded polymer generates the formation of active fragments in the condensed phase. When those fragments volatilise in the gas-phase, they can react with oxygen to form non-flammable gases. Scheme 4 demonstrates how halogenated flame retardants react through such mechanism.



Scheme 1-5: Gas phase reaction of halogenated flame retardants (X = Cl, Br).¹²

- Char formation: under thermal exposure the formation of a thermally stable layer at the surface of polymer can be enhanced by the presence of a flame retardant. This insulating char layer reduces the volatilisation of the reactive fragments and prevents the heat from reaching the combustible polymer.^{13,29,30}

1.4 Alternative to halogen flame retardants

As mentioned in section 1.2, the introduction of legal directive restricting the use of halogenated flame retardants, stimulated the flame retardant community to develop environmentally friendlier alternatives. This section will give a brief overview of the three main classes of non-halogenated flame retardants and their flame retardant mechanism. For a more detailed discussion, several reviews and book chapters have been published on this subject.^{4,31-33}

1.4.1 Inorganic flame retardants

The most common inorganic flame retardants are metal hydroxide such as Aluminum hydroxide (ATH), Boehmite and magnesium hydroxide (MDH). They are relatively inexpensive and environmentally friendly. During a fire scenario, metal hydroxides decompose to metal oxides and water in a highly endothermic reaction. The deviation of energy, away from the ignition source, leads to the interruption in the flame cycle and consequently to the extinguishment of the flame. Moreover, the water produced during the decomposition evaporates, thus cooling the polymer surface and diluting the burnable gases.³⁴ However, due to their relatively low flame retardant efficiency, high loading (~30-60 %) are necessary, which has a negative impact on the physical properties of the cured resin. The thermal stability of ATH has proved problematic when lead-free soldering was introduced. Indeed, ATH starts to decompose at 250 °C, releasing water and leading to the delamination of the epoxy resin composite during the soldering process.

The use of nanocomposite materials such as nanoclays based on magnesium-aluminium hydroxide layers (Montmorillonite) or nanostructured polyhedral oligomeric silsesquioxane (POSS) have been subject to increasing interest.³⁵⁻⁴⁰ Organically modified nanoclay have demonstrated promising flame retardant results in epoxy resins both with and without other flame retardant additives. The use of nanoclay allows a lower loading of mineral flame retardant. Nanoclays are reported to reduce the relative heat release rate (HRR) which is directly related to the flame spreading ability. They are also found to reduce the smoke generation and promote the char formation.^{37,41-43}

1.4.2 Nitrogen-based flame retardants

The most commonly used nitrogen based flame retardant in EE application is melamine based. Under thermal stress, melamine is thought to favour the formation of non-flammable cross-linked structures that act as a thermal barrier (charring). Simultaneously, the release of molecular nitrogen and NH_3 in the flame can contribute to the dilution of the flammable particles.^{29,44-46}

1.4.3 Phosphorus-based flame retardants

Most of the literature dealing with non-halogenated flame retardant focuses on phosphorus derivatives.⁴⁷⁻⁵⁰ Both additive and reactive phosphorus compounds demonstrated good flame retardant efficiency in epoxy resin systems. Under thermal stress, phosphorus derivatives tend to oxidise to form phosphorus pentoxide (P_2O_5).^{31,51} The latter undergoes hydrolysis to yield polyphosphoric acid ($\text{H}_x\text{P}_y\text{O}_z$) that can catalyse the formation of carbonaceous char. Non-halogenated phosphorus flame retardant were found to have an environmentally friendly profile.^{4,31} 9,10-dihydro-9-oxa-10-phosphaphenanthrene-10-oxide (DOPO) and its hydroquinone derivative (DOPO-HQ) are both commercially available reactive organophosphorus flame retardant for EE applications.

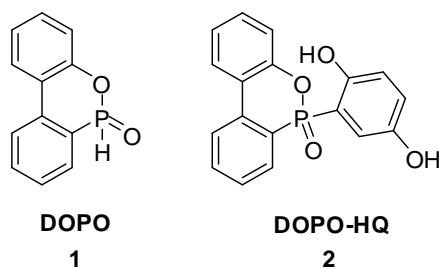
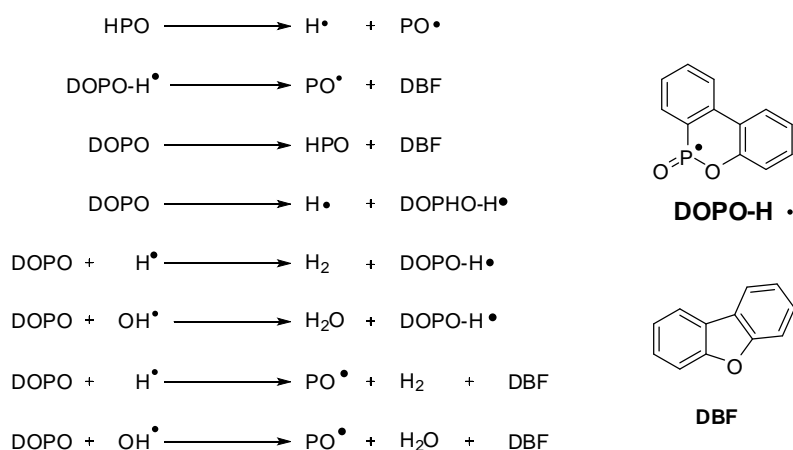


Figure 1-8: Commercially available organophosphorus flame retardants for EE application.

The reactive P-H bond of DOPO allows its chemical incorporation in the epoxy resins also known as a fusion process (Section 4.1). The direct bond between the flame retardant and the epoxy resin remove the concerns about the possible leaching out of the phosphorus compound into the environment also known as blooming.

Even though both gas phase and condensed were reported for phosphorus flame retardants, in the case of DOPO the gas phase mechanism is thought to be predominant.



Scheme 1-6: Proposed mechanism for flame retardant reactivity of DOPO in the gas phase.

Theoretically, chemical tailoring of the phosphorus derivatives can favour one flame retardant mechanism over the other. However, reports on the chemical tailoring of phosphorus derivatives for specific flame retardant mechanism remain scarce.

1.5 Objectives

The aim of the work presented in this thesis is to synthesise and investigate a variety of heterocyclic organophosphorus compounds that act as flame retardants for epoxy resin systems used in the electrical and electronic applications.

In order to investigate the influence of the environment around the phosphorus atom on the flame retardancy, the synthesis of heterocyclic organophosphorus compounds containing nitrogen and sulphur atom with similar structure to DOPO will be presented.

Prior to investigating their flame retardant activity, the reactivity of the newly synthesised compounds will be tested and compared to other organophosphorus molecules.

Then, the synthesised heterocyclic organophosphorus compounds will be grafted onto epoxy resins. The grafted resin will be cured using the similar hardener and accelerator system used for printed wiring board. Finally, the flame retardant properties of the new organophosphorus compounds will be investigated and compared to those of DOPO.

CHAPTER 2: EVALUATION OF FLAME RETARDANCY

The following describes the different techniques used to assess the flame retardancy of epoxy resin systems including composite materials.

2.1 Thermal Gravimetry Analysis (TGA)

TGA determines the thermal stability of the cured formulation by monitoring the loss of mass of a heated sample with increasing temperature. When discussing the flame retardancy of a polymer, one commonly quotes the decomposition temperature (T_d), which represents the temperature at which 10 % of the initial weight is lost. The charring ability of the formulation can also be extrapolated from the residual weight once all solid is thermally stable ($T > 600$ °C).

2.2 Differential Scanning Calorimetry (DSC)

DSC measures the difference between the amount of heat required to increase the temperature of a sample and a reference as a function of time or temperature. In polymer science, DSC enables to determine the glass transition temperature of the cured formulation (T_g). The T_g of the formulation containing modified resin should vary as little as possible from the pristine resin.

2.3 UL 94 test

UL 94 test is a common test for flame retardancy. It measures the flammability of a material by a defined ignition source. During the test, a small sample (13 mm width x 4 mm thick x 50 -125 mm high) is exposed for 10 s, either vertical or horizontally, to a small calibrated Bunsen burner flame (25 mm of height). To test a specific formulation, five samples are ignited twice and the time to extinguishment after each ignition is recorded. The flammability is rated as a function of the time the specimen keeps on burning after the removal of the flame and the total time to extinguishment to the set of five samples (Table 2-1). A material is considered non-flammable once it is classified as V0 (ISO 1210).

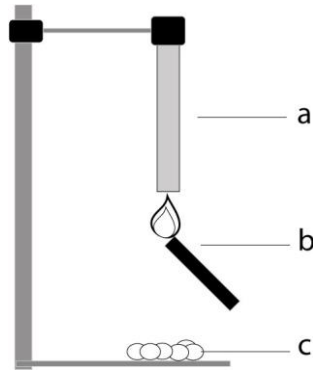


Figure 2-1: Schematic representation of the apparatus set-up for UL 94 vertical test. a) sample; b) bunsen burner; c) cotton.

Table 2-1: Definition of UL 94 Vertical test classifications.

Classification	V0	V1	V2	n.c.
Afterflame time t1	< 10 s	< 30 s	< 30 s	> 30 s
Afterflame time t2	< 30 s	< 60 s	< 60 s	-
Afterflame time, 10 flame applications	< 50s	< 250 s	< 250 s	> 250 s
Ignition of cotton	No	No	Yes	Yes

2.4 Oxygen Index Test

LOI measures the minimum concentration of oxygen in the atmosphere required to maintain a candle like burning of a material. Materials with a higher LOI value are less flammable. Materials with LOI under 21 %, which is the concentration of oxygen in air, are considered as flammable (ISO 4589-2). On the other hand, materials with LOI over 26 % are considered self-extinguishing.

$$LOI = \frac{[O_2]}{[O_2] + [N_2]}$$

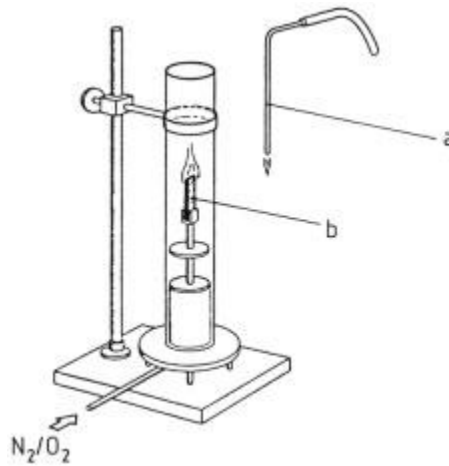


Figure 2-2: Schematic representation of the set-up apparatus for the oxygen index test. a) flame source; b) sample.⁵²

2.5 Cone Calorimetry

Similarly to UL 94 and LOI, cone calorimetry is another standard test to evaluate the flame retardancy of a material. This technique is based on the fact that the heat output during the combustion of materials is almost always directly proportional to the consumption of oxygen (13.6 kJ/g O_2). While a specimen of specific dimensions is exposed to a controlled radiant heat flux, the rate of the gas flow and the concentration of oxygen are measured and the rate of heat release and the effective heat of combustion can be extrapolated (ISO 5660 Part 1). This allows to determine how fast a fire will spread on a material once it has been lit. Simultaneously, the weight loss of the specimen, as well as the concentration of gases evolved (e.g. CO, CO₂, H₂O, HCN, HCl, HBr, SO₂, NO_x and other volatile carbonous molecules) are monitored.

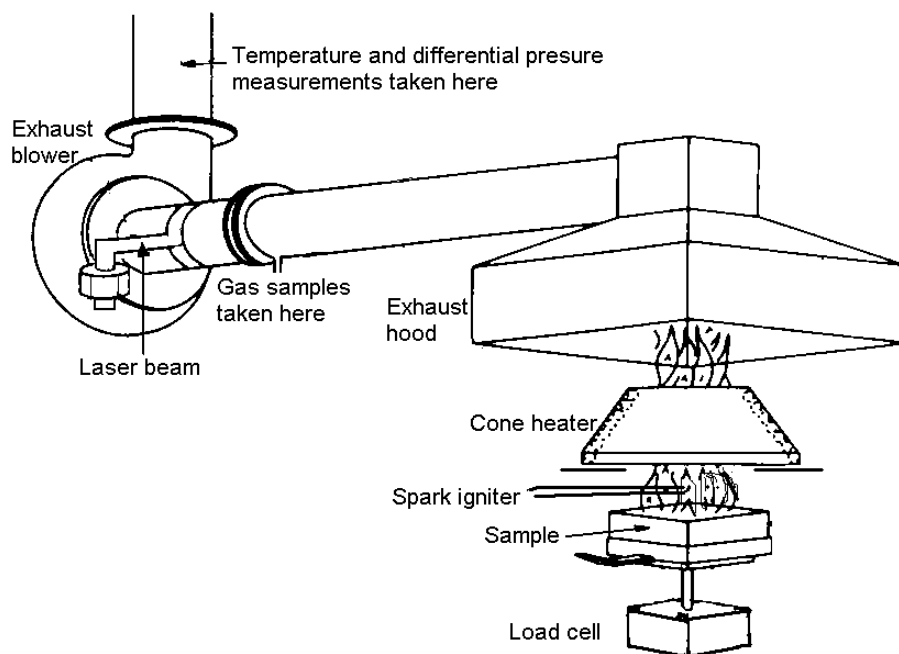


Figure 2-3: Schematic representation of the apparatus set up for cone calorimetric measurements.⁵²

2.6 Thermal desorption Mass Spectroscopy (TD-MS)

Thermal desorption mass spectroscopy is used to observe the volatile decomposition products of polymers when exposed to a heat flux. The extrapolated data allows an insight in the flame retardant mechanism. During the experiment, a small amount of flame retardant polymer is placed into a stainless steel crucible. The crucible is then heated under high vacuum using a thermal element and the molecular weight of volatile decomposition products are monitored by a mass spectrometer.

In the case of phosphorus based flame retardants, volatile fragments containing phosphorus such as PO , POO and HPO are plotted against the temperature. This enables to grasp a deeper understanding of the mechanism of action and decomposition of phosphorus flame retardants.^{53,54}

CHAPTER 3: SYNTHESIS OF ORGANOPHOSPHORUS COMPOUNDS

The section below describes the efforts invested toward the synthesis of heterocyclic organophosphorus compounds with different chemical environment around the phosphorus atom that could act as flame retardants for epoxy resins used in PWB.

3.1 Introduction

Since the pioneering work of Michealis and Arbuzov in the late 19th and early 20th century, the field of organophosphorus chemistry has been the subject of extensive research activity.⁵⁵ The discovery of the insecticidal activity of a number of phosphoric acid and phosphonic ester highly contributed to the development of new phosphorous derivatives. Nowadays, organophosphorus derivatives can be found in a wide spectrum of applications such as agrochemicals, catalysis, pharmaceutical and flame retardants.⁵⁵⁻⁵⁸

The majority of phosphorus compounds are synthesised using phosphorus chlorides, white phosphorus or red phosphorus as reactants.⁵⁹ For instance, as shown in figure 3-1, the commercially available flame retardant 9,10-dihydro-10-oxaphosphophenanthrene-10 oxide (DOPO) is synthesised by phosphorylation of 2-hydroxybiphenyl with PCl_3 , followed by an intramolecular Friedel-Crafts alkylation to form the phosphonous chloride (DOP-Cl) that undergoes hydrolysis with water to yield the phosphinate (DOPO).

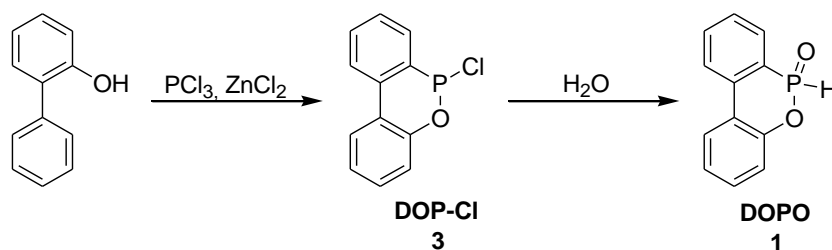


Figure 3-1: Synthesis of DOPO from 2-hydroxy biphenyl.

The phosphorus atom can undergo a series of chemical reactions to form new P-O, P-C or P-N bonds. The two most common methods to obtain new P-C bonds are the Michaelis-Becker reaction and the Michealis-Arbuzov reaction, commonly referred to as

the Arbuzov reaction (Figure 3-2). In the case of the Arbuzov reaction (Figure 3-2b), the phosphonic acid is formed by alkylation of a trialkyl phosphite. In the first case, the acidic proton of a dialkyl ester of phosphorus acid is removed using a strong base (Figure 3-2a). The formed anion act as a nucleophile in the presence of an alkylhalide to yield the corresponding phosphonic acid via rearrangement.

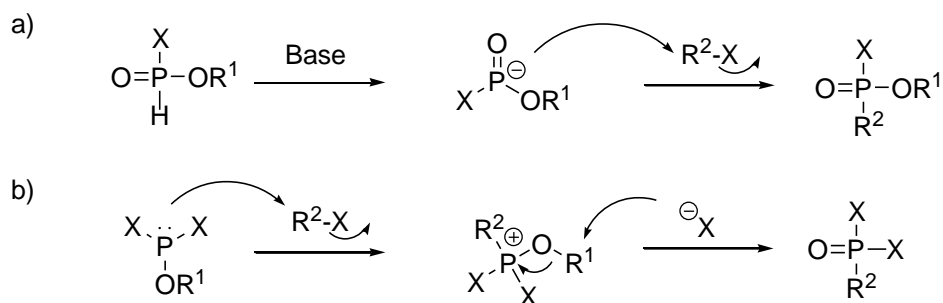


Figure 3-2: Mechanism of formation of phosphonic acid derivatives via a) Michaelis-Becker reaction and b) Arbuzov reaction.

Phosphinates, such as DOPO, are also known to form anions in the presence of base. The strong nucleophile formed allows addition reactions to α,β -unsaturated systems (i.e. Pudovik reaction) or carbonyl groups (i.e. Abramov reaction). The nucleophilicity of the phosphonate has been used to functional epoxy resin.⁵³

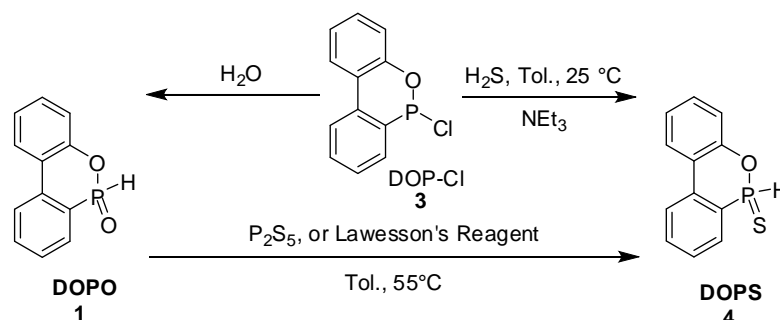
3.2 6H-dibenzo[c,e][1,2]oxaphosphinine 6-sulfide (DOPS) derivatives

This section was previously published in Heterocycles 2011, 83(4), 743-753.

3.2.1 Synthesis of 6H-dibenzo[c,e][1,2]oxaphosphinine 6-sulfide

To the best of our knowledge, 6H-dibenzo[c,e][1,2]oxaphosphinine 6-sulfide (**4**) had never been synthesised prior to our study. Krawiecki and Michalski showed that dialkyl phosphochloridates react readily with hydrogen sulphide in the presence of tertiary amines to yield tetra-alkyl thiopyrophosphates.⁶⁰ This method was then successfully used by Zwierzak to obtain a series of cyclic hydrogen thiophosphites.⁶¹ Therefore, our first synthetic approach consisted of reacting DOP-Cl and hydrogen sulphide gas as a source of sulphur in the presence of triethylamine (Scheme 3-1). Concentration of the reaction mixture *in vacuo* after removal of the formed triethylamonium salt yielded a white crystalline solid. Similarly to 9,10-dihydro-9-oxa-10-phosphaphenanthrene-10-oxide (**1**), the ¹H-NMR spectrum of the obtained solid showed a doublet in the aromatic region ($\delta = 8.4$ ppm) with a large coupling ($^1J_{\text{P-H}} = 536$ Hz) that

was associated with a P-H bond (Figure 3-3). An additional 8 aromatic protons associated with the rigid phosphaphenanthrene structure were also observed in the $^1\text{H-NMR}$ spectrum. The $^{31}\text{P-NMR}$ spectrum showed a single peak ($\delta = 57.1$ ppm) and the major peak in the mass spectra was at $m/z = 232$ strongly suggesting that the isolated product was the target molecule (4). The $^1\text{H-NMR}$ spectrum of (4) revealed well resolved signals which can be attributed *via* 2-D COSY methods involving both H-H (gCOSY, gDQFCOSY) and C-H correlations (gHSQC and gHMBC) (Figure 3-4).



Scheme 3-1: Synthesis of 6*H*-dibenzo[*c,e*][1,2]oxaphosphinine 6-sulfide (4) from 10-chloro-10*H*-9-oxa-10-phospha-phenanthrene (DOP-Cl) and 9,10-dihydro-9-oxa-10-phosphaphenanthrene-10-oxide (1).

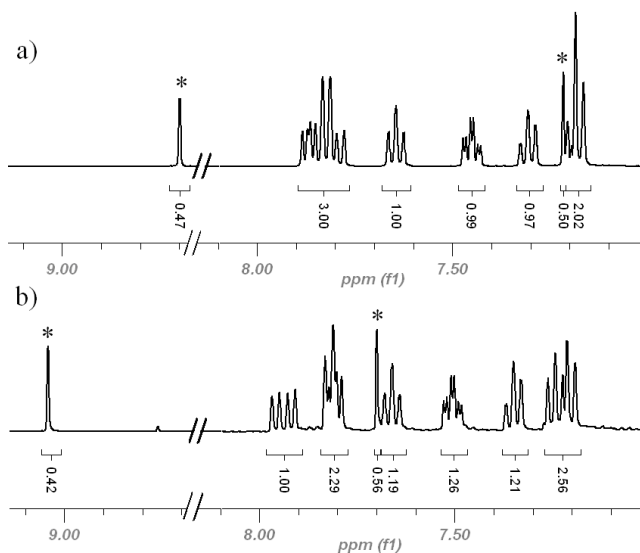


Figure 3-3: $^1\text{H-NMR}$ spectra of a) 9,10-dihydro-9-oxa-10-phosphaphenanthrene-10-oxide (1) and b) 6*H*-dibenzo[*c,e*][1,2]oxaphosphinine 6-sulfide (4) in CDCl_3 . * emphasize the doublets corresponding to the P-H bond.

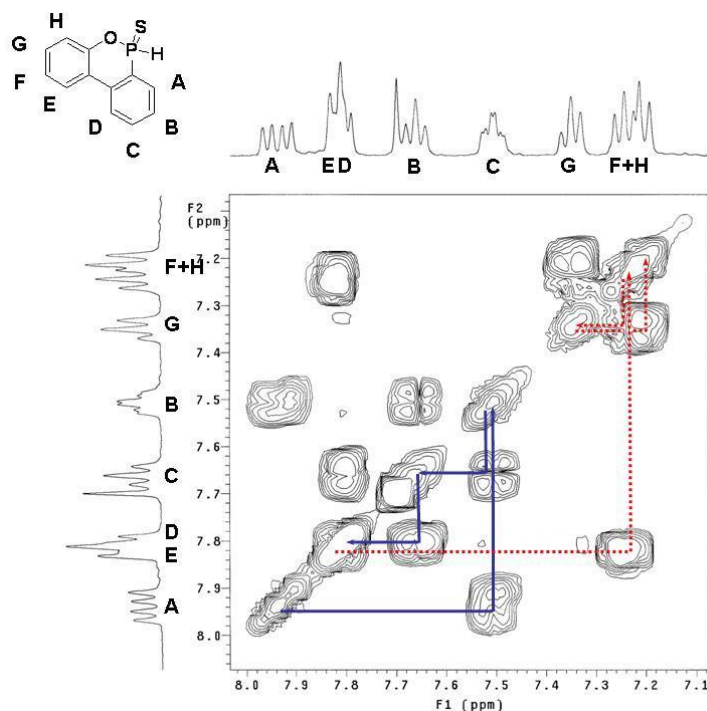


Figure 3-4: H,H-gCOSY of 6*H*-dibenzo[*c,e*][1,2]oxaphosphinine 6-sulfide (**4**) in CDCl₃.

Slow diffusion of a concentrated solution of (**4**) in dry dichloromethane into pentane yielded a single crystal that indisputably confirmed the isolation of the target molecule (Figure 3-5). The structure of (**4**) is similar to its parent oxide molecule (**1**) however (**4**) has an increased solubility in most organic solvents which is advantageous for formulations.⁶¹

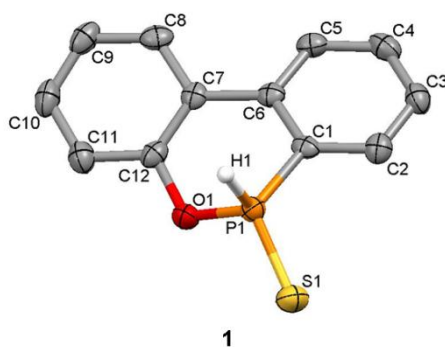


Figure 3-5: View of the molecular structure of (**4**) in the crystal, aromatic H atoms and solvent molecules omitted due to reasons of clarity. Selected bond lengths [pm]: (7) S1-P 190.94 (4), O1-P 161.77 (5), P-H1 138.03 (3).

However, during this synthesis, the use of large amounts of H₂S was not desirable as its toxicity is similar to that of hydrogen cyanide.⁶² The two most commonly used sources of sulphur are phosphorus pentasulfide and Lawesson reagent.⁶³ The use of

such thionation agents solved the toxicity issue and also allowed the use of the commercially available (1) as a starting material rather than DOP-Cl (3) which is highly air and moisture sensitive. Both thionation agents successfully yielded the desired molecule, however the yields were lower as side reactions occurred yielded a mixture of by-products that could not be separated for the target compound which is detrimental for further commercialisation.

3.2.2 Pudovik reaction of 6*H*-dibenzo[*c,e*][1,2]oxaphosphinine 6-sulfide

With several practical ways to synthesize molecule (4) in hand, we initiated the comparison of its reactivity with the parent phosphine oxide molecule (1) whose chemistry mainly involves the reactivity of the P-H bond. P-H bond are known to undergo nucleophilic addition onto unsaturated functionalities such as carbonyl group and acrylates.⁶⁴ The parent molecule (1) was reported to produce the hydroquinone derivative in very good yield when heated in toluene in presence of benzoquinone.^{49,65} The Pudovik product of DOPO with benzoquinone was reported to impart flame retardance to epoxy resins without detrimental impact on the glass transition temperature.⁶⁶ Hence, benzoquinone was chosen as α,β -unsaturated carbonyl to assess the reactivity of (4). When a solution of (4) was heated in the presence of equimolar amounts of benzoquinone, a single product from a Pudovik reaction could be isolated in high yields (Figure 3-6).⁶⁷

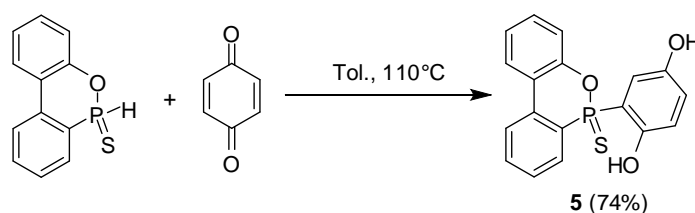


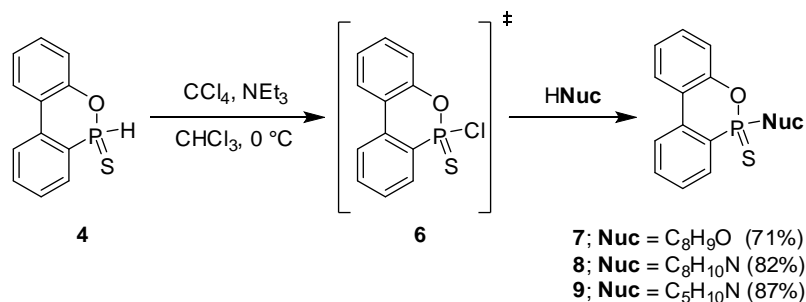
Figure 3-6: Synthesis of compounds (5) from (4).

3.2.3 Atherton-Todd reaction of 6*H*-dibenzo[*c,e*][1,2]oxaphosphinine 6-sulfide

Another organophosphorous reaction involving the reactive phosphorous-hydrogen bond in phosphites and phosphonites is the Atherton-Todd reaction.⁶⁷⁻⁷¹ The Atherton-Todd reaction, usually involving dialkyl and diaryl phosphites in the presence of carbon tetrachloride and a base, is known as an effective way to access functionalised

phosphine oxides, in particular phosphoramidates which are an important and versatile class of chemicals.

However, this reaction remains relatively unexplored for phosphorous sulfides. In an effort to deepen our understanding of its reactivity, (4) was reacted with different nucleophiles using the Atherton-Todd approach as shown in Scheme 3-2.^a



Scheme 3-2: Atherton-Todd approach of (4).

With this intention, (4) was dissolved in chloroform and carbon tetrachloride then a solution of triethylamine and a nucleophile diluted in chloroform was added drop wise. The different nucleophiles: 2-phenylethylamine, piperidine and 2-phenylethanol were chosen as models for primary and secondary amines as well as primary alcohols respectively (Scheme 3-2). All three desired products were obtained in good yields with fast reaction times (below 60 minutes). Hence, (4) proved to be an efficient reagent for the Atherton-Todd reaction. The *in situ* formation of 10-chloro-9-oxa-10-phosphaphenanthrene 10-sulfide (6) can be observed using NMR spectroscopy (δ (^{31}P , CDCl_3) 74.5 ppm) and HR-MS analysis (calculated for $[\text{C}_{12}\text{H}_8\text{OSP}_{35}\text{Cl}]^+$ 265.9722, found 265.9688). Even though primary alcohols are known to be problematic substrates for the Atherton-Todd reaction, the formation of compound (7) was observed in good yields.⁶⁹ Crystal structures of molecules (7), (8) and (9) were also obtained and indisputably verify the desired molecules. Figure 3-7 presents the crystal structures and selected bond lengths and torsion angles. The relatively low torsion angles are indicative of delocalisation. The P=S bond length in compound (7) was 191.1 pm (8(P=S): 193.6 pm, 9(P=S): 191.9 pm) which coincides with parent structures.^{72,73} The aliphatic phosphorus oxygen bond in (7) was 158.5 pm which was in agreement with the literature.^{72,74} The length of phosphorus nitrogen bond in molecule (8) (162.0 pm) and (9) (163.7 pm) is also comparable to similar structures.^{74,75} This set of experiments demonstrated that the

^aMolecules 5 and 7 were synthesised by Sebastian Wagner

Atherton-Todd reaction can be exploited to access different phosphine sulphide molecules.

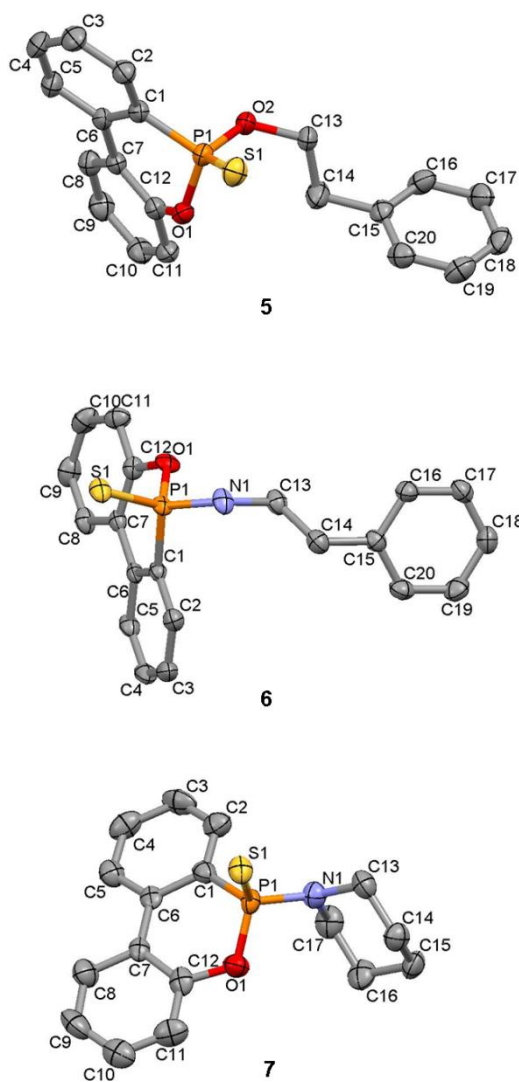


Figure 3-7: View of the molecular structure of (7), (8) and (9) in the crystal, H atoms and solvent molecules omitted due to reasons of clarity. Selected bond lengths [pm] and torsion angles [°]: (7) S1-P 191.15(4), O2-P 158.57(4), S1-P-O2-C13 37.72; (8) S1-P 193.65(6), N1-P 162.06(4), S1 P-N1-C13 10.07; (9) S1-P 191.96(6), N1-P 163.71(4), S1-P-N1-C13 20.40.

3.3 5,5-Dimethyl-[1,3,2]-dioxaphosphirane-2-sulfide (DDPS) derivatives

The relative ease of access to DOPS, motivated to investigate the possible thionation of other organophosphorus compounds used as flame retardant for epoxy resin materials.

5,5-dimethyl-[1,3,2]dioxophosphorinane 2-oxide (DDPO) (**10**) is another relevant organophosphorus flame retardant.⁷⁶ It is reported to successfully flameproof, cellulose materials, polyurethanes and more recently epoxy resins.⁷⁷⁻⁸⁰ DDPO was reported to increase the flame retardancy of DEN 438 and DGEBA resins.⁸¹ Similarly to DOPO, under thermal stress, DDPO produces phosphonic acids that promote the formation of carbonaceous char. However, unlike DOPO, the condensed phase mechanism is predominant.⁸¹ In order to compare the influence of sulphur on the mode of action, the synthesis of sulfide derivatives of DDPO was initiated.

3.3.1 Synthesis of 5,5-dimethyl-[1,3,2]dioxophosphorinane 2-thionic acid

First, as seen in Figure 3-8, DDPO^b was heated in toluene in the presence of equimolar amount of sulphur.⁸² Concentration of the yellow solution *in vacuo* yielded a shiny yellow powder. The absence of the doublet at 6.89 ppm ($J_{P-H} = 676$ Hz) in the ¹H-NMR spectrum of the obtained powder confirmed that the P-H bond had reacted. In addition, the presence of a broad singlet at 8.08 ppm indicated the presence of a –OH functionality. The molecular ion peak at $m/z = 182.01$ in high resolution mass spectrum confirmed the synthesis of the target molecule DDPS-OH (**11**). This confirmed that DDPO could undergo thionation reaction in a similar way to DOPO.⁸³

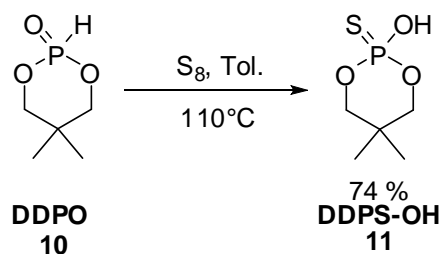


Figure 3-8: Synthesis of DDPS-OH (**11**) from DDPO (**10**).

^b Compound 10 was kindly provided by Patrick Mueller and Kai Stoess.

with the target addition product of DDPS to benzoquinone *via* a Pudovik reaction (14). The second peak, at $m/z = 438.05$, was associated with a double addition of DDPS to benzoquinone (15). Nonetheless, the successful Pudovik reaction demonstrated that the P-H bond could potentially react with catalytic amount of base, thus allowing DDPS to act as a nucleophile without losing the sulphur moiety. Hence, DDPS could potentially be grafted onto epoxy moieties. The reaction of DDPO with benzoquinone in toluene was also reported to yield to addition products.⁵⁰ However, in the latter case, the single addition product could be isolated in relatively good yields. Efforts to reproduce this synthesis however, yielded the double-addition product as the major compound.⁸⁷ In addition, unlike suggested by Worku *et al.*, X-Ray analysis of a single crystal confirmed that the addition of the second phosphorus moiety occurred at the ortho position to the first phosphorus moiety.⁸⁷

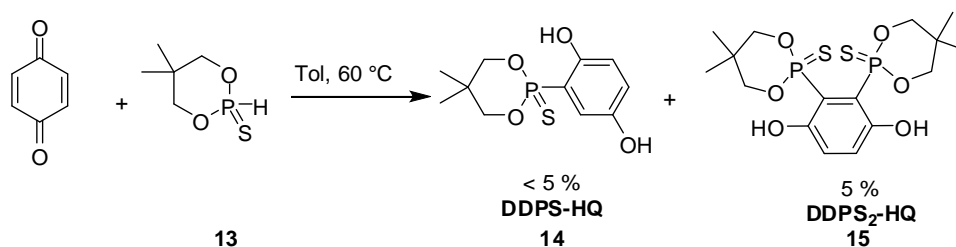


Figure 3-10: Reactivity of DDPS with benzoquinone.

3.4 9,10-dihydro-9-azaphosphaphenanthrene-10- oxide (DAPO) derivatives

Our group has investigated a series of phosphacyclic analogues to phenanthrene and anthracene (Figure 3-11).^{88,89} As with DPPA, the introduction of the amine functionality in the phosphaphenanthrene cycle would result in a bifunctional reactive material that could simultaneously be used as a flame retardant and a cross-linker.⁸⁹ Such bifunctional additives would therefore remove the necessity of adding an extra flame retardant, thus reducing the possible detrimental effect of on the material properties.

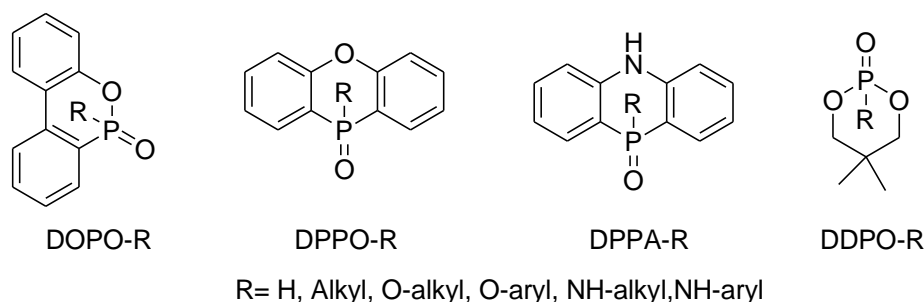


Figure 3-11: Heterocyclic phosphorus substrates investigated as HFFR in epoxy resins.

In order to investigate the influence of an amine functionality on the flame retardancy of the phosphaphenanthrene cycle, 9,10-dihydro-9-azaphosphaphenanthrene-10-oxide (DAPO) (**16**) was synthesised. The synthesis of DAPO from 2-aminobiphenyl was previously reported by Dewar and Kubba as well as Campbell and Way.^{90,91} However, the large discrepancy in the melting points of the hydrolysed compounds reported combined with the lack of NMR analysis prompted the investigation of the reaction conditions.

First, the synthesis of DAPO was attempted in a one-pot reaction of 2-aminobiphenyl with equimolar amount of phosphorus trichloride in refluxing benzene, to form the dichlorophosphine derivative followed by a Friedel-Crafts reaction in the presence of a AlCl_3 to yield the azaphosphaphenanthrene chloride derivative (DAP-Cl). Then, similarly to Dewar and Kubba, a solution of the cyclic phosphine chloride in dichloromethane was washed with water in order to form the target azaphosphaphenanthrene oxide DAPO. However, $^1\text{H-NMR}$ analysis of the solid isolated after hydrolysis showed only the presence of the starting material. This suggested either that the cyclisation was not complete or that the P-N bond was highly water sensitive.

In order to further understand the formation of the phosphine chloride, alternative reaction conditions were investigated. The use of ZnCl_2 , used for the cyclisation of DOP-Cl, instead of AlCl_3 , as Friedel-Crafts catalyst also failed to yield the target molecule.⁹² The use of PCl_3 as a solvent followed by a Friedel-Crafts alkylation in the presence of catalytic amount of AlCl_3 , successfully yielded a single heterocyclic organophosphorus molecule that rapidly hydrolysed with air ($\delta^{31}\text{P} = 84.2$ ppm in CDCl_3). Mass spectroscopy confirmed that the synthesised compound was the targeted DAP-Cl (**17**) ($m/z = 233$). Eventhough the rapid hydrolysis of DAP-Cl was also observed by Campbell and Way, it was stable enough in a solution of CDCl_3 to observe the characteristic aromatic fingerprint of phosphaphenanthrene derivatives (Figure 3-12).

Moreover, a doublet associated with the amine functionality with a large coupling ($J_{\text{P-H}} = 25 \text{ Hz}$) was observed ($\delta = 6.05 \text{ ppm}$). The chemical shift of this doublet confirmed the presence of an aminic proton while the large ${}^2J_{\text{P-H}}$ coupling indicated that it was directly bound to the phosphorus atom.

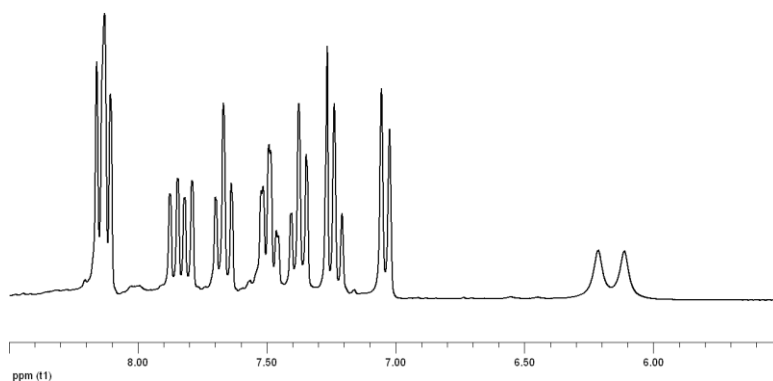
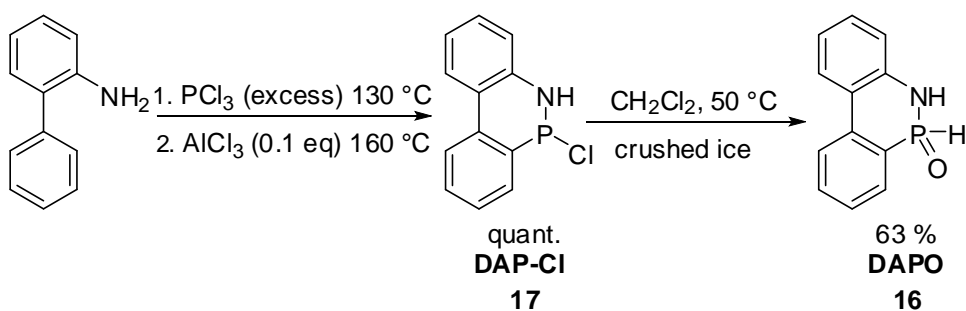


Figure 3-12: ${}^1\text{H}$ -NMR spectrum of DAP-Cl in CDCl_3 .

Once DAP-Cl was successfully synthesised, the investigation of the hydrolysis condition was carried out. Dissolution of DAP-Cl in chloroform followed by a water extraction yielded the starting material back. On the other hand, hydrolysis of a hot solution of DAP-Cl in dichloromethane, using crushed ice, yielded a single phosphorus compound (63 %) ($\delta^{31}\text{P} = -4.6 \text{ ppm}$) with $m/z = 215$ and $\text{mp } 196^\circ\text{C}$ that was isolated as an insoluble white solid. The melting point was coherent with the product isolated by Kubba and Dewar (

Scheme 3-3).⁹¹ Moreover, the ${}^1\text{H}$ -NMR spectra showed similar features to that of DOPO (

Figure 3-13). However, the chemical shift in the ${}^{31}\text{P}$ -NMR ($\delta^{31}\text{P} = -4.6 \text{ ppm}$) spectrum was more upfield than predicted from DOPO itself ($\delta^{31}\text{P} = 15.3 \text{ ppm}$).



Scheme 3-3: Synthesis of DAPO starting from 2-aminobiphenyl.

Concentration of the organic mother liquor yielded a single organophosphorus compound ($\delta^{31}\text{P} = 14.4 \text{ ppm}$) as a purple solid with a molecular ion peak at m/z 215 and mp $179 \text{ }^\circ\text{C}$ which coincided with the compound isolated by Campbell and Way.⁹⁰ Unlike the first organophosphorus compound isolated by filtration from the aqueous phase, the ^{31}P -NMR spectrum was in accordance with the DOPO molecule. However, significant discrepancies between the ^1H -NMR spectra were observed (Figure 3-13). The use of COSY, NOESY and HMBC enabled us to determine that the molecule isolated from the mother liquor had a more localized ring system and was the targeted azaphosphaphenanthrene analogue of the DOPO molecule: DAPO (figure 3-13). Moreover, the presence of a broad singlet at 9.2 ppm indicated that a phosphamidic acid was present in the compound isolated by filtration (figure 3.14).

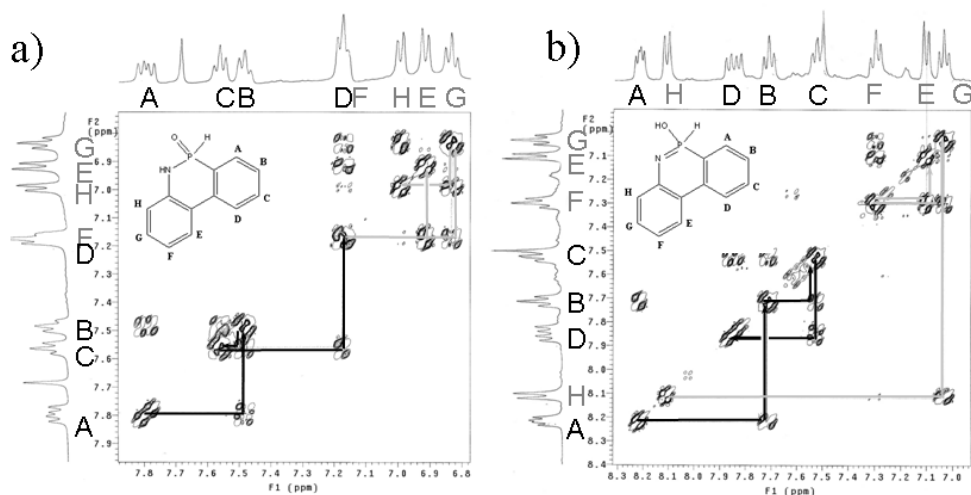


Figure 3-13: ^1H , ^1H -gCOSY of DAPO (a) and its tautomer (b).

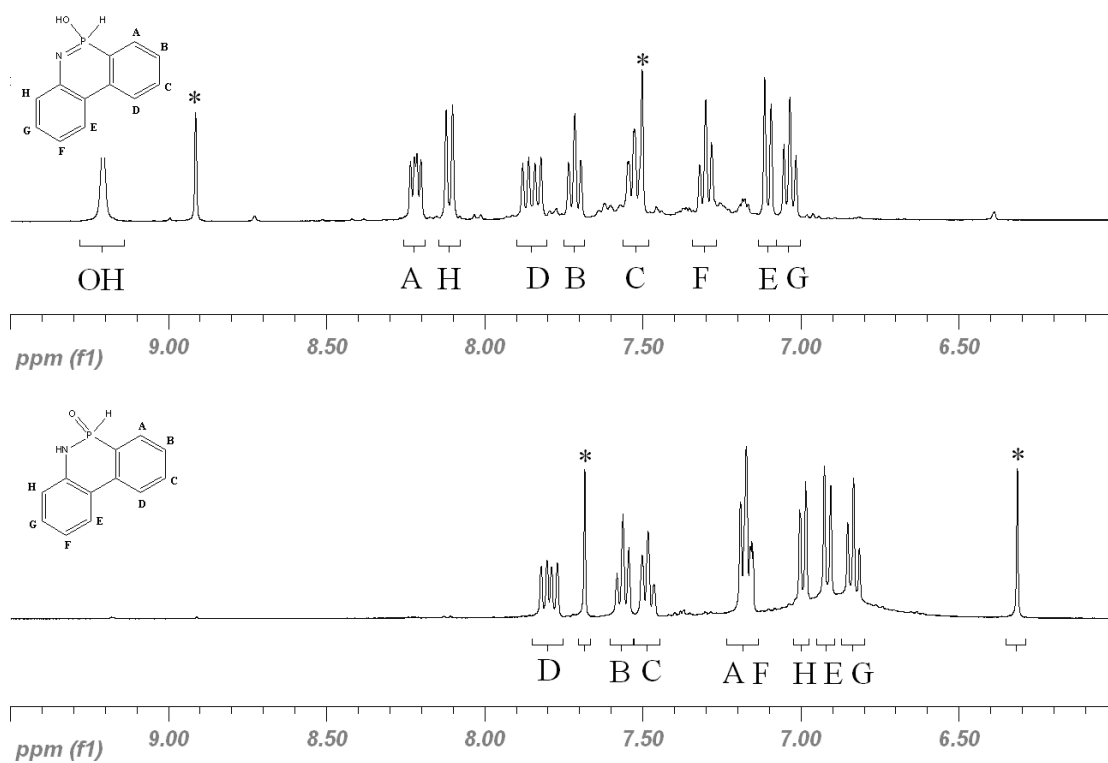


Figure 3-14: ^1H -NMR spectra of the two isolated tautomers of DAPO (16). The asterisks specify the signal corresponding to the P-H bond.

Thus, it can be concluded that the two phosphorus containing molecules isolated after hydrolysis of the DAP-Cl are tautomers (Figure 3-15). However, the factors favoring the formation of one tautomer over the other, such as heat or pH, are still under investigation. Unlike the tautomerism of 3-phosphorus acids, the prototropic transfer of phosphamidates has been reported on a few accounts.⁹³⁻⁹⁶ Moreover, to the best of the author's knowledge, its flame retardant activity has not been reported.

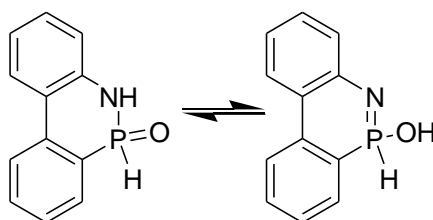


Figure 3-15: Equilibrium between the two tautomeric forms of DAPO.

3.4.1 Abramov reaction of 9,10-dihydro-9-azaphosphaphenanthrene-10-oxide

In order to test the reactivity of its P-H bond, DAPO was reacted with benzaldehyde in a solution of toluene under mild heating (Figure 3-16). ^{31}P NMR analysis of the crude solid isolated after removal of the toluene showed two peaks at $\delta = 24.5$ and

24.2 ppm in CDCl₃. The presence of two phosphorus-containing molecules was however not surprising as the nucleophilic attack on the carbonyl functionality yielded a new stereogenic centre. This was confirmed by the presence on a single ion peak in the mass spectroscopy at $m/z = 321$. Hence, the two organophosphorus compounds observed in solution are stereoisomers of the target molecule. The shift towards lower field was indicative of a shielding of the phosphorus atom in accordance with the replacement of P-H bond by a P-C bond. Moreover, two sets of doublet at 5.05 and 4.09 ppm in the ¹H-NMR spectra confirmed the presence of a benzylic carbon directly bound to a phosphorus ($^2J_{P-H} = 10.9$ and 8.9 Hz respectively). Hence, similarly to DOPO, under those reaction conditions, DAPO formed a new carbon-phosphorus bond *via* an Abramov reaction (Figure 3-16). This demonstrated that, the hydrogen of DAPO was labile and that the formed anion could act as a nucleophile.⁸⁸ The acidic proton could therefore potentially react with catalytic amount of base to activate the nucleophilic intermediate that can react with electrophilic groups such as epoxy group.

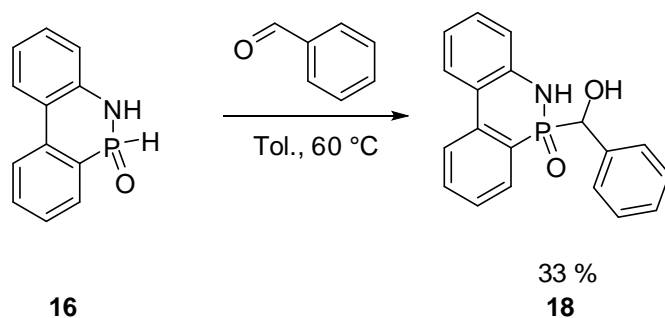


Figure 3-16: Reaction of DAPO with benzaldehyde in toluene.

When the same reaction was carried out in ethanol instead of toluene, a different product was formed (Figure 3-17). Similarly to the reaction carried out in toluene, ³¹P NMR analysis of the white powder, isolated after removal of the solvent, indicated the formation of an organophosphorus compound where the phosphorus atom was more shielded than DAPO ($\delta = 40.5$ ppm). ¹H-NMR analysis indicated the presence of aliphatic protons at $\delta = 0.85$ (3H), 3.88-3.74 (1H) and 3.49-3.33 (1H) ppm which suggests a nucleophilic attack of ethanol with the Abramov product (Figure 3-18).

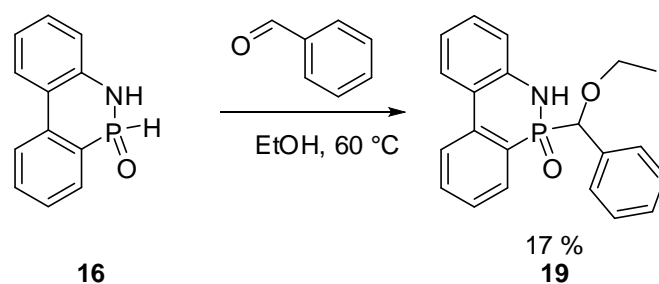


Figure 3-17: Reaction of DAPO with benzaldehyde in ethanol.

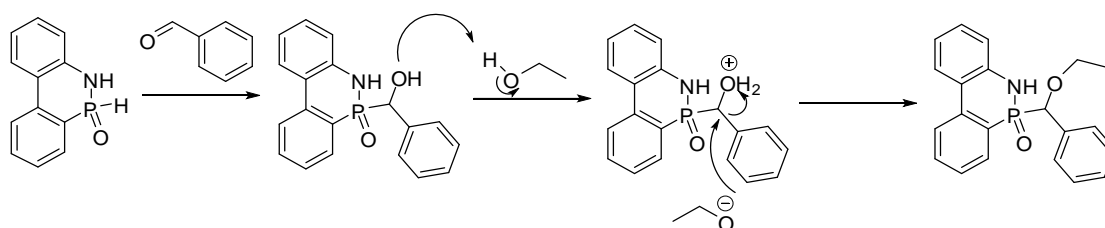


Figure 3-18: Suggested mechanism for the formation of compound 19.

3.4.2 Oxidation of 9,10-dihydro-9-azaphosphaphenanthrene-10- oxide

The successful Abramov reaction motivated the investigation of the other possible reaction of DAPO. Like most phosphinates, DOPO readily undergoes oxidation to form the corresponding phosphinic acid (DOPO-OH) (Figure 3-19). Similarly to DOPO, DOPO-OH was found to undergo nucleophilic addition and was successfully reacted with epoxy resins.⁵⁴ Chemical addition of DOPO-OH was found impart flame retardancy to DEN 438.^{54,81} Hence, the investigation of the oxidation of DAPO was initiated.

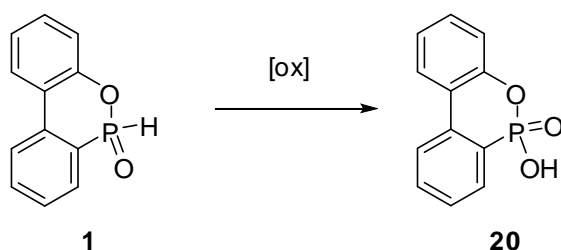


Figure 3-19: Oxidation of DOPO to form DOPO-OH.

First, DAPO was stirred in a solution of hydrogen peroxide in ethyl acetate.⁹⁷ Even though the disappearance of the doublet characteristic of the P-H bond in ¹H-NMR analysis indicated that DAPO had reacted, the ³¹P-NMR spectrum showed the

presence of several organophosphorus compounds in solution. Hence, this method was not the optimal route to access DAPO-OH since the use of peroxide yields water and consequently possible hydrolysis by-products. Wang and Shau synthesised phosphonamidic compounds by oxidation of a solution azaphosphine oxide in pyridine using KMnO_4 as oxidation agent.⁹⁸ Thus, in an attempt to obtain DAPO-OH, DAPO was heated with KMnO_4 in pyridine and water (Figure 3-20). ^{31}P -NMR analysis of the crude reaction mixture in D_2O showed the presence of an organophosphorus compound where the phosphorus atom is deshielded in comparison to the starting material ($\delta = 49.5$ ppm). However, the ^1H -NMR was inconclusive. Removal of the solvent *in vacuo*, followed by acidification using concentrated sulphuric acid, yielded a brown precipitate that was isolated by filtration. However, ^{31}P -NMR analysis of the brown powder failed to show any organophosphorus compound. Hence, KMnO_4 was ruled out as an oxidation agent for the formation of DAPO-OH.

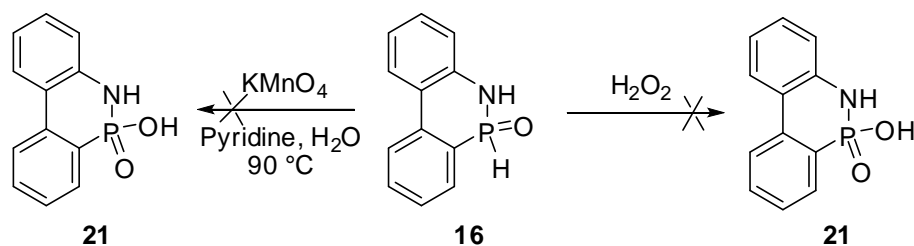


Figure 3-20: Synthesis of DAPO-OH (21) by oxidation of DAPO (16).

Quin *et al.* reported the successful synthesis of N-(1-Adamantyl) phenylphosphonamidic acid by hydrolysis of the N-(1-Adamantyl) phenylphosphonochloro amidate.⁹⁹ Hence, the synthesis of 9-hydro-10-chloro-10-azaphosphaphenanthrene oxide (DAPO-Cl) (22) was initiated (Figure 3-21). Reaction of 2-aminobiphenyl with phosphorus oxychloride in ether in the presence of triethylamine led to the precipitation of a white solid.¹⁰⁰ ^{31}P -NMR analysis of the dried white powder showed the presence of a single phosphorus compound (δ (CDCl_3) = 9.82 ppm) which suggested that the target DAPO-Cl was formed. However, the characteristic splitting pattern of phosphaphenanthrene derivatives was not observed in the ^1H -NMR spectrum. Nonetheless, mass spectroscopic analysis of the white powder confirmed the successful synthesis of DAPO-Cl as an ion peak at m/z 282, corresponding to the target compound with hydrochloric acid, was observed. Treatment of the chloro derivative with an aqueous solution of sodium hydroxide to form the sodium phosphonate salt was followed by acidification with hydrochloric acid which led to the precipitation of a white

solid. ^{31}P -NMR analysis of the filtered white powder indicated the presence of an organophosphorus compound (δ (CDCl_3) = 0.58 ppm) which could be associated with a phosphamidic functionality. However, the ^1H -NMR spectrum did not show the characteristic phosphaphenanthrene structure. This indicated that the azaphosphophenanthrene ring was unstable in solution. Quin *et al.* also discussed the thermal fragmentation of the P-N bond yielding an anhydride.⁹⁹ Hence, it can be concluded that the targeted 9-hydro-10-chloro-10-azaphosphophenanthrenic acid suffers from the same thermal instability.

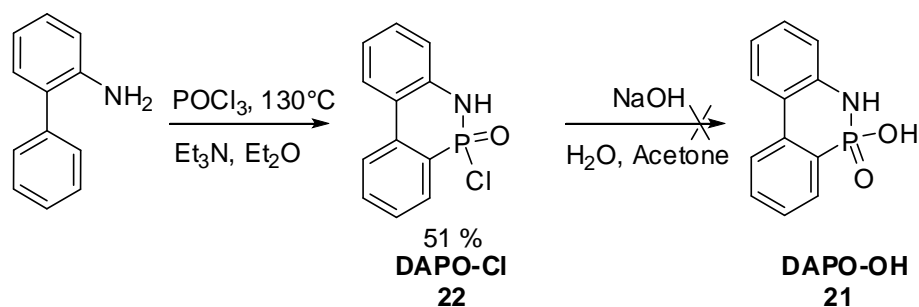


Figure 3-21: Synthesis of DAPO-OH from DAPO-Cl.

In order to test the resistance of the P-N bond to hydrolysis in alkali solution, DAPO was reacted in acetone with a solution of sodium hydroxide (Figure 3-22). ^{31}P -NMR analysis of the reaction mixture after removal of the solvent showed the presence of a single organophosphorus compound (δ = 15.9 ppm). In contradiction with the reported instability of the P-N bond, the ^1H -NMR showed the characteristic phosphaphenanthrene structure in the aromatic region which indicated that the phosphaphenanthrene structure remained intact.¹⁰¹⁻¹⁰³ In addition, the absence of the doublet at δ = 8.46 ppm confirmed that the P-H bond had reacted. Moreover, the mass spectroscopic analysis of the white solid showed an ion peak at m/z = 253, confirming the formation of the sodium phosphonate ion. Treatment of an aqueous solution of the sodium phosphonate ion with hydrochloric acid led the formation of a white precipitate. The ^{31}P -NMR spectrum of the white powder isolated by filtration indicated the presence of a single organophosphorus compound (δ = 6.77 ppm). Similarly to the hydrolysis product, the characteristic pattern of the phosphaphenanthrene compounds was observed in the ^1H -NMR spectrum. However, an additional broad singlet, associated with the acidic functionality, was observed at δ = 5.63 ppm. The formation of the targeted DAPO-OH was confirmed by mass spectroscopic analysis (m/z = 231).

Nonetheless, further investigation of the reactivity of DAPO-OH were not carried out as its solubility in organic solvent was very poor.

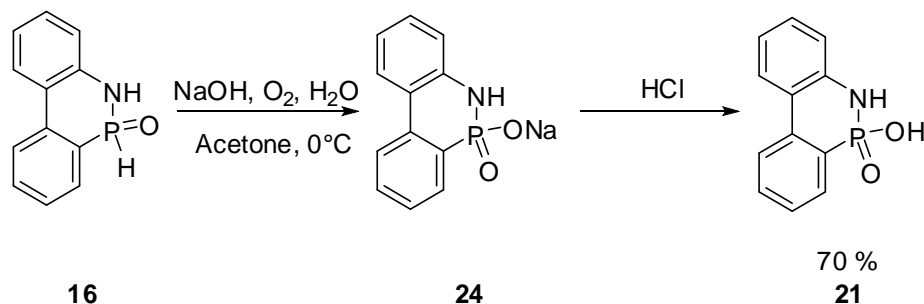


Figure 3-22: Oxidation of DAPO with sodium hydroxide.

3.4.3 Synthesis of 9,10-dihydro-9-azaphosphaphenanthrene-10- thionic acid

In order to study the possible synergism between phosphorus, nitrogen and sulphur of organophosphorus compounds in the flame retardancy of epoxy resin, the investigation of the synthesis of sulphur derivatives of DAPO was initiated.

The first attempt to obtain a azaphosphaphenanthrene sulphide derivative was achieved by heating a solution of DAPO in toluene in the presence of sulphur (Figure 3-23).⁸⁵ Concentration *in vacuo* of the filtered solution yielded a pale orange powder. The ¹H-NMR spectrum of the isolated powder showed the presence of 8 aromatic protons that were associated with the phosphaphenanthrene structure and a broad peak ($\delta = 5.44$ ppm, 2H) that was attributed to the acidic and amine functionality. In addition, the ³¹P-NMR showed the presence of one major peak ($\delta = 55.0$ ppm), which coincided with the parent 10-oxaphosphaphenanthrenethionic acid derivative (DOPS-OH). The formation of the targeted DAPS-OH (25), was also confirmed by mass spectroscopy ($m/z = 247$).

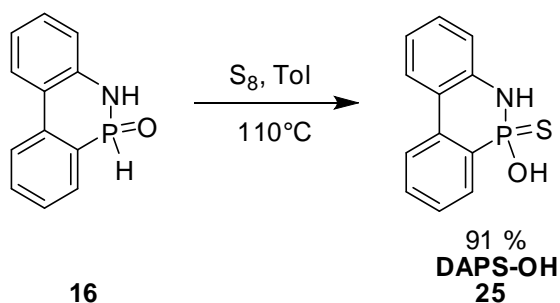


Figure 3-23: Synthesis of DAPS-OH from DAPO.

3.4.4 9,10-dihydro-9-azaphosphaphenanthrene-10- sulfide

The successful synthesis of DAPS-OH motivated the investigation of the synthesis of DAPS (**26**). Similarly to DOPS (3.2.1), our first attempt to obtain the target molecule was achieved by reacting a solution of DAP-Cl in toluene with H₂S and trapping the formed acid with triethylamine at room temperature (Figure 3-24). After removal of the triethylammonium salt by filtration, the reaction mixture was concentrated *in vacuo* to yield a light brown crystalline solid. ¹H-NMR analysis of the obtained solid revealed the presence of a rigid aromatic structure containing 8 protons which was associated with the phosphaphenanthrene ring. In addition, the presence of a doublet at 8.59 ppm (*J*_{P-H}=506 Hz) confirmed the presence of a P-H bond.

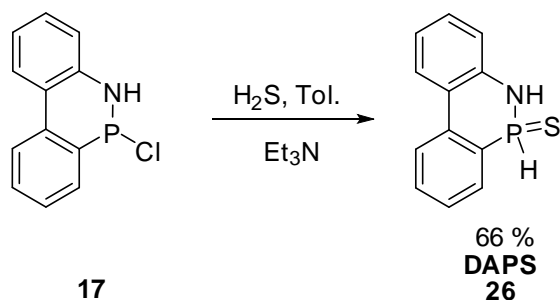


Figure 3-24: Synthesis of DAPS (26) from DAP-Cl (17).

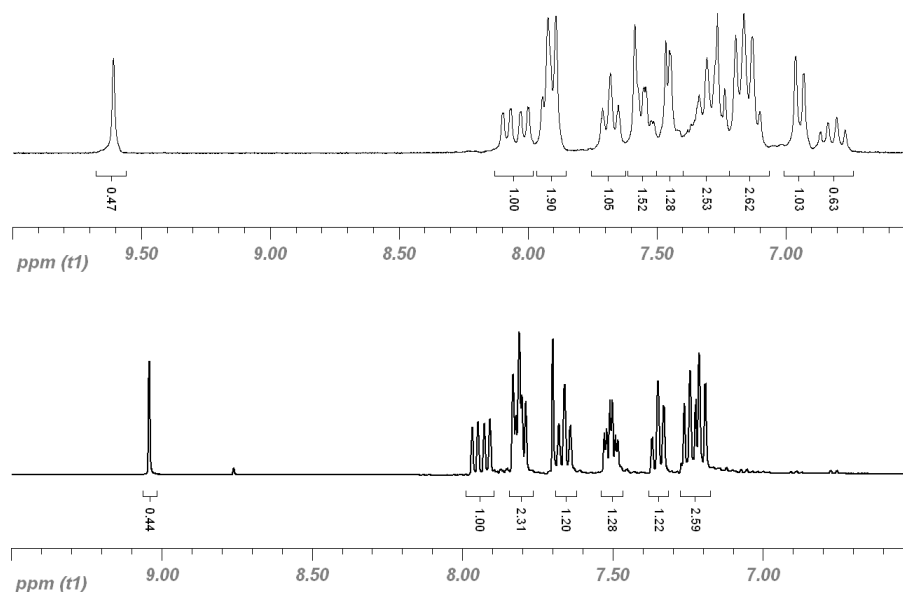


Figure 3-25: $^1\text{H-NMR}$ spectra of DAPS (top) and DOPS (bottom) measured in CDCl_3 .

3.5 Summary

The synthesis of a series of heterocyclic derivatives of DOPO with different chemical environment around the phosphorus was presented.

Firstly, the synthesis of the new 6*H*-dibenzo[*c,e*][1,2]oxaphosphinine 6-sulfide (**4**) (DOPS) was presented. Compound (**4**) can be obtained using different thionation agents and undergoes nucleophilic additions such as the Pudovik reaction as well as the Atherton-Todd reaction. The ease of synthesis of molecule (**4**) combined with its broad range of reactivity makes it a promising compound for a wide spectrum of molecules and applications. Secondly, the thionation procedure used for the synthesis of DOPS was applied to obtain DDPS. Similarly to DOPO, and DDPO, the P-H bond could be activated to generate the phosphonate nucleophilic species that could react with unsaturated functionality. The successful Abramov reaction of DDPS indicated that it could react with oxirane rings in a similarly to DDPO. Then, the synthesis of DAPO was optimised and the reactivity of P-H bond was compared to the other phosphine oxides. DAPO successfully underwent an Abramov reaction with benzaldehyde, which confirmed its potential use as a reactive flame retardant for epoxy resins. Lastly, two new sulphur derivatives of DAPO, DAPS and DAPS-OH were synthesised using the synthesis route developed for the DOPO and DDPO derivatives.

All the compounds shown in Figure 3-26, were synthesised using 1 or 2 steps synthesis from commercially available starting materials. Moreover, all heterocyclic

organophosphorus compounds presented were obtained in high yield and with high level of purity. Hence, such compounds are potentially commercialisable. The variety of environment around the phosphorus atom also makes such compounds interesting for studies where the binding properties of phosphorus are investigated.

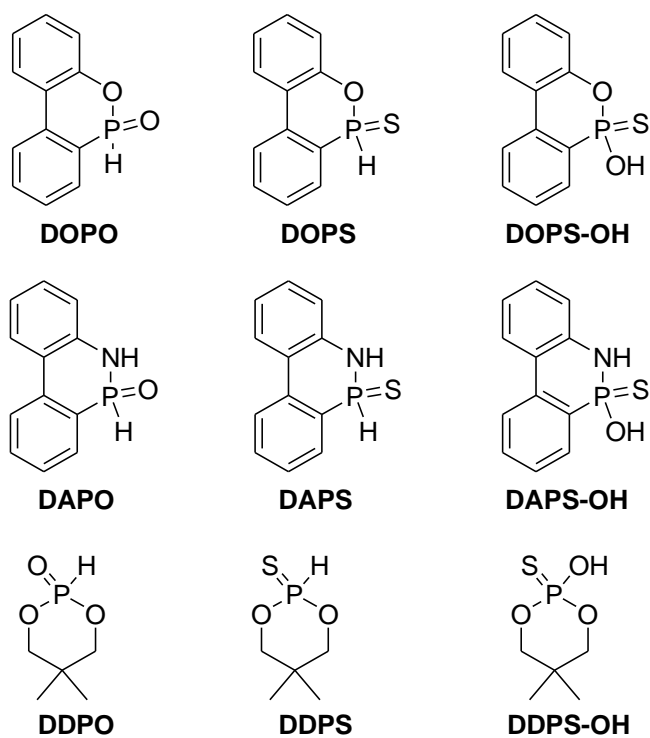


Figure 3-26: Summary of the heterocyclic organophosphorus compounds.

The evaluation of the reactivity of the P-H bond of the newly synthesised phosphine oxides and phosphine sulphides suggested that phosphonate nucleophilic species could be generated in the presence of base. Hence, the newly synthesised organophosphorus compounds could be chemically reacted with epoxy functionalities and their efficiency as flame retardant evaluated and compared to the already commercialised phosphine oxides. Such study will be presented in chapter 4.

CHAPTER 4: INVESTIGATION OF THERMAL STABILITY OF EPOXY PHENOL NOVOLAC RESIN MODIFIED WITH ORGANOPHOSPHORUS FLAME RETARDANTS

4.1 Formulation and curing

Unlike their non-reactive counter parts, reactive flame retardants require to be grafted onto the polymer matrix before curing. This solves the migration problem encountered with non-reactive flame retardants as the polymer itself becomes inherently flame retardant through the chemical bond formed between the organophosphorus moiety and the epoxy group. Figure 4.1 shows a typical preformulation process using a phosphorus compound as flame retardant, DEN 438 as novolac epoxy resin and triethanol amine as grafting catalyst.^{54,88}

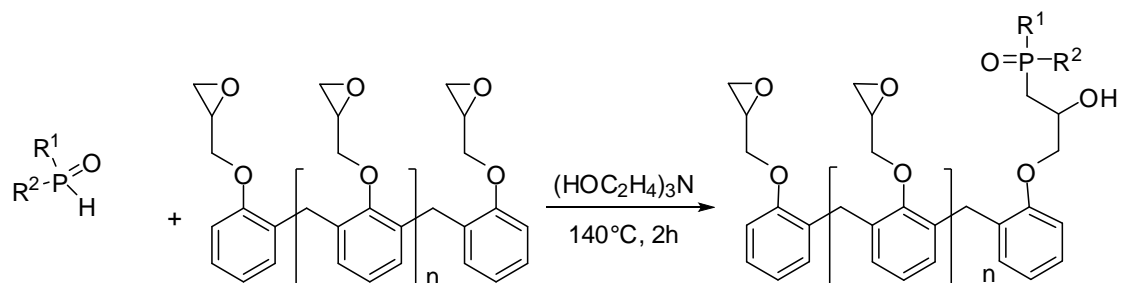


Figure 4-1: Chemical addition of Phosphorus molecules to DEN 438.

Once DEN 438 was grafted with the phosphorus flame retardant, it was cured according to literature using DICY as a hardener and Fenuron as an accelerator in a ratio 100 to 6 to 2 (Figure 4-2).⁵³

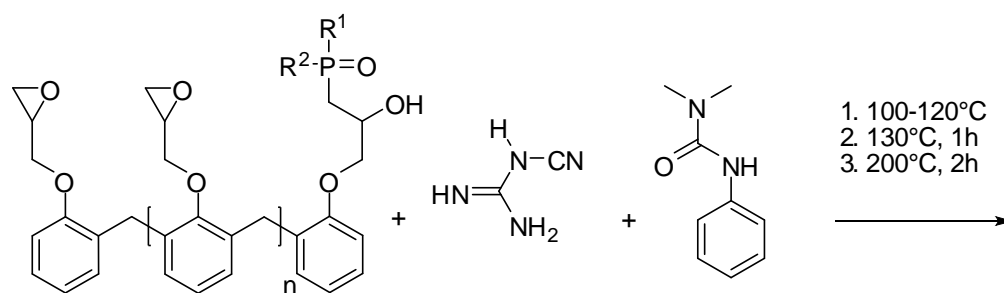


Figure 4-2: Curing condition of chemically modified DEN438 with DICY (middle) and Fenuron (right).

The formulations for the newly synthesised phosphorus heterocyclic compounds presented in Chapter 3 are summarised in Table 4-1, Table 4-2 and Table 4-3.

Table 4-1: Overview of the composition of DEN 438 resin chemically modified with DOPO, DAPO and DOPS.

DEN 438 (g)	DOPO (g)	DAPO (g)	DOPS (g)	P %	FR wt %
55.56				0.00	0.0
53.62	2.02			0.50	3.5
51.68	4.18			1.00	7.0
50.13	5.86			1.40	9.8
49.36	6.69			1.60	11.2
51.69		4.17		1.00	6.7
50.92		5.00		1.20	8.3
50.15		5.84		1.40	9.7
49.38		6.67		1.60	11.1
53.47			2.25	0.50	3.8
52.43			3.37	0.75	5.6
51.39			4.5	1.00	7.5
50.56			5.4	1.20	9.0
49.73			6.3	1.40	10.5
48.89			7.2	1.60	12.0
48.06			8.1	1.80	13.5

Table 4-2: Overview of the composition of DEN 438 resin chemically modified with DOPO-OH, DAPS-OH and DOPS-OH.

DEN 438 (g)	DOPO-OH(g)	DAPS-OH (g)	DOPS-OH (g)	P %	FR (wt %)
51.39	4.50			1.00	7.50
49.73	6.30			1.40	10.49
53.70		2.01		0.50	3.35
49.60		6.43		1.60	10.72
51.69			4.17	1.00	6.95
50.15			5.84	1.40	9.73

Table 4-3: Overview of the composition of DEN 438 resin chemically modified with DDPO, DDPS and DDPS-OH.

DEN 438 (g)	DDPO (g)	DDPS (g)	DDPS-OH	P%	FR (Wt %)
55.56				0.00	0.00
52.86	2.91			1.00	4.85
47.46	8.74			3.00	14.56
52.68		3.11		1.00	5.18
46.92		9.33		3.00	15.54
53.98			1.70	0.50	2.84
49.24			6.82	2.00	11.35

4.2 Influence of the fusion process on glass transition temperature (T_g) of the cured epoxy phenol novolac resin

As mentioned in chapter 1, in order to reduce the possible leaching of flame retardants out of the polymer matrix, the reactive approach has been adopted. However, the fusion process is often accompanied by a reduction of the functionality.⁴ Such is detrimental for the processability of the resin. This section will discuss the impact of the heterocyclic organophosphorus compounds discussed in chapter 3 on the glass transition temperature of DEN 438.

4.2.1 Influence of phosphaphenanthrene derivatives

Table 4-4 and Table 4-5 show the variation of the glass transition temperature of the cured novolac epoxy resin chemically modified with different phosphorus loading of DOPO, DAPO and DOPS as well as the oxidised derivatives DOPO-OH, DAPS-OH and DOPS-OH. As seen in Figure 4-3, the glass transition temperature of the cured modified resin decreases with increasing phosphorus loading. This can be rationalised by the decreased epoxy functionality in the uncured resin because of the fusion process. The reduced epoxy functionality causes a reduced cross-linking density in the cured polymer that is reflected in the decreased glass transition temperature.¹⁰⁴ The azaphosphaphenanthrene derivatives (DAPO and DAPS-OH) have less impact on the Tg than the oxaphosphaphenanthrene ones (DOPO and DOPS-OH). Unlike the DOPO derivatives, the presence of the amine functionality balances out the effect of functionalising the epoxy resin during the fusion process. Hence, similarly to the DOPO-HQ, which is a multifunctional flame retardant, the chemical addition of DAPO does not result in a drastic loss of functionality.⁶⁶ Figure 4-3 shows that the oxide compounds have a lesser influence on the glass transition temperature than their sulphide derivatives. When compared to the oxygen atom, the bulky sulphur atom has a larger plasticising effect, hence, a larger influence on the glass transition temperature can be observed. Nonetheless, this plasticising effect can be balanced out when the oxidised derivatives are used as flame retardants instead of the phosphine derivatives. As seen in Figure 4-3, DOPS-OH has less impact on the Tg than DOPS and the same trend is observed for the oxide derivatives. The additional oxygen in the polymer structure can contribute to additional hydrogen bonding which is reflected by an increase in glass temperature.

Table 4-4: Tg of DEN438 modified with DOPO, DAPO or DOPS and cured with DICY / Fenuron (neat DEN 438 182 °C).

	P	FR	Tg		P	FR	Tg		P	FR	Tg
	%	%	(°C)		%	(%)	(°C)		%	(%)	(°C)
DOPO	0.50	3.5	172	DAPO	1.00	6.7	170	DOPS	0.50	3.8	175
DOPO	1.00	7.0	162	DAPO	1.20	8.3	169	DOPS	1.20	9.0	159
DOPO	1.40	9.8	157	DAPO	1.40	9.7	171	DOPS	1.40	10.5	144
DOPO	1.60	11.2	151	DAPO	1.60	11.1	171	DOPS	1.60	12.0	142

Table 4-5: Tg of DEN438 modified with DOPO-OH, DAPS-OH or DOPS-OH and cured with DICY / Fenuron (neat DEN 438 182 °C).

	P	FR	Tg		P	FR	Tg		P	FR	Tg
	%	%	(°C)		%	%	(°C)		%	(%)	(°C)
DOPO-OH	0.50	3.5	172	DAPS-OH	0.50	4.0	176	DOPS-OH	0.50	3.8	175
DOPO-OH	1.00	7.0	162	DAPS-OH	1.20	8.3	169	DOPS-OH	1.20	9.0	159

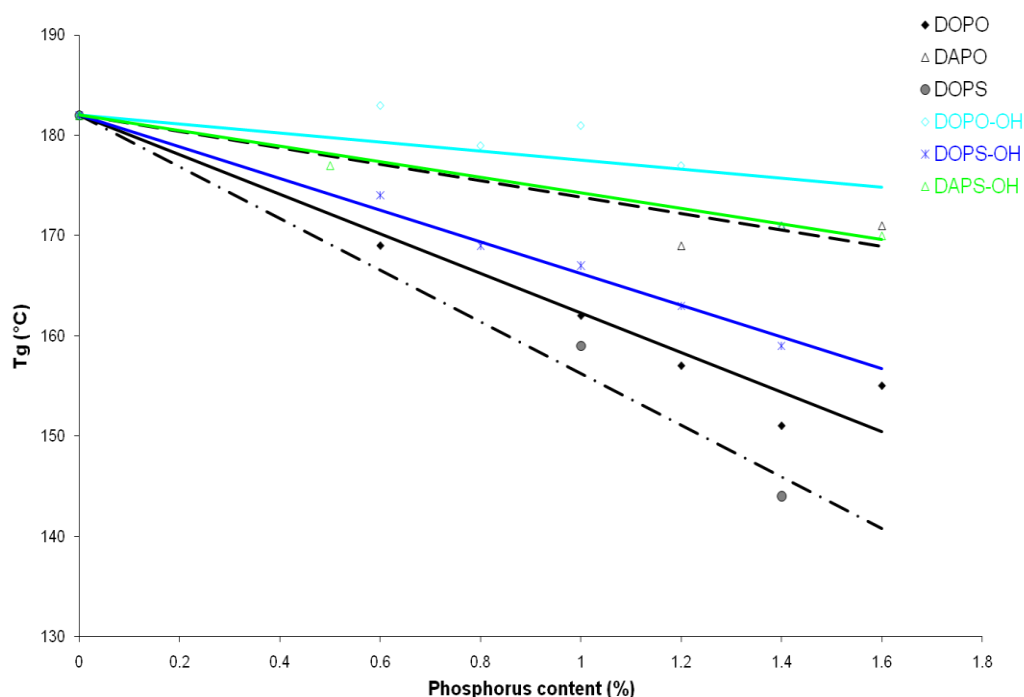


Figure 4-3: Influence of phosphaphenanthrene derivatives on the glass transition temperature of DEN 438 cured with DICY and Fenuron.

4.2.2 Influence of dimethyldioxophosphorinane derivatives

Table 4-6 summarises the glass transition temperature of DEN 438 chemically modified with DDPO, DDPS and DDPS-OH cured with DICY and Fenuron following the procedure described in section 4.1. Similarly to the trend observed for the phosphaphenanthrene derivatives, the chemical addition to the epoxy resin resulted in a loss of functionality. This was reflected in a decrease in the glass transition temperature with increase phosphorus loading (Figure 4-4). In addition, the plasticising effect of sulphur was also observed.

Table 4-6: Tg of DEN438® modified with DDPO, DDPS, DDPS-OH and cured with DICY / Fenuron(neat DEN 438 182 °C).

	P %	FR wt %	Tg (°C)		P %	FR (%)	Tg (°C)		P %	FR (%)	Tg (°C)
DDPO	1.00	4.85	168	DDPS	1.00	5.18	164	DDPS-OH	0.5	2.68	182
DDPO	3.00	14.56	148	DDPS	3.00	15.54	132	DDPS-OH	2.0	10.73	182

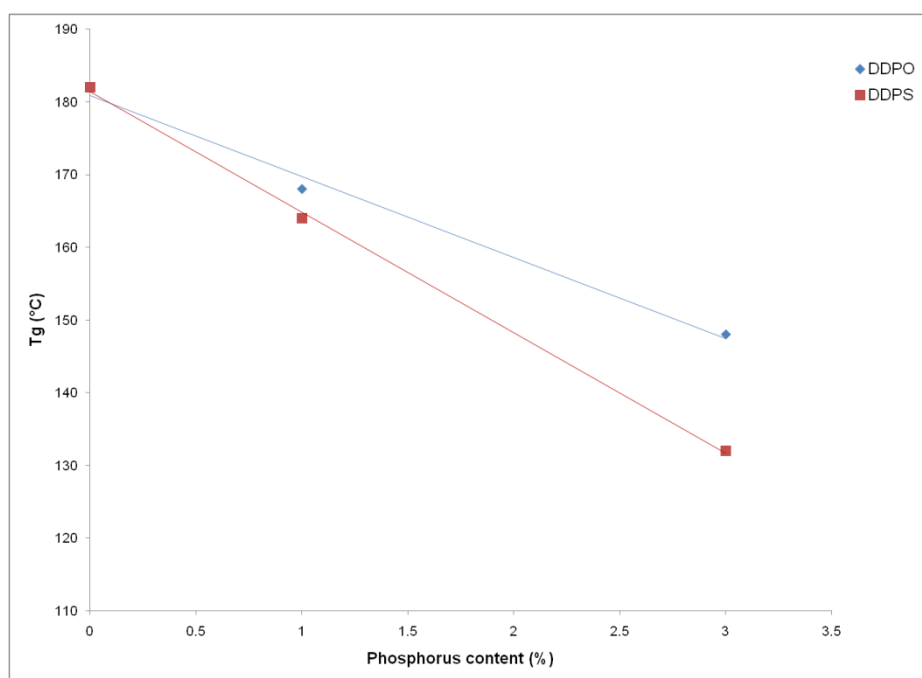


Figure 4-4: Influence of DDP derivatives on the glass transition temperature of DEN 438 cured with DICY fenuron.

4.3 Influence of phosphacyclic flame retardants on decomposition temperature (Td)

The thermal decomposition of the virgin DEN 438 cured with DICY and Fenuron is characterised by an onset decomposition temperature (mass loss of 5%) of 365 °C, followed by a single step with a maximum loss a 410 °C and subsequent decomposition leaving 29.4 wt% of thermally stable residue at 800°C (Figure 4-5). When DOPO (1.6 %P) was added, the onset decomposition was lowered from 365 °C to 355 °C and the residual char increased slightly to 31 %. The decomposition behaviour was more influenced when DOPS was used as reactive-flame retardant. The onset decomposition was reduced to 325 °C and the residual char was increased to 32 %. The reduced thermal stability is coherent with the plasticising effect of sulphur observed in section 4.2. Evnethough a loss 10 °C in the thermal decomposition temperature (Td) is observed, such decrease is not detrimental as the flame retardant resins used FR-4

composites need to be stable above 280 °C. Similarly to DOPS, the addition of DAPO induced a decrease of the onset decomposition temperature to 323 °C (Figure 4-5). However, a second decomposition step was observed at 470 °C and the thermally stable residue at 800 °C was increased to 35 % of the original weight. The slight reduction of weight loss rate observed at 470 °C can be attributed to the formation of carbonaceous char layer that protects the polymer from the heat source. However, as the temperature increases, this char layer decomposed which results in the second decomposition step observed. Nitrogen containing flame retardants are known to promote such char formation.¹⁰⁵ The decrease of the decomposition temperature (Td) with addition of flame-retardant is in agreement with the trends observed for Tg using DSC. The significant change in onset decomposition temperature between DOPS and DOPO suggests that the presence of sulphur lowers the thermal stability of the cured resin. Similarly to Tg, the depression in Td can be justified by the lower cross-linking density in the cured resin resulting from the replacement of epoxy group by bulky flame-retardant molecules.

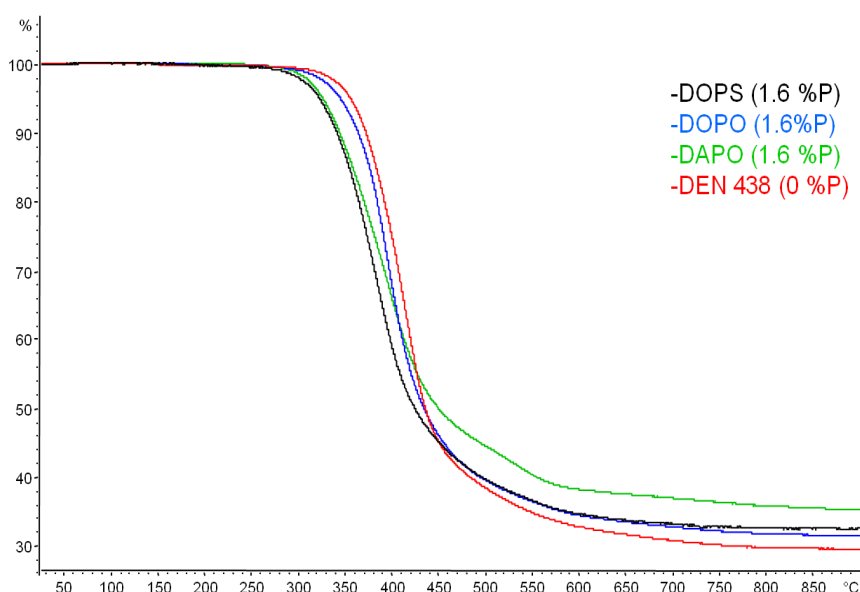


Figure 4-5: TGA traces of DEN 438 cured with DICY and Fenuron containing phosphaphenanthrene derivatives DOPS, DOPO and DAPO.

4.4 UL-94 measurements of cured epoxy phenol novolac resin

Table 4-7 summarises the UL-94 classifications obtained for the DEN 438 resin chemically modified with DOPO, DAPO and DDPO cured with DICY and Fenuron according to the procedure described in section 4.1. The phosphorus loading required to

impart UL-94 V0 rating is directly related to the flame retardant efficiency of the organophosphorus compound added. DOPO, DDPO and DAPO all render the cured novolac resin resistant to fire (V0 rating) with phosphorus loading above 1.4 %P. When DOPO and DAPO are used as flame retardants, a similar phosphorus loading was required to impart flame retardancy. This indicates that the addition of an amine functionality did not have a significant impact on the mode of action phosphaphenanthrene. Due to practical restrictions, DAPO could not be tested over such a large range of concentration as DOPO because the cured resin was very brittle and the plates often fractured during the curing stages. The increase in brittleness of the cured resins reflects the higher cross-linking density obtained and is in accordance with the reactivity of the amine functionality. However, when DDPO was used as flame retardant, 3.0 % phosphorus loading is required to meet the V0 rating. This indicates that DDPO is a less efficient flame retardant for the DEN 438/DICY/Fenuron system than the aromatic compounds DOPO and DAPO. This can be justified by the required gas phase mechanism for the DEN 438/DICY/Fenuron used. Indeed, DDPO was reported to be an efficient flame retardant for DGEBA/Dimethyldicykane system that require a condensed phase mechanism.⁸¹

Table 4-7: UL-94 V rating of the oxide derivatives: DOPO, DAPO and DDPO.

	X	Y	Z	%P	Wt %	Tg (°C)	UL 94	Char (%)
DEN 438	-	-	-	0	0	182	n.c.	29.04
DOPO	O	O	H	1.60	11.20	155	V0	31.60
DAPO	NH	O	H	1.60	11.20	171	V0	35.30
DDPO	O	O	H	3.00	14.60	148	V0	34.40

Table 4-8 summarises the minimum concentration required to impart UL-94 V0 rating when DOPS, DAPS and DDPS were used as flame retardants. Surprisingly DOPS imparted V0 rating to sample with lower phosphorus loading (1.0 %P) and V1 rating was achieved with only 0.5 %P. This suggests that the presence of sulphur enhances the flame retardant mechanism of oxa-phosphaphenanthrene compounds. The investigation of the mechanism of action of sulphur is presented in section 4.5. Similarly to DDPO, higher loading (3 %P) were required when DDPS was chemically added to impart flame retardancy to DEN438 (Table 4-6) which is consistent with the predominant condensed phase activity of dioxophosphorinane derivatives.

Table 4-8: UL-94 V rating of the sulfide derivatives: DOPS and DDPS.

	X	Y	Z	%P	Wt %	Tg (°C)	UL 94	Char (%)
DEN 438	-	-	-	0	0	182	n.c.	29.04
DOPS	O	S	H	1.00	7.30	159	V0	30.90
DDPS	O	S	H	3.00	15.50	138	V0	35.00

Table 4-7 summarises the phosphorus loading required to impart V0 rating when thionic acid flame retardants DOPS-OH, DAPS-OH and DDPS-OH are used in epoxy phenol novolac resin. In the case of the DOPS-OH, phosphorus loadings similar to DOPO are required to impart UL-94 V0 rating. On the other hand, 1.6 %P of DAPS-OH failed to impart flame retardancy to the epoxy phenol novolac resin. Eventhough, the extinguishment after the first ignition occurs within one second of the flame removal, the lit materials required between 5 and 15 s to self-extinguish after the second flame application (10 s required for UL-94 V0 rating). Unfortunately, similarly to DAPO, higher phosphorus loading could not be tested as the modified resins with phosphorus loading higher than 1.6 %P gelled during the fusion process. Hence, formulation could not be achieved. As predicted from the results reported earlier, the material with 2.0 P% of DDPS-OH was not flame retardant. However, similarly to DAPS-OH higher phosphorus loadings could not be tested has the preformulation could not be processed at 80 °C.

Table 4-9: UL-94 –V ratings for the thionic acid DOPS-OH, DAPS-OH and DDPS-OH.

	X	Y	Z	%P	Wt %	Tg (°C)	UL 94	Char (%)
DEN 438	-	-	-	0	0	182	n.c.	29.04
DOPS-OH	O	S	OH	1.40	11.20	159	V0	33.50
DAPS-OH	NH	O	OH	1.60	12.80	170	V1	35.60
DDPS-OH	O	S	H	2.00	11.36	181	n.c	33.40

4.5 Oxygen index measurements

As mentioned in chapter 2, LOI is another method used to assess the flame retardancy of polymeric materials.⁴ Even though in most cases the sole limiting index concentration is quoted as a measure of flammability of a material, the oxygen index test

(OIT) allows a more thorough investigation of the mechanism of action of a flame retardant additive. Indeed, the substitution of oxygen by nitrous oxide can help evaluate if the added flame retardant acts as a flame poison in the gas phase. As seen in Figure 4-6 and Figure 4-7, the LOI was measured for samples of DEN 438 cured with DICY and Fenuron using DOPO, DOPS, DDPO and DDPS as reactive flame retardant. The flammability of the cured DEN 438 was evaluated in an O₂-N₂ atmosphere to determine the LOI and in an N₂O-N₂ atmosphere to determine the nitrous oxide index (LNI).

4.5.1 Oxa-phosphaphenanthrene derivatives

A summary of the oxygen indexes for the epoxy phenol novolac resin materials modified with DOPO can be seen in Table 4-10.

Table 4-10: Summary of the Oxygen Index test for oxa-phosphaphenanthrene derivatives DOPO and DOPS in DEN 438 resin cured with DICY and Fenuron.

FR	% P	UL 94	LOI (%)	LNI (%)	IOI (%)	BOI (%)
None	0	n.c.	26.7	47.2	24.0	23.0
DOPO	1.6	V0	38.1	57.4	31.0	31.0
DOPO	0.5	n.c.	31.1	52.8	24.0	30.5
DOPS	1.6	V0	36.6	58.3	36.0	31.0
DOPS	0.5	V1	30.7	53.7	27.0	37.5

The LOI value for the cured virgin resin was 26.7 while its LNI value was 47.2. The higher value of LNI with respect to LOI value can be explained by the lower effectiveness of N₂O as an oxidant compared to O₂. For DOPO and DOPS, the addition of flame retardant (0.5 %P) resulted in an increase of LOI, 31.1 and 30.7 respectively, in comparison to the neat resin. The LOI value increased with increasing flame retardant loading (1.6 %P) to 38.7 and 36.6 for DOPO and DOPS respectively. This is consistent with the UL 94 results. Indeed with low loading (0.5 %P), the cured resin is classified V1 whereas with higher loading (1.6 %P), the cured DEN438 is classified as V0 corresponding to a non-flammable polymer material. Thus, with higher flame-retardant loading (1.6 %P), there is higher oxygen demand to sustain the combustion cycle. A similar trend is observed when O₂ was replaced by N₂O. The LNI value increased from 52.8 to 57.4 for DOPO and from 53.7 to 58.3 for DOPS with increasing phosphorus content.

The efficiency of a flame retardant acting as flame poison in the gas phase in an oxygen atmosphere should be diminished when acting in a nitrous oxide atmosphere. As seen in Figure 4-6, the OI trend with increasing phosphorus content is similar to that of LNI for DOPO and DOPS. When the respective LOI values are plotted against the LNI at equal loading, the slope obtained for DOPO and DOPS are 1.6 and 1.3 respectively. This indicates that the effectiveness of the flame retardants is slightly lower in nitrous oxide than in oxygen. Therefore, the larger oxidant content required to sustain burning when oxygen is substituted by nitrous oxide indicates that a gas-phase mechanism could impart the flame retardancy to DEN 438 modified with DOPO and DOPS.

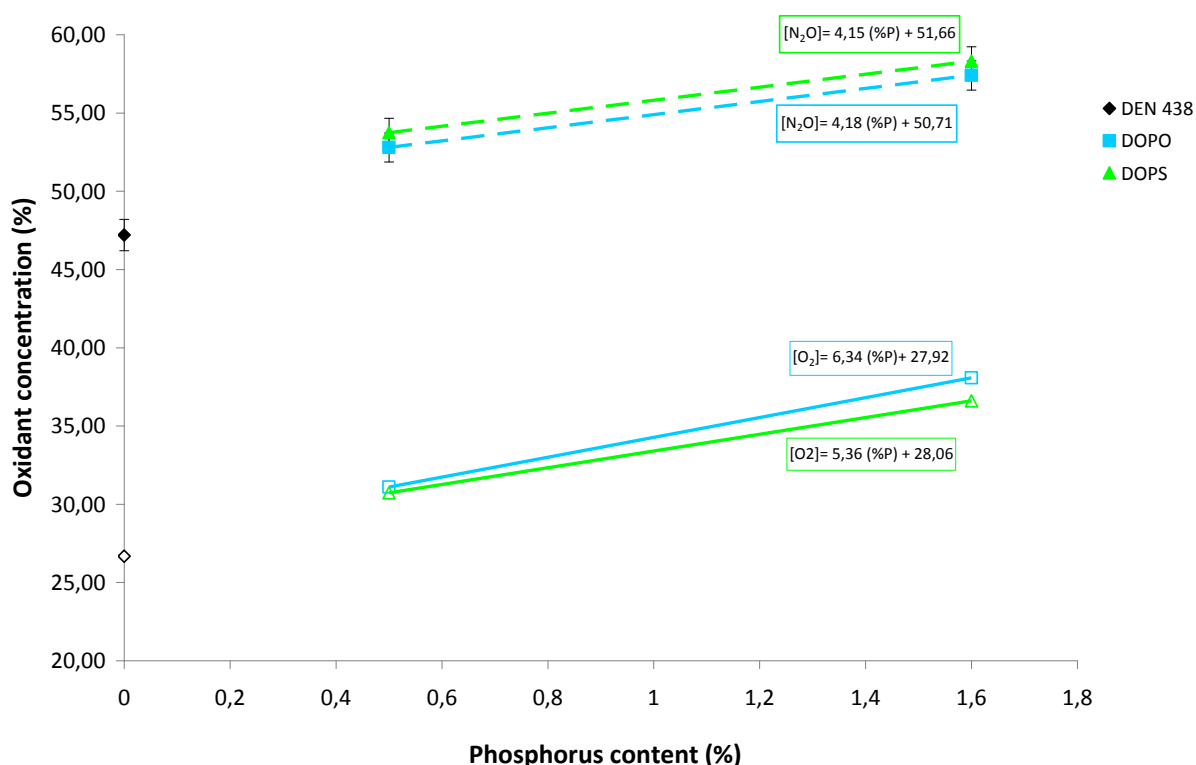


Figure 4-6: Plot of OI and NI vs. phosphorus content for DOPO and DOPS modified DEN438 measured in oxygen atmosphere (solid lines) and nitrous oxide atmosphere (dashed lines).

4.5.2 Dioxophosphorinane derivatives

Similarly to the trends observed with the addition of DOPO and DOPS, the oxidant content required to sustain burning generally increased with increasing phosphorus content. However, the difference in OI between the virgin resin and the flame retardant specimens was much lower. Table 4-11 summarises the oxygen indexes

measured for the cured samples containing the DEN 438 modified resin with DDPO and DDPS.

Table 4-11: Summary of the Oxygen Index test for dimethyldioxophosphorinane derivatives DDPO and DDPS in DEN 438 resin cured with DICY and Fenuron.

FR	% P	UL 94	LOI (%)	LNI (%)	IOI (%)	BOI (%)
DEN 438	0.0	n.c.	26.7	47.2	24.0	23.0
DDPO	1.0	n.c.	27.5	49.1	25.0	26.0
DDPO	3.0	V0	27.2	48.1	25.0	23.0
DDPS	1.0	n.c.	23.8	47.2	23.0	20.0
DDPS	3.0	V0	26.7	49.1	24.5	21.5

When oxygen was used as oxidant, the LOI value for the non-flammable specimens (V0 rating in the UL 94 test) for the samples with DEN 348 resin modified with DDPO and DDPS were 26.7 and 27.2 respectively compared to 27.6 for the virgin resin,. Figure 4-7shows the LOI and LNI value of DEN 438 modified with the DDPO and DDPS. When oxygen was substituted by nitrous oxide, the LNI values were 48.1 for DDPO and 49.1 for DDPS, compared to 47.2 for the unmodified resin. The absence of significant oxidant dependence with increasing phosphorus content indicates that the flame retardant efficiency is not dependent on the concentration of oxygen for either DDPO or DDPS. This suggests that neither of the aliphatic reactive additives acts as a flame poison when covalently bound to DEN 438, even when present in high loading (3.0 %P). A slight decrease in OI was observed with increasing loading of DDPO such trend was previously observed with a halogen-bismuth flame retardant in polypropylene acting in the condensed phase.¹⁰⁶

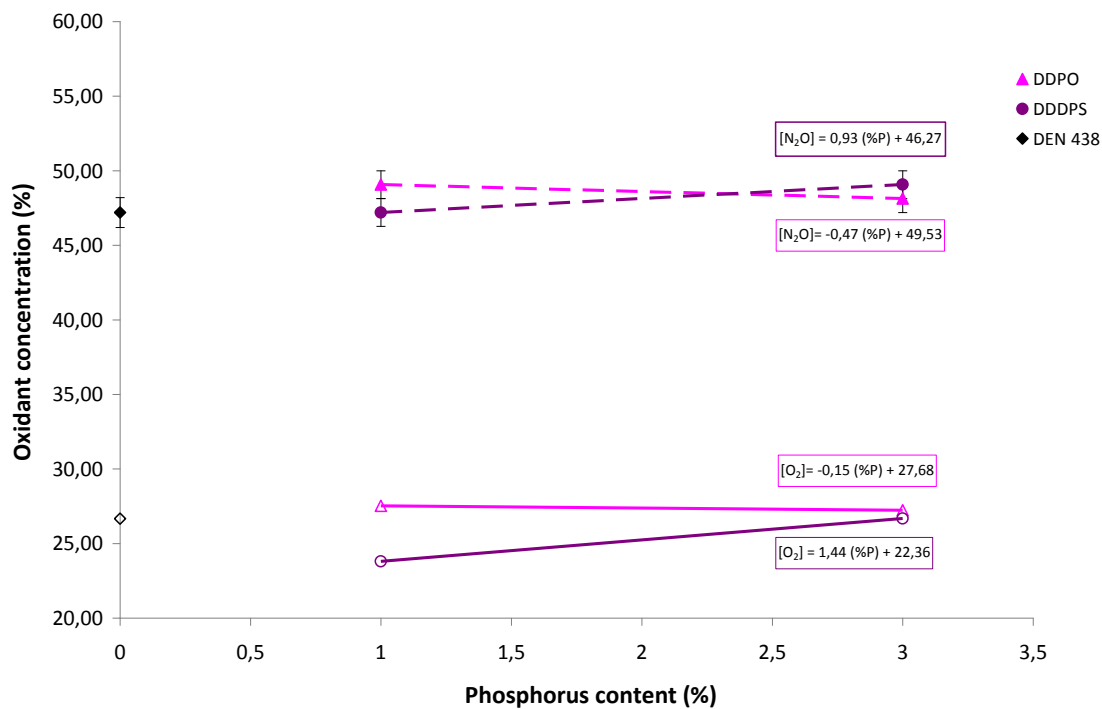


Figure 4-7: Plot of OI vs. phosphorus content for DDPO and DDPS-modified DEN 438 measured in oxygen atmosphere (solid line) and nitrous oxide atmosphere (dashed line).

When the increase of LOI is plotted against the increase of LNI for equivalent phosphorus content, the straight line obtained has a negligible slope. The lack of influence of the oxidant source indicates that the contribution of the gas phase mechanism to the flame retardant action of DDPO is negligible. Interestingly, when DDPS is used at lower loading (1.0 %P), the oxygen index is lower than that of the virgin resin. This reveals that, unless the required concentration of flame retardant to render the polymer non-flammable (V_0 in UL94) is reached, addition of DDPS increases the flammability of the novolac resin. When the LOI is plotted against the LNI for equivalent concentrations of DDPS, the obtained straight line has a slope of 1.5 similar to DOPO and DOPS suggesting that it may also be partially active in the gas-phase. Hence, when DDPS is used as a reactive flame retardant in DEN 438, a competition between the gas-phase and the condensed phase mechanism might be taking place. It is possible that, when the resin is under thermal stress, the presence of DPPS at low concentration enhances the production of flammable volatile species which would in turn contribute to maintain the combustion cycle. However, with higher loading, the char formation process could dominate. This thermally stable char layer would prevent the volatile particle from reaching the gas phase, which in turn would result in extinguishment of the flame. Such competition of mechanisms needs to be investigated in further details.

Nonetheless, according to Fenimore and Jones, the efficiency of pure gas-phase flame retardants should not depend on the polymer matrix since the reactions happening in the gas-phase occur above the burning material and are therefore thought to be independent from the condensed-phase pyrolysis.¹⁰⁷ Hence, a change of polymer matrix should not have any significant repercussion on the efficiency of a gas-phase active flame retardant such as DOPO. On the other hand, for flame retardants thought to act in the condensed phase such as DDPO, a change of polymer matrix should have a strong influence on the flame-retardant efficiency.¹⁰⁸ This suggests that if a similar set of experiment was carried out in DGEBA, the OI of the sample with DDPO and DDPS would vary more than those with DOPO and DOPS.

4.5.3 Self-quenching time (SQT) measurements

4.5.3.1 Self-quenching time (SQT) of oxa-phosphenanthrene derivatives

A plot of the time required for the flame to extinguish itself after removal of the ignition flame, the self quenching time (SQT), as a function of oxygen concentration is shown in

Figure 4-8 and

Figure 4-9. For each specimen, the graph can be split in two linear regions. In the first region, a large increase in OI is required to increase the SQT. However, in the second region, a small increase in OI results in a large increase in SQT. The transition between the two regions is recognised as the transition from unstable to stable burning condition.¹⁰⁸ Extrapolation of the first linear region to $SQT = 0$ enables to determine the oxygen content at which ignition of polymeric material is just possible. This ignition OI (IOI) allows the evaluation of the ease of ignition of a material. For the cured virgin resin, the IOI is ~24.

Figure 4-8 shows that the chemical addition of DOPO and DOPS to DEN 438 prior to curing increases the IOI. For non-flammable samples (V0 in UL 94), the IOI was significantly increased to 31 for DOPO and 36 for DOPS. On the other hand, the large change in oxygen content required to change from unstable to stable burning suggests that DOPO also prevents the flame propagation. Interestingly, unlike DOPO, the SQT trace for DOPS (1.6 %P) was composed of only one linear section. This indicates that once IOI is reached, only a small increase in oxygen content is required to reach a stable burning. Hence, DOPS could be considered to render a DEN438®

resistant to fire by preventing ignition. This is in agreement with a gas-phase mechanism observed in the NOI experiment.

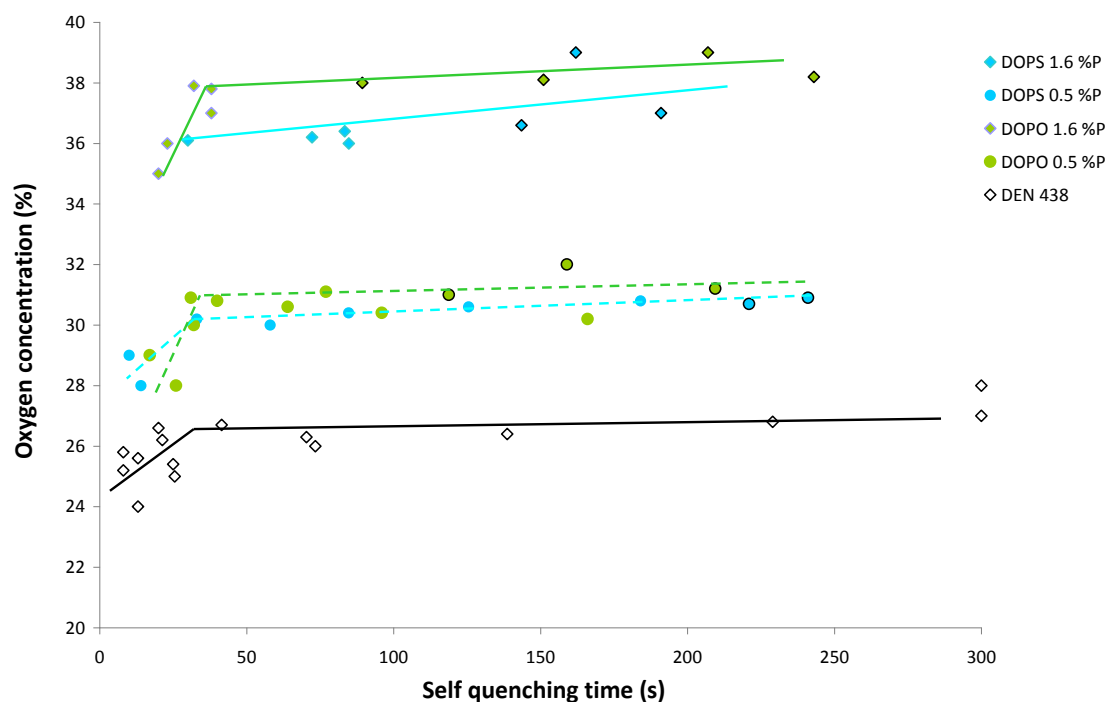


Figure 4-8: Plot of Oxygen content vs. Self quenching time of virgin, DOPO-modified and DOPS-modified DEN 438 measured in oxygen atmosphere. Points with black contour line correspond to specimens burned more than 5 cm.

4.5.3.2 Self-quenching time(SQT) of dimethyldioxophosphorinane derivatives

Figure 4-9 shows the influence of the oxygen content on the SQT of DEN 438 chemically modified with DDPO and DDPS prior to curing. Unlike DOPO, a relatively small change in IOI was observed between the virgin resin and the DDPO and DDPS modified DEN 438 ($> 0.5 \% O_2$). This suggested that, contrary to their aromatic analogues, DDPO and DDPS did not render DEN438 resistant to fire by preventing ignition. The small change in oxygen content required to change from unstable to stable burning, indicates that the addition of aliphatic phosphorus flame retardants did not prevent the combustion cycle as efficiently as DOPO, even though those modified resins were classified as non-flammable in the UL 94 test. As mentioned earlier, DDPO is thought to act predominantly through a condensed phase mechanism. In the UL 94 test, the flame propagates upwards. Hence, when the flammability of the polymer is considered, the hot part of the flame is in direct contact with the polymeric material. This means that the char formation, theoretically responsible for the flame retardant

mechanism, is occurring between the flame front and the polymeric material. Thus, the flame cannot feed on the flammable volatile particles that are being blocked by the insulating char. This in turn leads to the extinguishment of the flame. However, in the OIT, the specimen is burnt downwards. This means that the hottest part of the flame is not in contact with the burning polymeric material surface that is above the travelling (cooler) flame front. Thus, not enough thermal energy is present at the burning polymer surface to assist the char formation responsible for the flame retardancy. This char formation mechanism was practically observed during the OI measurements of DDPO-modified DEN 438. Indeed, the flame was propagating down the sample at a relatively slow rate and the swollen char would only form once the hot part of the flame reached the already partially thermally decomposed sample (

Picture 4-1).

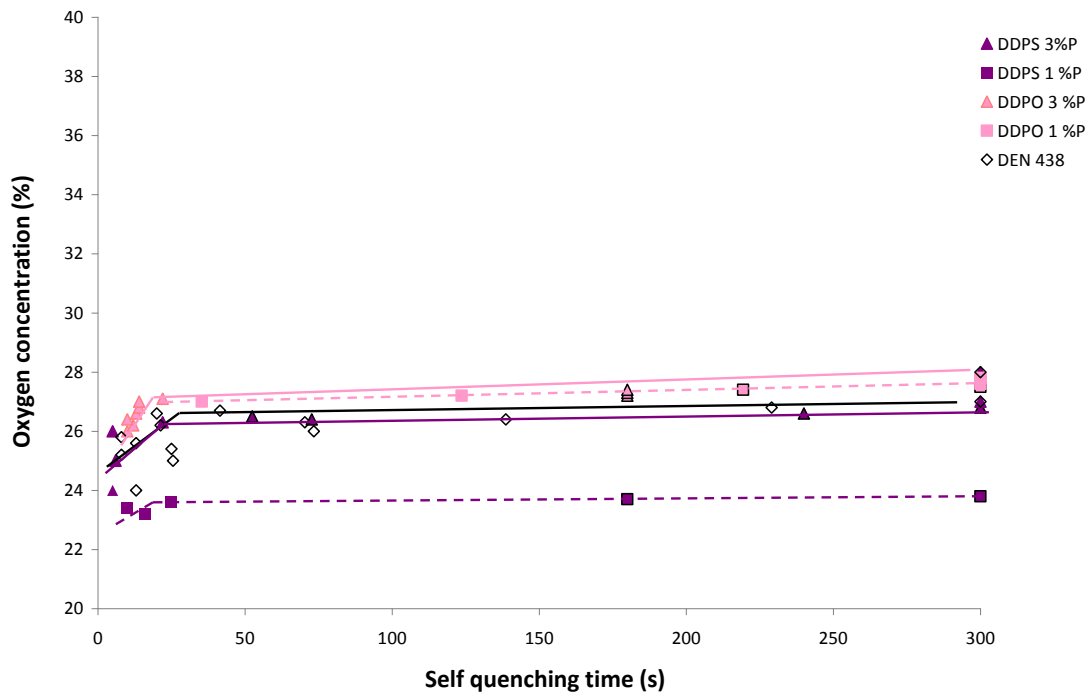
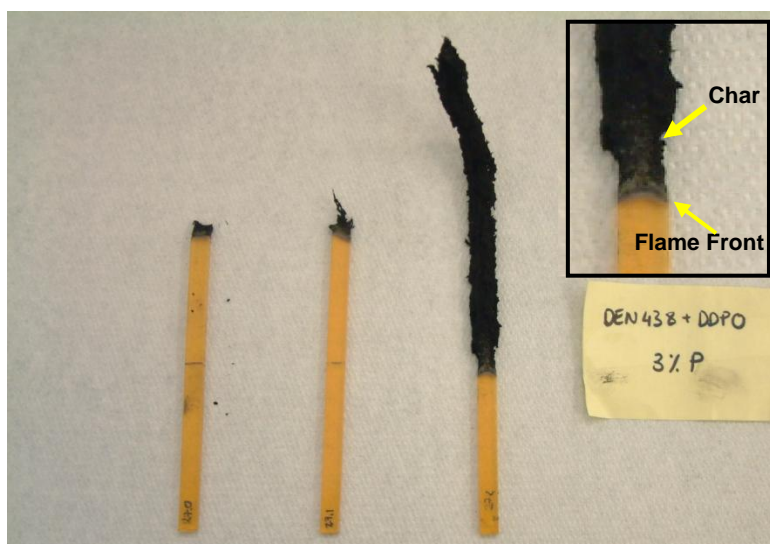


Figure 4-9: Plot of Oxygen content vs. Self-quenching time of virgin, DDPO-modified and DDPS-modified DEN 438 measured in oxygen atmosphere. Points with black contour line correspond to specimens burned more than 5 cm.



Picture 4-1: Specimens of DDPO-modified DEN 438 at 27.0 (left), 27.1 (middle) and 27.2 (right) % oxygen.

4.5.4 Burning rate measurements

Figure 4-10 and 4-11 show the burning rate DEN 438 chemically modified with oxaphosphaphenanthrene and dioxophosphorinane derivatives respectively. As seen in Figure 4-10 the addition of DOPO and DOPS resulted in an increase of the burning rate of DEN 438 cured with DICY and fenuron. However, the addition of DOPS seems to have a weaker impact on the burning rate than DOPO. The same ability of sulphur to slow the burning rate down was also observed for DDPS (Figure 4-11). The burning rate is dependent on the efficiency of the energy back feed toward the polymer. In the neat cured resin, the sample burns to completion. However, when DEN 438 is modified with DDPO, the formation of an insulating char layer prevents the heat from reaching the polymer. Hence, the burning rate slows down. In the case of DDPS, it is possible that the release of non-flammable volatile particles also contributes to altering the flame cycles. However, further investigations are required (section 4.6).

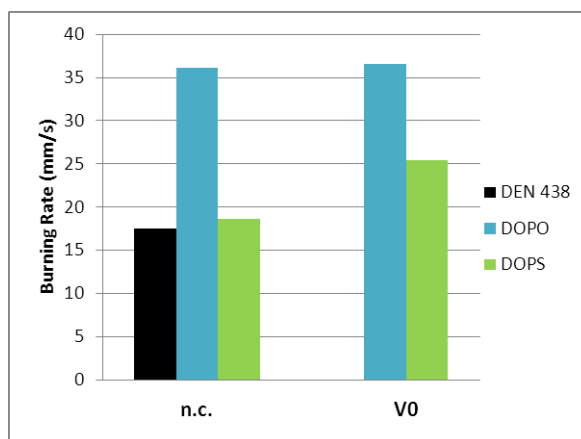


Figure 4-10: Burning rate of DEN 438 resin modified with oxaphosphaphenanthrene derivatives DOPO and DOPS.

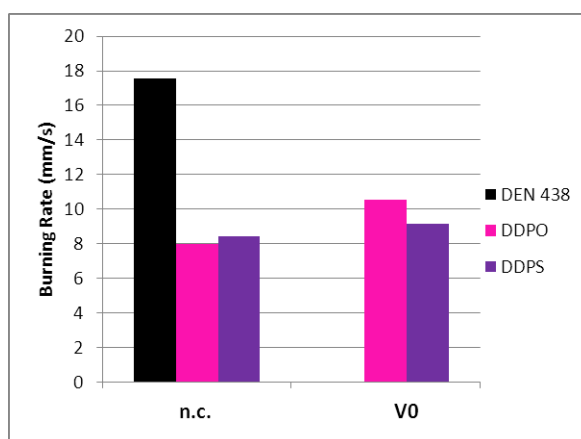
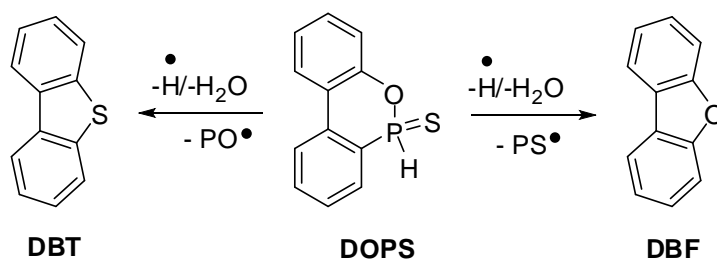


Figure 4-11: Burning rate of DEN 438 resin modified with dioxophosphorinane derivatives DDPO and DDPS.

4.6 Thermal degradation mechanism of organophosphorous derivatives

As mentioned in chapter 1, phosphorus flame retardants can act both in gas and condensed phase. However, in the case of DOPO, the release of PO radicals in the gas phase the predominant mechanism of flame retardancy. DFT calculations predicted that, similarly to DOPO, DOPS would release PO and PS radicals under thermal stress to yield dibenzothiophene and dibenzofuran respectively (Scheme 4-1). Hence, the abundance of volatile phosphorus containing radicals during controlled exposure to a heat source was monitored by thermal desorption mass spectroscopy (TDMS).



Scheme 4-1: Decomposition reactions of DOPS.

Figure 4-12 shows the variation of phosphorus containing radical concentrations plotted as a function of temperature for the flame retardant modified DEN 438 resin cured with DICY and Fenuron. Each phosphaphenanthrene cycles shows different thermal desorption behaviour. Nonetheless, for all samples, the release of PO and PO₂ radicals are predominant while the release of HPO appears to be the smallest. For the samples containing DOPS and DOPO-OH, the production of phosphorus containing radicals reached a maximum before the temperature reached 500 °C. This is coherent with the observed degradation temperature in section 4.3. Indeed, at equal phosphorus loading, the onset degradation temperature of DOPS is 20 °C lower than that of DOPO. Hence, the release of volatile phosphorus containing radicals should be observed at lower temperature in the TDMS spectra. However, a noticeable first release of phosphorus radicals is observed in the DOPO sample between 225 and 400 °C. This is indicative of the formation of an insulating char layer that prevents the volatilisation of phosphorus radicals. Then, once the temperature reached 400 °C, the formed char decomposes and simultaneously releases the trapped gases that can be observed the increased release rate above 425 °C. However, as seen in Figure 4-12, the two steps release of phosphorus radicals is the most pronounced for the DOPO samples and practically non-existent for the DOPO-OH sample. Indeed, for the DOPO-OH sample, the release of PO and PO₂ occurs in a single step. The delayed release of radicals suggests that, during the thermal oxidation DOPO-OH modified resin, the char is formed much earlier and that it is less permeable than one formed when the DOPO modified resin is exposed to heat. Such observation agrees with the ability of phosphoric acid derivatives to promote char formation.^{109,110}

The delay in the release of phosphorus radicals was also observed when the DOPS-OH-containing cured resin was compared to the DOPS modified resin. Indeed, for the DOPS sample, the first release started at ~ 225 °C followed by a faster release at 350 °C. In contrast, for the cured resin containing DOPS-OH, the release of phosphorus

radical started relatively slowly at ~ 260 °C and the rate gradually increased with the increase of temperature.

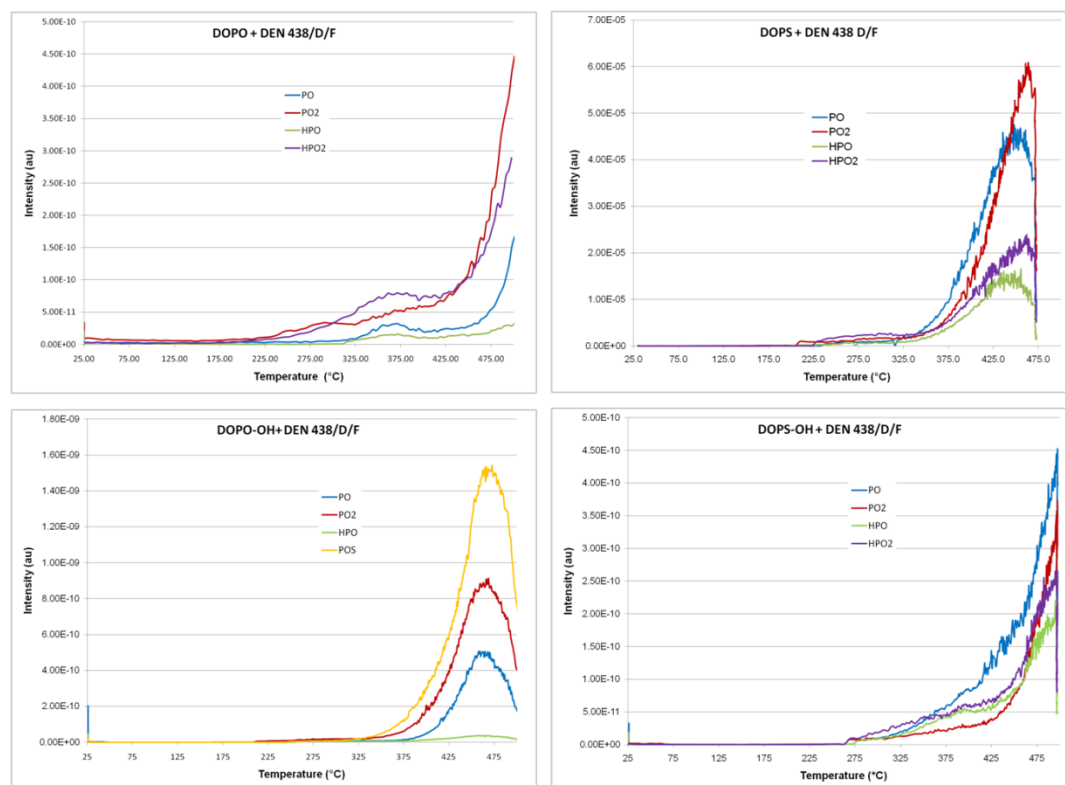


Figure 4-12: Thermal desorption mass spectrum of the DEN 438 cured resins preformulated with DOPO (top-left), DOPS (top-right), DOPO-OH (bottom left) and DOPS-OH (bottom-right). The abundance of PO (blue), PO₂/PS (red), HPO (green), POS (yellow) are plotted as a function of temperature.

The relative intensity for each phosphorus radical did not vary with the oxidation of the phosphorus however, a variation was observed between the sulphide and oxide derivatives. As mentioned earlier, the PO and PO₂/PS radicals are the dominant species in the gas phase. As shown in Figure 4-12, the order of release of the radicals depends on the chemical environment around the phosphorus. For the phosphaphenanthrene oxide derivative DOPS, the PO₂ radicals are release before PO, which suggests that the PO radicals are produced from the reaction of PO₂ radicals with oxygen. On the other hand, for the phosphaphenanthrene sulfide derivatives, the release of PO radicals occurs before the release of PO₂/PS radicals. Moreover a higher initial rate is observed for the DOPS-OH cured resin. In addition, the release of PO₂/PS exceed that of PO radicals for DOPS and not for DOPS-OH. This suggest that the release PO radicals initiate the flame retardant mechanism of phosphaphenanthrene sulphide however, recombination in the gas flame allows the formation of PS radicals that can enhance the gas phase efficiency.

This could rationalised the lower phosphorus loadings required to impart UL-94 V0 rating when DOPS is used a flame retardant for DEN 438 resin cured with DICY and fenuron.

4.7 Summary

The thermal stability and flame retardancy of materials containing the organophosphorus compounds synthesised in chapter 3 was tested.

All heterocyclic organophosphorus compounds were grafted on the epoxy phenol novolac resin commercialised by Dow Chemicals using the fusion process. The modified resins were then cured with DICY and Fenuron. Functionalisation of the epoxy resin resulted in a decrease of the T_g for all samples presented. The sulfide derivatives (DOPS, DOPS-OH, DAPS-OH, DDPS and DDPS-OH) had a more pronounced effect on the T_g than their oxide analogs (DOPO, DOPO-OH, DAPO, DDPO and DDPO-OH). This detrimental effect could however be diminished when the oxidised compounds were used. On the other hand, modification of DEN438 with the nitrogen derivatives (DAPO and DAPS-OH) had a lesser impact on the glass transition temperature of the cured resin. The beneficial influence of nitrogen derivatives can be attributed to the reactivity of the amine functionality. As predicted, during the curing process, the amine can contribute to the cross-linking reaction thus minimising the detrimental effect of reducing the number of epoxy groups during the fusion process. Nonetheless, the increase of viscosity generates during the preformulation processed rendered, DAPS-OH and DDPS-OH not adequate for application in FR-4 composite as the preformulations were almost solid.

TGA analysis of the cured materials indicated that the presence of phosphorus containing moieties slightly increased the char formation. DAPO was found to have the most beneficial impact on the char formation from all the studied compounds. The ability of nitrogen containing molecules to promote the char formation was previously reported, and used in the melamine polyphosphate flame retardant.^{110,111}

UL-94 test of the modified epoxy phenol novolac resins cured with DICY and Fenuron showed that DOPS was the best flame retardant as only 1.0 % phosphorus loading was required to impart UL-94 V0 rating. The DAPO modified resin could reach UL-94 V0 rating with similar loading to the commercially available DOPO. Hence, DAPO represents a viable flame retardant for FR-4 composites as it does not generated

any drastic loss of functionality. The acid derivatives demonstrated better flame retardant performance than their sulphide and oxide analogues, which is in agreement with the observations from Braun *et al.*⁵¹ As predicted, the dioxophosphorinane derivatives required higher loading to impart flame retardant ratings.

In order to further understand the influence of sulphur on the flame retardancy, the limiting oxygen index (LOI) and burning rate were measured. The presence of sulphur did not increase the LOI of the modified resins. In addition, no significant change in mechanism of flame retardancy was observed for the phosphaphenanthrene derivatives. Nonetheless, the presence of sulphur increased the ease of ignition of dioxophosphorinane derivatives, suggesting that sulphur promotes the gas phase mechanism. The possible competition of mechanism was validated when the structures of the chars were observed. Indeed, in comparison to DDPO modified resin, the char formed was less voluminous, which indicated that the intumescence of DDPO was reduced.

The influence of PS radicals in the gas phase was verified using TD-MS analysis of DOPO, DOPS, DOPO-OH and DOPS-OH. Indeed, the resin preformulated with DOPS showed a sequential release of PO and PS radical that can rationalise the low phosphorus loading required to impart UL-94 V0 rating to DEN438.

CHAPTER 5: SYNERGISM OF DOPO WITH EXFOLIATED NANOCCLAY IN EPOXY RESIN

5.1 Introduction

Despite their high flame retardant efficiency, organophosphorus compounds suffer from a relatively high production price in comparison to inorganic flame retardants. This increase in production cost contributes to delaying their use in polymeric systems. In order to counter-affect the increases in cost, the combination of organophosphorus compounds with inorganic clay has been investigated.¹¹²⁻¹¹⁴

Unlike organophosphorus flame retardants whose flame retardant activity is generally associated with the gas phase, inorganic fillers act in the condensed phase.⁴³ Their main mechanism of action consists of reducing the available combustible fuel during the fire event. In addition, metal hydroxide can act as heat sinks. During the combustion of the polymeric material, aluminium hydroxide undergoes an endothermic decomposition that removes energy away from the flame cycle and produces water as a flame diluent.[c.f. Chapter 1]

5.2 Influence of Cloisite 30B

The use of nanoclay to enhance the fire resistance of polymeric materials has been the subject of increasing interest in the past decade.³⁶ In addition to enhancing the fire resistance of polymeric materials, nanoclays were also reported to improve other properties.^{115,116} However, the solubility of inorganic nanoclays in polymeric is very reduced. Hence, nanoclays are organically modified in order to improve their solubility.

The intercalation of different organoclays was reported to impart flame retardancy to DGEBA cured with methyl tetrahydrophthalic anhydride.⁴¹ Out of the wide range of nanoclays investigated, the organically modified montmorillonite Cloisite 30B was reported to have the best fire retardant performance as it reduced the heat release rate of the cured DGEBA resin by 68 %. The reduction of heat release was attributed to the formation of a protective layer at the surface of the burning polymer.

In order to study the possible synergism of nanoclay on the flame retardancy of DOPO in DEN 438, functionalised resins were mixed with Cloisite 30B and the retardancy was investigated.^c

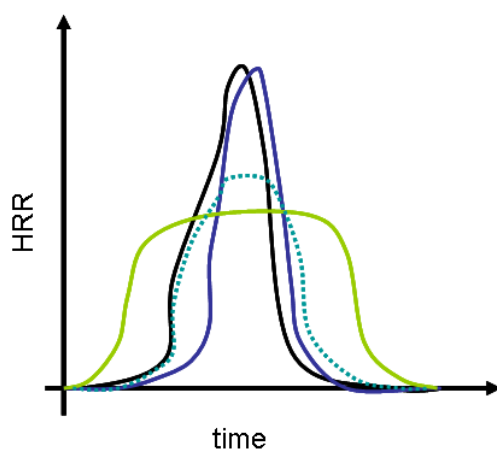


Figure 5-1: Idealised Heat Release Rate (HRR) of for the combustion of DEN 438 (black) with DOPO (blue), nanoclay (light green), or DOPO and nanoclay (dashed dark green).

5.2.1 Formulation

The flame retardant efficiency of organoclays is linked to the extent of dispersion within the epoxy resin matrix.^{41,112,117,118} Nonetheless, prior to investigating the level of exfoliation of the epoxy resin in different concentration of cloisite 30B, four materials were prepared (Table 5-1).

Table 5-1: Summary of formulations investigated.

Sample	Resin	DOPO (%P)	Cloisite 30B (Wt %)
1	DEN 438	0	0
2	DEN 438	1	0
3	DEN 438	0	1
4	DEN 438	1	1

5.2.2 Thermal stability investigation

The thermal decomposition of the exfoliated materials in oxidative atmosphere is shown in Figure 5-2. All the cured samples show a two steps decomposition process. The first step is associated with dehydration reactions and the dissociation of the weak P-

^c This project is part of a collaboration with Prof. G. Camino at the Politecnico di Torino in Italy.

O and P-N bonds, whereas the second step is related to the oxidation of the dehydration products, which involve C-C bond breaking and radical recombination (c.f. Chap 1). As seen in Figure 5-2, the onset decomposition temperature (T_d) is similar for all materials studied. However, the second step occurs at different temperatures. In the case of the neat DEN 438 resin, the temperature at which 50 % of the mass is lost ($T_{d_{50}}$) is at 475 °C, while the materials containing flame retardants decompose at 515 °C and 534 °C, for the DOPO-modified resin and exfoliated DOPO-modified resin respectively. The increase in decomposition temperature indicates that the presence of phosphorus promotes the formation of non-volatile residues.

When the same samples were heated in a N_2 atmosphere, a different decomposition pattern was observed (Figure 5-3). Similarly to the onset decomposition observed in air, the chemical addition of phosphorus resulted in a decrease of the onset decomposition temperature (Table 5-2). However, unlike the thermograms in air, only one step was observed. The absence of the second oxidative step is rationalised by the absence of O_2 . As seen in Figure 5-3, the addition of phosphorus resulted in a slight increase of char formation, which is in agreement with the decomposition observed in air. However, no synergism between Cloisite 30B and DOPO was observed in the TGA analysis.

Table 5-2: Summary of UL-94, T_g measured using differential scanning calorimetry and TGA data.

#	UL 94 rating	T_g (°C)	Td Air		N_2		% Char N_2
			5%	10%	5%	10%	
1	n.c	182	363	383	355	372	29
2	V1	162	351	375	342	361	32
3	n.c.	188	366	391	355	371	31
4	V0	167	356	381	336	366	34

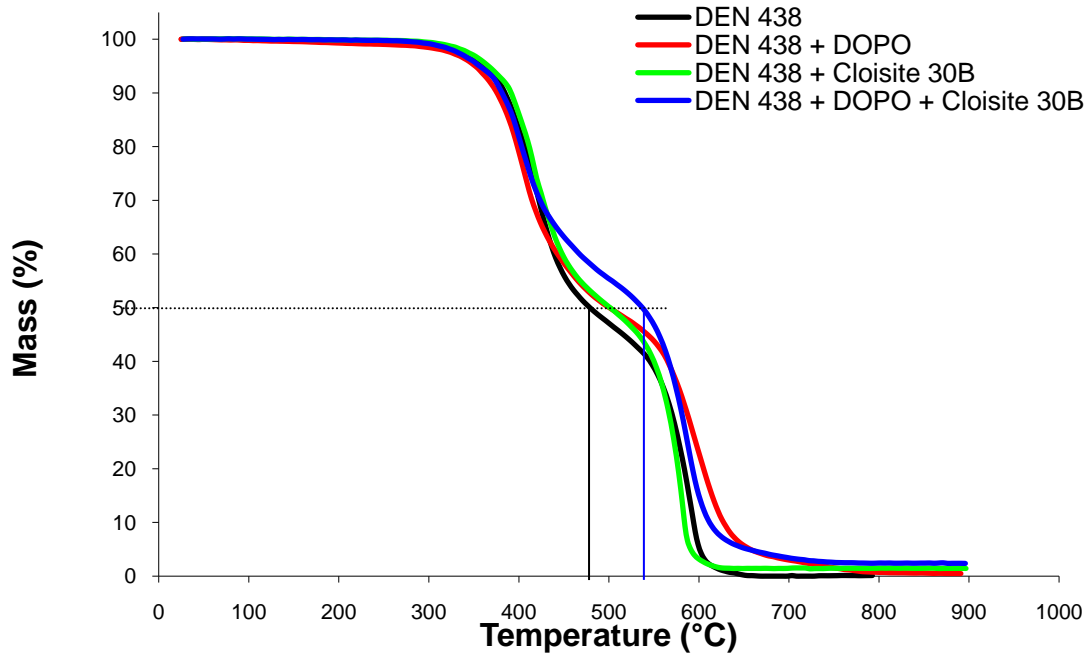


Figure 5-2: Thermal gravimetric curves in air of cured DEN 438 (black); with DOPO (1 %P) (red); with Cloisite 30B (red); with DOPO and Cloisite 30B (blue). The vertical blue line emphasises the temperature at which 50% of the initial weight is lost.

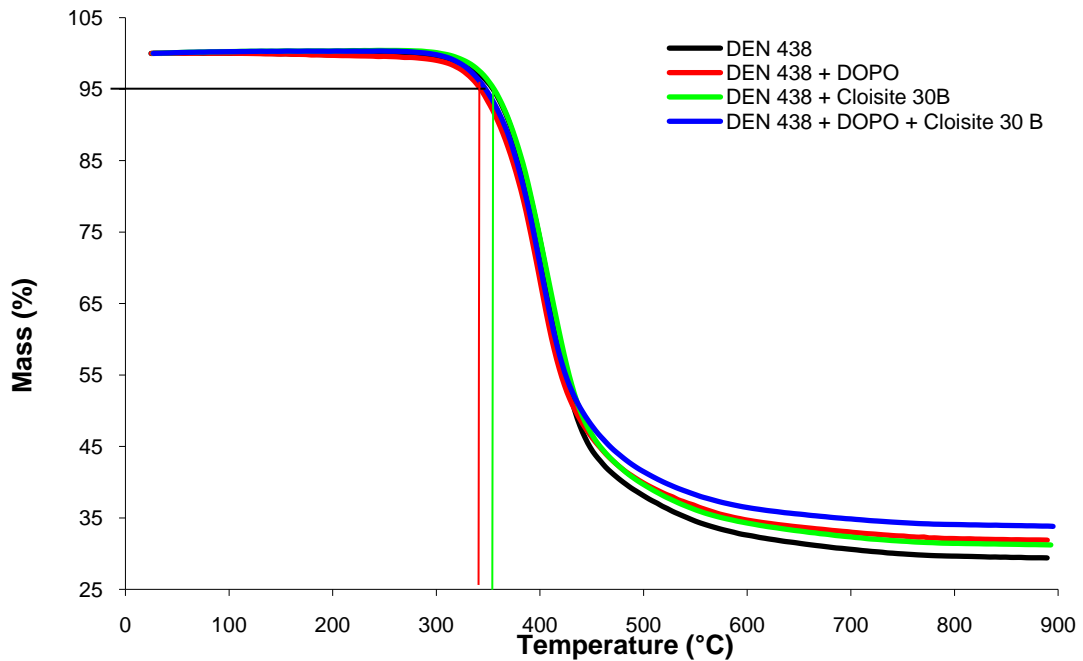


Figure 5-3: Thermal gravimetric curves in N₂ of cured DEN 438 (black); with DOPO (1 %P) (red); with Cloisite 30B (red); with DOPO and Cloisite 30B (blue). The vertical lines emphasises the temperature at which 95% of the initial weight is lost.

5.2.3 Oxygen index test (OIT)

The Limiting Oxygen Index of the four samples was measured.^d As seen in table 5-2, the addition of DOPO to DEN 438 resulted in a 10 % increase of the LOI. This increase of LOI is coincident with the reduced flammability observed in section 4.5. Similarly to the observation by Camino et al in DGEBA, the addition of Cloisite 30B did not have any significant impact on the flammability of DEN 438. Correspondingly, the presence of 1 wt% Cloisite 30B did not influence the flammability of the DOPO-modified epoxy phenol novolac resin. In addition no significant impact on the burning rate were observed.

Table 5-3: LOI and combustion rates.

Sample	LOI (%O ₂)	σ (%O ₂)	Rate(mm/min)	σ (mm/min)
1	27.4	0.16	28.4	6.1
2	37.0	0.10	32.7	5.8
3	27.3	0.14	29.8	2.4
4	36.8	0.29	30.4	2.4

The effect of the addition of the limiting nitrogen protoxide index (LNI) are summarised in Table 5-3. As expected, the replacement of oxygen by the less powerful oxidand N₂O resulting in higher LNI values than the LOI value observed in Table 5-2. Nonetheless, the trends observed are almost identical. The modification of the epoxy phenol novolac resin with DOPO resulted in a 10 % increase of the LNI, whereas no significant impact was observed whether Cloisite 30B was dispersed into the pristine or the modified resin. Similarly to the rates measured in oxygen atmosphere, the addition of Cloisite 30B did not result in any significant changes. However, DOPO-modified resin burnt faster than the pristine resin. Moreover the addition of Cloisite 30B to the DOPO-modified resin resulted in a further increase of the rate of combustion.

Table 5-4: LNI and combustion rates.

Sample	NOI (%N ₂ O)	σ (%N ₂ O)	Rate (mm/min)	σ (mm/min)
1	49.1	1.05	25.7	3.3
2	58.3	<1.8	29.5	2.8
3	49.1	1.05	22.8	4.15
4	56.5	1.27	32.2	2.7

^d The measurement were carried out by Matteo Lavaselli in the Politecnico di Torino, Italy

5.2.4 Cone calorimetry measurements

In order to gain a better understanding of the decomposition process of the DOPO-modified epoxy phenol novolac resin and its possible synergism with the organically modified montmorillonite nanoclay Cloisite 30B, cone calorimetry measurement were carried out. The main parameters of the test are summarised in Table 5-5:

- Time to ignition (TTI): time at which the ignition occurs;
- Peak of heat release rate (pkHRR): peak value of the curve of heat release rate, for these materials two main peaks are recorded;
- Heat release rate (HRR): average value of the heat release rate;
- Total heat released (THR);
- Total smoke released (TSR): total quantity of smoke released during the test;
- Self extinguishing area (SEA): represent the optical density of the smoke;
- Carbon monoxide (CO);
- Carbon dioxide (CO₂).

Table 5-5: Summary of the cone calorimetric measurements

	TTI [sec]	pkHRR 1 [kW/m ²]	pkHRR 2 [kW/m ²]	HRR [kW/m ²]	THR [MJ/m ²]	TSR [m ² /m ²]	SEA [m ² /kg]	CO [kg/kg]	CO ₂ [kg/kg]
1	122	455	428	134	138	3674	611	0.0761	2.32
2	115(- 7")	285 (37.4%)	306 (28.5%)	111 (-17%)	122 (11.6%)	4506 (+22.7%)	729 (+19.3%)	0.1305 (+71%)	1.94 (16.4%)
3	122	467 (+2.%)	440 (+2.%)	141 (+5.%)	141 (2.2%)	3701 (+0.7)	614 (+0.5)	0.0693 (-8.9%)	2.32
4	110 (12)	282 (-38%)	362 (15.%)	119 (11.%)	109 (-21%)	4289 (+16%)	723 (+18%)	0.1188 (+56.1%)	1.8 (22.4%)

As seen in Figure 5-4, the HRR curve of the neat DEN 438 is characterised by the presence of two peaks. During the combustion of the sample, the formation of a carbonaceous layer on the surface that acts as a protective barrier results in decrease the HRR curve. However, as the combustion proceeds, the insulating layer degrades and the underlying material becomes exposed to the heat source, which results in the appearance of second peak. This two peak values are comparable and the first one is slightly higher.

The chemical addition of DOPO to the epoxy phenol novolac resin led to a noticeable decrease of the peak value of 37.4% and 28.5%, for the first and second peak respectively (Table 5-5). Similarly, the presence of DOPO had a positive effect on both the average value of the heat release rate and the total heat released, as they were significantly reduced. On the other hand, an increase of the total production and density of the smoke was observed. Moreover, a strong increase (+71%) in the production of carbon monoxide was recorded.

The addition of a small amount of Cloisite 30B led to variations of the studied parameters lower than the analytical error (10%) (Table 5-5).

No synergism among the additives was observed. Indeed, the material with both Cloisite 30B and DOPO presents values comparable with those of the material with DOPO alone.

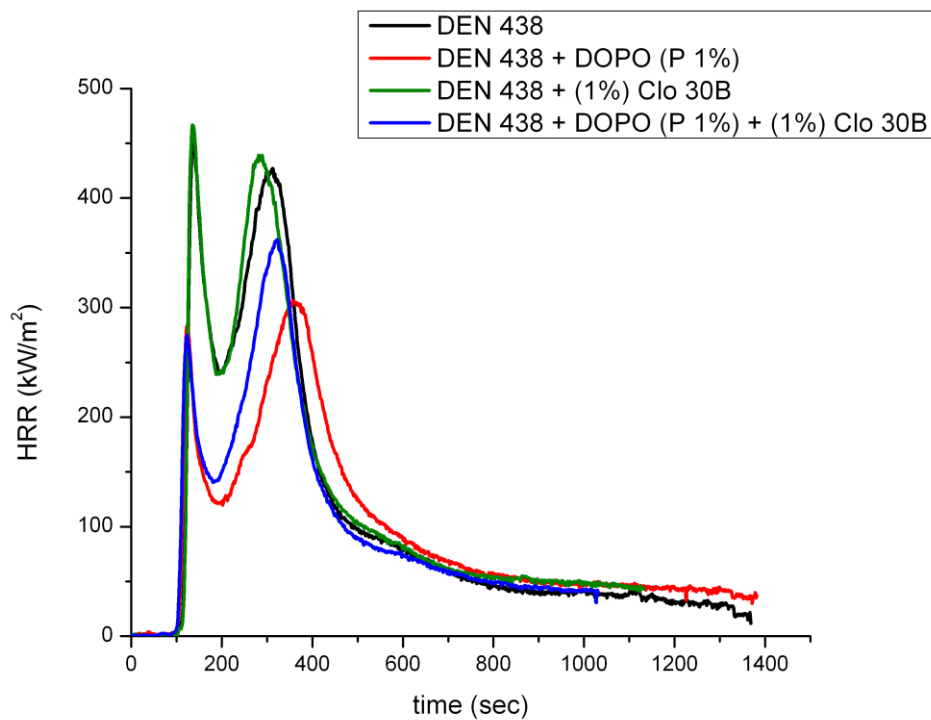


Figure 5-4: Heat release rate (HRR) for of the DEN 438 samples.

5.3 Summary

The effect of a phosphorous based flame retardant (DOPO) and of a commercial organomodified clay (Cloisite 30B) on the flammability and combustion behaviour of an epoxy phenol novolac resin (DEN 438) were tested by differential scanning calorimetry (DSC), thermal gravimetry analysis (TGA), limiting oxygen index (LOI), limiting nitrogen protoxide index (LNI), vertical UL-94 and cone calorimeter.

The addition of DOPO leads to the improvement of the flammability and combustion behaviour of the resin indeed an enhancement of LOI and LNI and a decrease of about 40% of the main peak of the HRR curve were obtained.

The addition of Cloisite 30B did not lead to noticeable improvement of the resin flame resistance: this behaviour could be due to the very low concentration of the clay (1%); future studies could be conducted on resin with an higher concentration of additive, for example 3-5%.

The UL-94 was the only test that showed a synergy among the two additives. The material with DOPO and Cloisite was classified V0, whereas the material with DOPO alone reached the V1 classification. This classification has very important commercial interest. The UL-94 result was surprising because, as discussed above, the nanoclay alone did not modify the horizontal burning (Cone calorimeter) and the vertical burning with the flame from the top (LOI – LNI).

The results confirms that the DOPO acts in the condensed phase as, increasing the flame retardant concentration, the LOI and LNI have the same behaviour.

CHAPTER 6: CONCLUSION

In the course of this doctoral work, the influence of organophosphorus compounds containing different heteroatoms in the chemical environment on the flame retardancy of epoxy phenol novolac resin was studied.

Prior to investigating their flame retardant properties, the synthesis of a series of derivatives of the heterocyclic DOPO with different chemical environment around the phosphorus was presented. Firstly, in order to investigate the role of PS radicals in the flame retardancy of epoxy phenol novolac resin DEN 438, the synthesis of the new 6H-dibenzo[*c,e*][1,2]oxaphosphinine 6-sulfide (**4**) (DOPS) was investigated. Compound (**4**) was successfully obtained using different thionation agents and underwent nucleophilic additions such as the Pudovik reaction as well as the Atherton-Todd reaction. Secondly, the thionation procedure used for the synthesis of DOPS was applied to obtain DDPS. Similarly to DOPO, and DDPO, the P-H bond could be activated to generate the phosphonate nucleophilic species that could react with unsaturated functionality. Then, the synthesis of DAPO was optimised and the reactivity of P-H bond was compared to the other phosphine oxides. DAPO successfully underwent an addition reaction with benzaldehyde, which confirmed that its potential use as reactive flame retardant for epoxy resins. Lastly, two new sulphur derivatives of DAPO, DAPS and DAPS-OH were synthesised using the synthesis route developed for the DOPO and DDPO derivatives.

All the compounds shown in Figure 3-26, were synthesised using 1 or 2 steps synthesis from commercially available starting materials. Moreover, all heterocyclic organophosphorus compounds presented were obtained in high yield and with high level of purity. The variety of environment around the phosphorus atom also makes such compounds interesting for studies where the binding properties of phosphorus are investigated. The ease of synthesis of the organophosphorus molecules presented combined with their broad range of reactivity make them promising compounds for a wide spectrum of molecules and applications.

In order to investigate the thermal stability and flame retardancy of materials containing the organophosphorus compounds synthesised in chapter, all heterocyclic

organophosphorus compounds were grafted on the epoxy novolac resin commercialised by Dow Chemicals using the fusion process. The modified resins were then cured with DICY and Fenuron. Functionalisation of the epoxy resin resulted in a decrease of the T_g for all samples presented. The sulfide derivatives (DOPS, DOPS-OH, DAPS-OH, DDPS and DDPS-OH) had a more pronounced effect on the T_g than their oxide analogs (DOPO, DOPO-OH, DAPO, DDPO and DDPO-OH). However, modification of the resin with the nitrogen derivatives (DAPO and DAPS-OH) had a lesser impact on the glass transition temperature of the cured resin. The beneficial influence of nitrogen derivatives can be attributed to the reactivity of the amine functionality. As predicted, during the curing process, the N-H group can contribute to the cross-linking reaction thus minimising the detrimental effect of reducing the number of epoxy groups during the fusion process.

UL-94 test of the modified epoxy phenol novolac resins cured with DICY and Fenuron showed that DOPS was the best flame retardant as only 1.0 % phosphorus loading was required to impart UL-94 V0 rating. DAPO represents a viable flame retardant for FR-4 composites as it does not generated any drastic loss of functionality and impart UL-V0 rating with similar phosphorus loading to DOPO. Moreover, DAPO was found to have the most beneficial impact on the char formation from all the studied compounds. The ability of nitrogen containing molecules to promote the char formation was previously reported, and used in the melamine polyphosphate flame retardant. The acid derivatives demonstrated better flame retardant performance than their sulphide and oxide analogues, which is in agreement with the observations from Braun et al.⁵¹

In order to further understand the influence of sulphur on the flame retardancy, the limiting oxygen index (LOI) and burning rate were measured. The presence of sulphur did not increase the LOI of the modified resins. Nonetheless, the presence of sulphur increased the ease of ignition of dioxophosphorinane derivatives, suggesting that sulphur promotes the gas phase mechanism. The possible competition of mechanism was validated when the structures of the chars were observed. Indeed, in comparison to DDPO-modified resin, the char formed from the decomposition of the DDPS containing resin was less voluminous, which indicated that the intumescence of DDPO was reduced.

TD-MS analysis was used to gain further understanding the influence of PS radicals in the gas phase of DOPO, DOPS, DOPO-OH and DOPS-OH-modified epoxy

phenol novolac resins. Indeed, the resin preformulated with DOPS showed a sequential release of PO and PS radical that can rationalise the low phosphorus loading required to impart UL-94 V0 rating to DEN438.

Since the past decade, there has been a raise of interest towards the development of nanocomposite flame retardant solutions. The DFT calculations, LOI, and TD-MS experiments suggested that PO radicals were the active flame retardant species in the DOPO derivatives. Hence, the addition of a condensed phase active material could potentially lead to a synergistic flame retardancy. Such synergism would enable to reduce the production costs as inorganic additives are generally cheaper organophosphorus compounds. With this aspiration, the effect of a phosphorous based flame retardant (DOPO) and of a commercial organomodified clay (Cloisite 30B) on the flammability and combustion behaviour of an epoxy phenol novolac resin (DEN 438) were tested by differential scanning calorimetry (DSC), thermal gravimetry analysis (TGA), Limiting oxygen index (LOI), limiting nitrogen protoxide index (LNI), vertical UL-94 and cone calorimeter.

The addition of DOPO leads to the improvement of the flammability and combustion behaviour of the resin indeed an enhancement of LOI and LNI and a decrease of about 40% of the main peak of the HRR curve were obtained.

The addition of Cloisite 30B did not lead to noticeable improvement of the resin flame resistance: this behaviour could be due to the very low concentration of the clay (1%); future studies could be conducted on resin with a higher concentration of additive, for example 3-5%.

The UL-94 was the only test that showed a synergy among the two additives. The material with DOPO and Cloisite was classified V0, whereas the material with DOPO alone reached the V1 classification. This classification has very important commercial interest. The UL-94 result was surprising because, as discussed above, the nanoclay alone did not modify the horizontal burning (Cone calorimeter) and the vertical burning with the flame from the top (LOI – LNI). Hence, further studies using higher loadings or different organophosphorus compounds are required to obtain a better understanding of the synergism observed in the UL-94 tests.

In summary, a series of organophosphorus compounds with different heteroatoms around the phosphorus was synthesized and their reactivity was tested prior to grafting on epoxy phenol novolac resin. All compounds enhanced the flame retardant

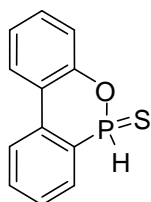
efficiency of DEN 438. TD-MS showed that sequential release of PS and PO radicals participated to its high flame retardant properties. The addition of an organically modified montmorillonite clay to a DOPO-modified resin did not result in any observable synergism in the cone calorimetry. Nonetheless, cone calorimetry represents an excellent tool to investigate the mechanism of thermal decomposition and the PS-PO synergism should be further studied using this method.

CHAPTER 7: EXPERIMENTAL SECTION

7.1 General experimental

Unless stated otherwise, solvents and chemicals were obtained from commercial sources and used without further purification. With the exception of DOP-Cl and DOPO which were provided by Krems Chemie and Schill & Seilacher respectively, all starting materials were purchased from Sigma-Aldrich. NMR spectra were recorded with a Varian INOVA-400 (400 MHz). Chemical shifts are reported as δ values relative to the solvent peak. Trimethylsilane was used as a standard. All ^{31}P -NMR spectra are measured proton decoupled. All ^{13}C -NMR spectra were measured proton decoupled and phosphorus coupled. ^1H -NMR spectra were measured phosphorus coupled. Melting points are uncorrected and measured with a Büchi B-545. High resolution mass spectrometry (HR-MS) analyses were performed on a MicroMass GCT (time of flight (TOF); electron ionization (EI), 70 eV). IR spectra were recorded with a Varian 660-IR (FT-IR). Crystal structure analyses were conducted on a Siemens SMART-1000-CCD with Mo-K α ($\lambda=0.71073$, graphite monochromator) at 200 K. A Lorentz and Polarisation correction was applied. Experimental absorption correction were done with SADABS, structure solving and refining was done with SHELX 97. XPMA and Mercury 2.2 were used for visualisation.

7.2 Synthesis



Chemical Formula: C₁₂H₉OPS
Molecular Weight: 232.24

6*H*-dibenzo[*c,e*][1,2]oxaphosphinine 6-sulfide (4):^{60,119} In a flame-dried three neck round bottom flask fitted with a gas inlet, a thermometer and a gas outlet leading to a NaOH aqueous solution, H₂S gas was bubbled through a solution of DOP-Cl (40.0 g, 171 mmol) in dry toluene (120 mL) at room temperature. The released acid was then

trapped with triethylamine (19.0 g, 188 mmol). The suspension was filtered and concentrated *in vacuo* to yield a colorless powder (35.2 g, 152 mmol, 89 %). mp 88 °C; ³¹P NMR (101 MHz, CDCl₃) δ 57.1 ppm; ¹³C NMR (101 MHz, CDCl₃) δ 149.7 (d, *J* = 11.2 Hz, 1C), 135.7 (d, *J* = 5.4 Hz, 1C), 134.9 (s, 1C), 131.7 (d, *J* = 14.0 Hz, 1C), 131.1 (s, 1C), 129.0 (d, *J* = 14.7 Hz, 1C), 125.6 (d, *J* = 5.2 Hz, 1C), 125.4 (s, 1C), 124.9 (d, *J* = 10.4 Hz, 1C), 124.2 (d, *J* = 9.5 Hz, 1C), 123.6 (d, *J* = 13.5 Hz, 1C), 120.8 ppm (d, *J* = 5.9 Hz, 1C); ¹H NMR (400 MHz, CDCl₃) δ 8.37 (d, *J* = 536.8 Hz, 1H), 7.95 (dd, *J* = 15.9 Hz, *J* = 7.6 Hz, 1H), 7.8 (d, *J* = 8.1 Hz, 1H), 7.83-7.80 (m, 2H), 7.66 (dt, *J* = 7.7 Hz, *J* = 1.1 Hz, 1H), 7.50 (dt, *J* = 7.5 Hz, *J* = 3.2 Hz, 1H), 7.35 (dt, *J* = 8.4 Hz, *J* = 1.1 Hz, 1H), 7.24 (dt, *J* = 8.0 Hz, *J* = 0.8 Hz, 1H), 7.20 ppm (dd, *J* = 8.1 Hz, *J* = 0.9 Hz, 1H); IR (KBr) ν 3061, 2364 (w, P-H), 1578 (m, P-C_{aryl}), 1194 (vs, P-O), 941 (vs, P=S), 758 (s, C-H bend) cm⁻¹; HR MS (EI) calcd for [C₁₂H₉OPS]⁺ 232.0112, found 232.0112.

Alternative experimental procedure for the synthesis of 1:

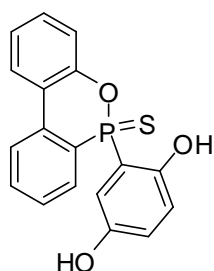
Using Phosphorus pentasulfide:

DOPO (54 g, 0.25 mol) and dry toluene (150 mL) were fed into a three neck round bottom flask equipped with a mechanic stirrer, a gas inlet and a thermometer. This mixture was heated up to 55 °C under an Ar atmosphere. P₄S₁₀ (13.9 g, 0.03125 mol) was then added and the reaction mixture was stirred at 55 °C. After 2 hours at 55 °C, a second portion (13.9g) of P₄S₁₀ was added and the mixture was stirred at 40°C over a period of 15 h under Ar atmosphere. The cloudy solution was decanted up from the phosphorus sulfides/oxides and was filtered through a thin layer of silica gel. Afterwards the toluene was removed *in vacuo*. The resulting oil was dissolved in chloroform (100 ml). A small amount of a precipitate was removed by filtration. The filtrate was then stirred with an aqueous solution of sodium hydrogen carbonate (100 ml) for 20 min under argon (the chloroformic phase became milk-like; evolution of CO₂). The cloudy chloroformic phase was collected dried over sodium sulphate and filtered over silica gel. The resulting clear solution was concentrated *in vacuo* to yield an oily product that gradually solidified (43.5g, 0.18mol, 70 %). mp 88 °C; ³¹P NMR (101 MHz, CDCl₃) δ 57.1 ppm.

Using Lawesson reagent:

DOPO (0.32 g, 1.50 mmol), Lawesson reagent (1.22 g, 3.0 mmol) and dry toluene (100 mL) were charged into a three neck round bottom flask equipped with a

mechanic stirrer, a gas inlet and a thermometer. While under Ar atmosphere, this mixture was heated up to 140 °C using an oil bath. After 1h at 140 °C, the oil bath was removed and the reaction mixture allowed to cool to room temperature. Once cooled the solvent was removed *in vacuo* to yield a brown solid. The unpure product was then redissolved in chloroform and filtered over silica gel. The resulting liquid was then concentrated *in vacuo* to yield a pale yellow syrup. The syrup was then recrystallised from acetonitrile to yield a crystalline white solid (0.118g, 0.51 mmol, 34 %). mp 88 °C; ³¹P NMR (101 MHz, CDCl₃) δ 57.1 ppm.

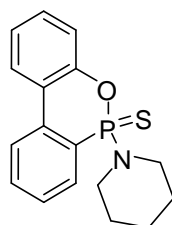


Chemical Formula: C₁₈H₁₃O₃PS
Molecular Weight: 340.33

2-(10-Thioxo-10H-9-oxa-10λ⁵-phospha-phenanthren-10-yl)-benzene-1,4-

diol (4): A thoroughly dried 2-neck round bottom flask fitted with a condenser and an Ar gas inlet was charged with DOPS (12.3 g, 53.0 mmol) and dry toluene (20 mL). This solution was heated under positive argon pressure using an oil bath at 110 °C. While under Ar atmosphere, benzoquinone (6.30 g, 58.0 mmol) was added in portions to the stirring solution over a period of 30 min. After 3.5 h under reflux, 4 was fully consumed and the heat source was removed to allow the reaction mixture to cool down to room temperature. The crude black reaction mixture was concentrated *in vacuo* to yield a black solid. The black solid was triturated with cold dichloromethane and the resulting suspension was filtered to yield a spectroscopically pure off-white solid (13.3 g, 39.2 mmol, 74 %). mp 127 °C; ³¹P NMR(101 MHz, DMSO-d₆) δ 73.6 ppm; ¹³C NMR (101 MHz, DMSO-d₆) δ 152.5 (s, 1C), 150.0 (d, *J* = 18.2 Hz, 1C), 149.7 (d, *J* = 9.8 Hz, 1C), 134.0 (d, *J* = 4.6 Hz, 1C), 132.8 (s, 1C), 131.1 (s, 1C), 130.1 (d, *J* = 14.2 Hz, 1C), 129.2 (d, *J* = 106.4 Hz, 1C), 129.2 (d, *J* = 14.6 Hz, 1C), 126.1 (s, 1C), 125.1 (s, 1C), 124.2 (d, *J* = 8.8 Hz, 1C), 123.4 (s, 1C), 122.5 (d, *J* = 12.4 Hz, 1C), 121.0 (d, *J* = 5.8 Hz, 1C), 120.4 (d, *J* = 14.2 Hz, 1C), 118.1 (d, *J* = 9.2 Hz, 1C), 116.8 (d, *J* = 111.8 Hz, 1C); ¹H NMR (400 MHz, DMSO-d₆) δ 9.53 (s, 1H), 9.21 (s, 1H), 8.11 (d, *J* = 7.8 Hz, 2H), 7.63 (dt, *J* = 6.6 Hz, *J* = 1.3 Hz, 1H), 7.47-7.36 (m, 4H), 7.24 (dt, *J* = 7.2 Hz, *J* = 0.8 Hz, 1H), 7.18 (dd, *J* = 8.1 Hz, *J* = 0.6 Hz, 1H), 6.85 (dd, *J* = 8.7 Hz, *J* = 2.8 Hz, 1H), 6.58 ppm (t, *J* = 5.6 Hz, 1H); IR (KBr) ν 3267 (br, -OH), 3190, 1591 (s, P-C_{aryl}), 1580, 1471, 1221 (vs, P-O), 1182 (vs, P-O), 901 (vs, P=S), 752 cm⁻¹; HRMS (EI) calcd for [¹²C₁₈H₁₃PO₃S]⁺ 340.0326, found 340.0323.

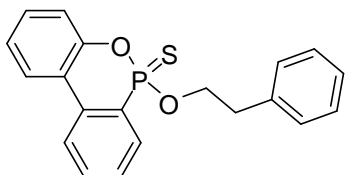
The experimental data for compound **9** is given as a typical representative of an Atherton-Todd reaction involving DOPS (**4**) as a substrate.



Chemical Formula: C₁₇H₁₈NOPS
Molecular Weight: 315.37

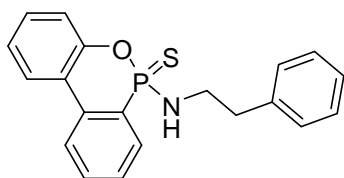
1-(10-Thioxo-10H-9-oxa-10λ⁵-phospha-phenanthren-10-yl)-piperidine (9):

A flame dried three neck flask with a condenser, thermometer and an addition funnel was charged with **1** (3.80 g, 16.4 mmol), carbon tetrachloride (2.77 g, 18.0 mmol) and 20 mL of dry chloroform. The reaction mixture was cooled with an ice bath to 5 °C. The addition funnel was charged with triethylamine (1.80 g, 18.0 mmol) and piperidine (1.39 g, 16.4 mmol) dissolved in 20 mL of dry chloroform. The triethylamine mixture was added dropwise under vigorous stirring. The reaction temperature was not allowed to exceed 10 °C. After 1 h the addition was complete and NMR analysis indicated complete conversion of the starting material. The reaction mixture was washed three times with 50 mL water to remove the triethylamine hydrochloride. The organic phase was isolated, dried over MgSO₄ and the solvent was removed *in vacuo*. The spectroscopically pure product was obtained as a brown solid (4.51 g, 14.3 mmol, 87%) mp 72-74 °C; ³¹P NMR (101 MHz, CDCl₃) δ 72.3 ppm; ¹³C NMR (101 MHz, CDCl₃) δ 149.2 (s, 1C), 136.0 (s, 1C), 132.1 (s, 1C), 130.2 (s, 1C), 129.1 (d, *J* = 11.0 Hz, 1C), 128.6 (d, *J* = 14.7 Hz, 1C), 128.2 (d, *J* = 137.0 Hz, 1C), 124.9 (s, 1C), 124.2 (s, 1C), 123.7 (d, *J* = 10.7 Hz, 1C), 122.5 (d, *J* = 11.8 Hz, 1C), 120.6 (d, *J* = 5.7 Hz, 1C), 46.0 (2C), 26.2 (s, 1C), 26.1 (s, 1C), 24.5 ppm (s, 1C); ¹H NMR (400 MHz, CDCl₃) δ=7.92–7.87 (m, 2H), 7.77 (ddd, *J* = 15.1 Hz, *J* = 7.6 Hz, *J* = 1.2 Hz, 1H), 7.60 (tt, *J* = 7.5 Hz, *J* = 1.3 Hz, 1H), 7.46 (ddt, *J* = 7.5 Hz, *J* = 3.1 Hz, *J* = 0.9 Hz, 1H), 7.35 (tt, *J* = 7.6 Hz, *J* = 1.2 Hz, 1H), 7.26–7.18 (m, 2H), 3.34–3.28 (m, 4H, N-CH₂), 1.63–1.60 (m, 2H, CH₂), 1.54–1.49 ppm (m, 4H, CH₂); IR (KBr) ν 3052, 2955, 2934, 2918, 2848, 1604 (w, P-C_{aryl}), 1580, 1474, 1443, 1425, 1206 (vs, P-O), 1164, 1113, 1059 (vs, P-N), 962 (vs, P=S), 783, 746, 725 cm⁻¹; HRMS (EI) calcd for [¹²C₁₇H₁₈NPOS]⁺ 315.0847, found 315.0852.



Chemical Formula: C₂₀H₁₇O₂PS
Molecular Weight: 352.39

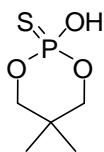
10-Phenethyloxy-9-oxa-10-phospha-phenanthrene 10-sulfide(7). The product was isolated as a white solid (4.31 g, 12.2 mmol, 75%). mp 102-104 °C; ³¹P NMR (101 MHz, CDCl₃) δ 76.9 ppm; ¹³C NMR (101 MHz, CDCl₃) δ 149.7 (d, *J* = 11.3 Hz, 1C), 136.7 (s, 1C), 134.4 (d, *J* = 4.9 Hz, 1C), 133.1 (s, 1C), 130.6 (*J* = 14.7 Hz, 1C), 130.2 (s, 1C), 128.6 (s, 2C), 128.4 (s, 2C), 128.0 (s, 1C), 126.8 (d, *J* = 145.7 Hz, 1C), 126.4 (s, 1C), 125.1 (s, 1C), 124.6 (s, 1C), 123.6 (d, *J* = 10.6 Hz, 1C), 122.6 (d, *J* = 12.2 Hz, 1C), 119.9 (d, *J* = 5.8 Hz, 1C), 66.9 (d, *J* = 6.7 Hz, 1C, CH₂), 36.3 ppm (d, *J* = 6.2 Hz, 1C, CH₂); ¹H NMR (400 MHz, CDCl₃) δ 7.91 (dd, *J* = 16.9 Hz, *J* = 7.6 Hz, 1H), 7.78–7.74 (m, 2H), 7.54 (dt, *J* = 7.5 Hz, *J* = 1.2 Hz, 1H), 7.35 (dt, *J* = 7.5 Hz, *J* = 3.7 Hz, 1H), 7.25–7.21 (m, 1H), 7.13 (t, *J* = 7.8 Hz, 1H), 7.08–7.02 (m, 4H), 6.88–6.86 (m, 2H), 4.24–4.18 (m, 2H, CH₂), 2.77–2.66 ppm (m, 2H, CH₂); IR (KBr) ν 3062, 3023, 2977, 2947, 2889, 1606 (w, P-C_{aryl}), 1580, 1559, 1496, 1474, 1447, 1429, 1194 (vs, P-O), 1115 (vs, P-O), 1045, 902 (vs, P=S), 754, 733, 716, 696 cm⁻¹; HRMS (EI) calcd for [¹²C₂₀H₁₇PO₂S]⁺ 352.0687, found 352.0721.



Chemical Formula: C₂₀H₁₈NOPS
Molecular Weight: 351.40

Phenethyl-(10-thioxo-10H-9-oxa-10λ⁵-phospha-phenanthren-10-yl)-amine

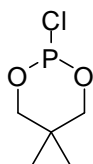
(8). The product was isolated as a white solid (5.76g, 16.4 mmol, 82 %). mp 106-109°C; ³¹P NMR (101 MHz, CDCl₃) δ 69.3 ppm; ¹³C NMR (101 MHz, CDCl₃) δ 137.2 (s, 1C), 133.7 (d, *J* = 6.6 Hz, 1C), 131.5 (s, 1C), 129.4 (s, 1C), 128.6 (d, *J* = 11.6 Hz, 1C), 127.8 (s, 2C), 127.6 (s, 1C), 127.5 (s, 1C), 126.5 (d, *J* = 133 Hz, 1C), 125.6 (s, 1C), 124.0 (s, 1C), 123.5 (s, 1C), 122.7 (d, *J* = 10.6 Hz, 1C), 121.6 (d, *J* = 12.1 Hz, 1C), 119.8 (d, *J* = 5.9 Hz, 1C), 42.5 (s, 1C), 36.8 ppm (d, *J* = 5.3 Hz, 1C); ¹H NMR (400 MHz, CDCl₃) δ 7.83 (d, *J* = 8.1 Hz, 1H), 7.82 (d, *J* = 6.5 Hz, 1H), 7.73 (dd, *J* = 14.9, *J* = 7.1 Hz, 1H), 7.55 (dt, *J* = 8.5 Hz, *J* = 1.3 Hz, 1H), 7.38 (dt, *J* = 7.5 Hz, *J* = 3.3 Hz, 1H), 7.31 (dt, *J* = 8.2 Hz, *J* = 1.1 Hz, 1H), 7.20-7.11 (m, 6H), 7.00 (dd, *J* = 8.0 Hz, *J* = 0.9 Hz, 2H), 3.30 (q, *J* = 6.7 Hz, 1H), 3.19-3.09 (m, 2H), 2.74-2.62 ppm (m, 2H); IR (KBr) ν 3301 (br, -NH), 3062, 3028, 2932, 1582 (m, P-C_{aryl}), 1477, 1211 (vs, P-O), 1092 (vs, P-N), 745 cm⁻¹; HRMS (EI) calcd for [¹²C₂₀H₁₈NPOS]⁺ 351.0847, found 351.0891.



Chemical Formula: C₅H₁₁O₃PS
Molecular Weight: 182.18

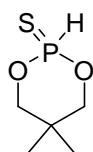
5,5-dimethyl-[1,3,2]-Dioxaphosphorinane thionic acid (DDPS-OH) (11):⁸²

In a 2 neck round bottom flask fitted with a condenser, DDPO (33.6 g, 224.0 mmol), toluene (100 ml) and sulphur (8.2 g, 246.0 mmol) were charged and heated at 110 °C using an oil bath. After 18 h at 110 °C, NMR analysis of an aliquot of the reaction showed the presence of unreacted DDPO. Hence, additional sulphur (3.6 g, 112.5 mmol) was added and the reaction was maintained at 110 °C. After 18h, the heat source was removed and the reaction mixture cooled to room temperature. The insoluble sulphur was filtered off and the clear yellow filtrate was concentrated *in vacuo* to yield a yellow syrup. Trituration of the syrup with cold toluene (80 ml) resulted in the precipitation of white solid. Filtration of the suspension yielded the target molecule DDPS-OH as a white powder (29.74 g, 163.6 mmol, 74 %). mp 73 °C, lit. 72-73;⁸² ³¹P-NMR δ 55.5 ppm; ¹³C-NMR δ = 77.3 (s, 1C), 77.2 (s, 1C), 32.3 (d, J = 6.1 Hz, 1C), 21.3 (s, 1C), 21.1 ppm (s, 1C); ¹H-NMR δ 8.04 (s, 1H), 4.16-3.94 (m, 4H), 1.12 (s, 3H), 1.00 ppm (s, 3H); HRMS (EI) calc for [¹²C₅H₁₁O₃PS]⁺ 182.0167 found 182.0185.



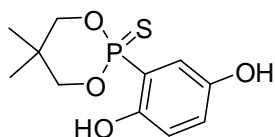
Chemical Formula: $C_5H_{10}ClO_2P$
Molecular Weight: 168.56

2-chloro-5,5-dimethyl-1,3,2-Dioxaphosphorinane, (DDP-Cl) (12):⁶¹ was synthesised using the literature procedure. Neopentylglycol (156 g, 1.5 mol) was added in portion to a thoroughly dried round bottom flask charged with PCl_3 (220 g, 1.6 mol), cooled with an ice bath and fitted with a condenser and an argon inlet tube. The reaction was stirred under argon pressure and HCl evolved. Once the HCl production ceased, the colourless translucent liquid was distilled (50 mbar, 80 C) to yield the target moisture sensitive DDP-Cl as a clear liquid (240 g, 95 %) ^{31}P -NMR ($CDCl_3$) δ = 147.6 ppm.

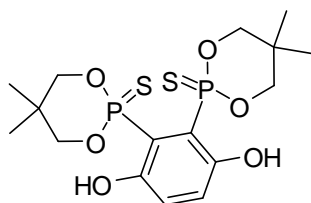


Chemical Formula: $C_5H_{11}O_2PS$
Molecular Weight: 166.18

5,5-dimethyl-1,3,2-Dioxaphosphorinane 2-sulfide (DDPS) (13):^{61,82} was synthesised using the procedure developed for the synthesis of DOPS. In a flame-dried three neck round bottom flask fitted with a gas inlet, a thermometer and a gas outlet leading to a NaOH aqueous solution, H_2S gas was bubbled through a solution of DDP-Cl (58.0 g, 348.0 mmol) in dry toluene (120 mL) at room temperature. The released acid was then trapped with triethylamine (53.0 g, 382.0 mmol). The suspension was filtered and concentrated *in vacuo* to yield a colorless powder (53.0 g, 320 mmol, 84 %) mp 84-85 °C, lit. 83-84.5 C;⁶¹ 1H -NMR ($CDCl_3$) δ = 7.77 (d, J_{P-H} = 600.9 Hz, 1H), 4.06-3.94 (m, 4H), 1.27 (s, 3H), 0.89 (s, 3H); ^{31}P -NMR ($CDCl_3$) δ 67.3 ppm.

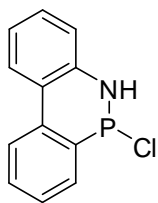


Chemical Formula: C₁₁H₁₅O₄PS
Molecular Weight: 274.27



Chemical Formula: C₁₆H₂₄O₆P₂S₂
Molecular Weight: 438.44

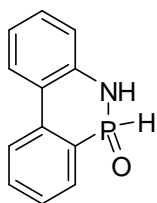
Reaction of DDPS with hydroquinone:⁵⁰ DDPS (6.2 g, 37.5 mmol) and dry toluene (20 ml) were charged in a thoroughly dried three-neck round bottom flask fitted with a condenser and a dropping funnel. While heating the solution at 80 C using an oil bath, a solution of benzoquinone (4.5 g, 41.3 mmol) in dry toluene (100 ml) was added dropwise under argon flow. Once the addition was completed, the temperature was raised to 110 C. After 4 h at 110 C, the heat source was removed and the brown reaction mixture was allowed to cool down to room temperature overnight. The insoluble black precipitate was removed by filtration and the filtrate was concentrated *in vacuo* to yield a brown solid containing multiple phosphorus compounds. Chloroform (100 ml) was added to the brown solid and the insoluble black solid was isolated by filtration. ¹H-NMR indicated that the insoluble compound was mainly hydroquinone while ³¹P-NMR showed the presence of traces of the target compound. ¹H-NMR (DMSO-d₆) δ= 9.67 (s, 1H), 9.13 (s, 1H), 7.11-6.72 (m, 3H), 4.2-4.01 (m, 2H), 3.89-3.79 (m, 2H), 1.04 (s, 3H), 0.99 (s, 3H); ³¹P-NMR δ = 82.8 ppm. Slow evaporation of the filtrate, yielded the precipitation of an insoluble white powder that was identified as the double addition product (2.25 g, 5.1 mmol, 27 %). m.p.>200 °C; ¹H-NMR (DMSO-d₆) δ 9.86 (s, 2H), 7.04 (t, J = 3.4 Hz, 2H), 3.80-3.37 (m, 8H), 1.12 (s, 6H), 0.64 (s, 6H); ³¹P-NMR (DMSO-d₆) δ 75.8 ppm;



Chemical Formula: C₁₂H₉ClNP
Molecular Weight: 233.63

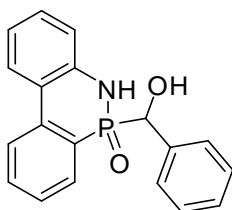
10-Chloro-9,10-dihydro-9-aza-10-phospha-phenanthrene (DAP-Cl) (17):⁹¹

PCl₃ (100 mL) was charged under Ar-flow in a moisture free 3 neck round bottom flask. 2-aminobiphenyl was added (25.0 g, 147.9 mmol) to the stirring solution of PCl₃ at room temperature. During the addition, HCl gas evolved. Using an oil bath, the reaction mixture at 130°C was heated. Once the evolution of HCl ceased (18 h), the heat source was removed and the reaction mixture was cooled to 40 °C. Once cooled, the excess PCl₃ was removed *in vacuo* to yield a thick dark brown solid. AlCl₃ was added (1.96 g, 14.8 mmol) to this dark solid and the mixture was heated to 165°C. When the solid melted, HCl gas evolved from the reaction. Once the evolution of HCl ceased (6h) the heat source was removed and the reaction mixture cooled down to room temperature to yield DAP-Cl as a brown solid (35 g, 147.0 mmol, 95 %). m.p. 132-134 °C, lit. 132-134 °C⁹¹; ¹H-NMR δ 8.21 (t, J = 6.5 Hz, 1H), 7.85 (dd, J = 14.0 Hz, J = 7.5 Hz, 1H), 7.68 (t, J = 7.7 Hz, 1H), 7.51 (t, J = 7.3 Hz, 1H), 7.39 (t, J = 7.5 Hz, 1H), 7.24 (t, J = 7.5 Hz, 1H), 7.04 (d, J = 7.8 Hz, 1H), 6.07 ppm (d, J = 25.0 Hz, 1H); ³¹P-NMR (CDCl₃) δ 84.2 ppm.



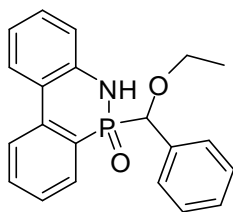
Chemical Formula: C₁₂H₁₀NOP
Molecular Weight: 215.19

9,10-dihydro-9-azaphosphaphenanthrene-10-oxide (DAPO) (16):⁹¹ In a 250 mL round bottom flask fitted with a condenser, DAP-Cl (35 g, 150.2 mmol) and CH₂Cl₂ (200 mL) were charged and heated up to 50 °C using an oil bath. After 1h at 50 °C, the hot purplish solution was poured over crushed ice (500 mL). HCl gas should evolve from the reaction mixture and an off-white solid should precipitate. Keep stirring while allowing the ice to melt. Once the ice is molten, filter the suspension to yield DAP-OH as an off white powder (22.56 g, 105.0 mmol, 63 %). m.p. 196 °C ³¹P-NMR (DMSO) δ = - 4.6 ppm The organic phase was reduced *in vacuo* to yield DAPO as a purple solid (9.03 g, 42.1 mmol, 28 %) m.p. 179 °C; ³¹P-NMR (DMSO-d₆) δ= 14.5 ppm.



Chemical Formula: C₁₉H₁₆NO₂P
Molecular Weight: 321.31

(10-Oxo-9,10-dihydro-9-aza-10λ⁵-phospha-phenanthren-10-yl)-phenylmethanol (18): DAPO (2.15 g, 10.0 mmol) and toluene were charged in a round bottom flask. The solution was heated to 110 °C using an oil bath and benzaldehyde (1.2 g, 12.0 mmol) was added dropwise using a syringe. The reaction mixture was maintained at 110 °C after the addition of benzaldehyde was completed. After 2h, the heat source was removed and the reaction mixture was cooled to room temperature. The cold brown suspension was filtered to yield a dark brown solid. The solid was then washed with cold acetone (3 x 20 mL) to yield the clean target compound as a white solid (1.06 g, 3.3 mmol, 33 %). ¹H-NMR (DMSO-d₆) δ = 8.49 (d, J = 2.35 Hz, 1H), 8.39 (d, J = 2.7 Hz, 1H); 8.13 (d, J = 6.4 Hz, 1H), 8.10 (d, J = 5.1 Hz, 1H), 7.98 (d, J = 8.4 Hz, 1H), 7.94 (d, J = 8.3 Hz, 1H), 7.89 (dd, J = 7.7 Hz, J = 0.9 Hz, 1H), 7.84 (dd, J = 7.6 Hz, J = 0.6 Hz, 1H), 7.65 (q, J = 7.5 Hz, 2H), 7.48 (dt, J = 7.4 Hz, J = 1.6 Hz, 2H), 7.36-7.30 (m, 2H), 7.20-7.16 (m, 12 H), 7.04 (t, J = 7.3 Hz, 2H), 7.97-6.87 (m, 2H), 6.09-5.90 (m, 2 H), 5.03 (d, J = 8.96 Hz, 1H), 4.93 ppm (d, J = 11.1 Hz, 1H); ³¹P-NMR (DMSO-d₆) δ = 21.5 (s, 1P), 21.0 ppm (s, 1P).

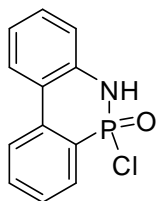


Chemical Formula: C₂₁H₂₀NO₂P
Molecular Weight: 349.36

10-(Ethoxy-phenyl-methyl)-9H-9-aza-10-phospha-phenanthrene 10-oxide (19): DAPO (1.19 g, 5.5mmol) and ethanol (80 mL) were charged into a round bottom flask fitted with a condenser and the reaction mixture was heated to 60 °C using an oil bath. Once DAPO was dissolved, benzaldehyde (0.71 g, 6.6 mmol) was added dropwise using a syringe. After 2.5 h, ³¹P-NMR analysis of a aliquot from the reaction mixture showed the presence of unreacted DAPO, hence the temperature of the oil bath was raised to 80 C. After reacting for 18 h at 80 °C, the heat source was removed and the reaction mixture allowed to cool to room temperature. The cold mixture was concentrated *in vacuo* to yield a pale orange syrup that had an almond smell. In order the unreacted benzaldehyde, the syrup was dissolved in hot toluene (40 ml) and the solution allowed to cool to room temperature. The precipitated white solid was isolated by filtration and identified as the reaction product of the Abramov product with ethanol (0.28 g, 0.8 mmol, 17 %) MS (EI)m/z = 349; ³¹P-NMR δ = 40.0 ppm; ¹³C-NMR (CDCl₃) 145.9 (s, 1C), 143.1 (d, 9.4 Hz, 1C), 138.1 (d, *J* = 4.8 Hz, 1C), 135.2 (s, 1C), 133.2 (s, 1C), 133.2 (s, 1C), 132.8 (d, *J* = 8.5 Hz, 1C), 129.9 (s, 1C), 129.7 (s, 1C), 128.9 (s, 1C), 128.3 (s, 1C), 127.7 (s, 1C), 127.4 (s, 1C), 127.4 (d, *J* = 2.8 Hz, 1C), 126.8 (s, 1C), 126.6 (s, 1C), 126.4 (s, 1C), 123.5 (d, *J* = 20.3 Hz, 1C), 70.2 (d, *J* = 105. 1 Hz, 1C), 60.2 (d, *J* = 7.2 Hz, 1C), 15.5 ppm (d, *J* = 6.8 Hz, 1C); ¹H-NMR (CDCl₃) δ = 7.97 (dd, *J* = 11.9 Hz, *J* = 7.7 Hz, 1H), 7.72 (t, *J* = 7.4 Hz, 1H), 7.53-7.48 (m, 2H), 7.42-7.23 (m, 8H), 7.09 (d, *J* = 7.4 Hz, 1H), 5.06 (d, *J* = 15.7 Hz, 1H), 3.88-3.74 (m, 1H), 3.59 (s, 1H), 3.49-3.34 (m, 1H), 0.84 ppm (t, *J* = 7.0 Hz, 3H).

Oxidation of DAPO using H₂O₂:⁹⁷ DAPO (4.30 g, 20.0 mmol) and ethanol (30 ml) were charged in a three-neck round bottom flask fitted with a condenser. The mixture was heated to 70 °C using an oil bath. While heating, H₂O₂ (30 ml, 30 % aq.) was added dropwise using a dropping funnel over a period of 30 min. The white suspension gradually became darker. After 1h at 70 °C, the suspension was fully black and the heat source was removed to allow the reaction to cool to room temperature. The ethanol was removed *in vacuo* to yield a black aqueous suspension. The aqueous mixture was extracted with dichloromethane (3 x 50 mL) and the combined organic fractions were dried over Na₂SO₄ and concentrated *in vacuo*. ¹H and ³¹P-NMR indicated the formation of multiple phosphorus compounds that could not be separated.

Oxidation of DAPO using KMnO₄:⁹⁸ DAPO (4.3 g, 20.0 mmol) and pyridine (50 ml) were charged in a round bottom flask fitted with a condenser. While heating to 80 °C, a solution of KMnO₄ (6.3 g, 40.0 mmol) in water (80 mL) was added in portions over 15 min. After 5h, the heat source was removed and the reaction cooled to room temperature. ¹H and ³¹P NMR of the brown solid obtained after removal of the solvent *in vacuo* did not indicate the presence of an organophosphorus compound.

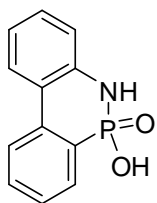


Chemical Formula: C₁₂H₉ClNOP
Molecular Weight: 249.63

6-chloro-5,6-dihydro- dibenz[c,e][1,2]azaphosphorine, (DAPO-Cl) (22):¹⁰⁰

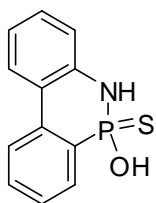
2-aminobiphenyl (8.46 g, 50.0 mmol) was added in portions over a period of 15 min to a round bottom flask charged with POCl₃ (8.43 g, 55.5 mmol) and fitted with a condenser and a bubbler. Once the addition was completed, the reaction mixture was heated up to 130 °C using an oil bath. After 9h at 130 °C, HCl gas stopped evolving, hence the heat source was removed and the reaction mixture cooled to room temperature. The resulting brown solid was dissolved in diethyl ether (100 ml) and a solution of triethylamine (5.6 g, 55.5 mmol) in diethylether (50 ml) was added drop-wise over a period of 90 min using a dropping funnel. During the addition HCl gas evolved and a white precipitate formed. After reacting for 3h at room temperature, the production of HCl had ceased. The formed triethyl amonium chloride salt was removed by filtration and the concentration of the filtrate yield the target molecule as a white powder (6.7 g, 4.6 mmol, 9.2 %). ³¹P-NMR (CDCl₃) δ = 9.77 ppm; MS(EI) m/z = 249.01

(DAPO-OH): under atmospheric pressure, an aqueous solution of NaOH (0.86 g, 22.0 mmol in 30 ml) and acetone (30 ml) were charged into a round bottom flask. DAPO-Cl (5.0 g, 20.0 mmol) was added in portions to the NaOH solution. After reacting for 1h at room temperature, ³¹P-NMR analysis indicated the presence of two phosphorus-containing molecules (δ = 0.58, -10.20 ppm). However neither the ¹H-NMR nor the mass spectroscopic analysis could confirm the formation of the target compound.



Chemical Formula: C₁₂H₁₀NO₂P
Molecular Weight: 231.19

9,10-dihydro-9-azaphosphaphenanthrenic acid DAPO-OH (21): Under atmospheric pressure, NaOH (0.44 g, 11.0 mmol) was charged in round bottom flask, dissolved in water (30 ml) and cooled using an ice bath. A suspension of DAPO (1.07 g, 5.0 mmol) in acetone (30 ml) was added drop-wise to the cold solution using a dropping funnel. After 1h at 0 °C, the solid was fully dissolved to yield a brown solution. ¹H and ³¹P- NMR analysis of reaction mixture after removal of the acetone *in vacuo* indicated the presence of a single organophosphorus compounds ($\delta = 15.9$ ppm) $m/z = 253$. The aqueous solution was used without further purification for the next step. HCl (0.36 % aq, 1.0 ml) was added dropwise to the aqueous solution. The white precipitate formed was isolated by filtration to yield a white powder (0.8 g, 3.4 mmol, 70 %) that was confirmed as the target compound by mass spectroscopy $m/z = 231$. ³¹P-NMR (CDCl₃) δ 6.77 ppm; HRMS (EI) calculated for [C₁₂H₁₀NO₂P]⁺ 231.0449 found 231.0472



Chemical Formula: C₁₂H₁₀NOPS
Molecular Weight: 247.25

9,10-dihydro-9-azaphosphaphenanthrene thionic acid DAPS-OH (23):

DAPO (21.5 g, 100.0 mmol), S₈ (3.8 g, 118.7 mmol) and toluene (100 ml) were charged in a round bottom flask fitted with a condenser and heat to 110 °C using an oil bath. After 4 h at 110 °C, the heat source was removed and the reaction mixture allowed to cool to room temperature. The cold reaction was concentrated *in vacuo* to yield a yellowish syrup. The syrup was washed with cold toluene (3 x 80 mL) to the target molecule as pale-yellow solid (22.6 g, 91.5 mmol, 91 %). ³¹P-NMR (CDCl₃) δ 56.3 ppm; ¹³C-NMR (CDCl₃) δ 137.7 (s, 1C), 135.2 (s, 1C), 131.8 (s, 1C), 129.7 (s, 1C), 129.4 (s, 1C), 128.3 (d, *J* = 162.3, 1C), 127.3 (s, 1C), 125.2 (s, 1C), 123.9 (d, *J* = 9.3 Hz, 1C), 121.8 (s, 1C), 118.8 ppm (d, *J* = 7.2 Hz, 1C); ¹H-NMR (CDCl₃) δ 8.27 (dd, *J* = 18.1 Hz, *J* = 7.6 Hz, 1H), 8.03 (t, *J* = 7.3 Hz, 2H), 7.68 (t, *J* = 7.7 Hz, 1H), 7.51 (dt, *J* = 7.4 Hz, *J* = 2.3 Hz, 1H), 7.33-7.23 (m, 2H), 7.19-7.12 (m, 2H), 6.93 (d, *J* = 7.9 Hz, 1H), 5.4 ppm (s, 2H). HRMS(EI) calculated for [C₁₂H₁₀NOPS]⁺ 247.0176 found 247.0229.



Chemical Formula: C₁₂H₁₀NPS
Molecular Weight: 231.25

9,10-dihydro-9-azaphosphaphenanthrene-10-sulfide DAPS (24) was synthesised according to the procedure developed for the synthesis of DOPS:¹¹⁹ DAPO (11.6 g, 50.0 mmol) was charged in a three neck round bottom flask and dissolved in toluene (100 mL). H₂S was bubbled through the reaction mixture for 2 h and the acid formed was trapped by addition of triethylamine (5.6 g, 55.3 mmol). After 1h at room temperature, the triethyl ammonium chloride salt was removed by filtration. The orange filtrate was concentrated *in vacuo* to yield the target molecule as an orange solid (7.6 g, 32.9 mmol, 66 %).³¹P-NMR (CDCl₃) δ 23.5 ppm; ¹H-NMR (CDCl₃) δ 8.60 (d, *J* = 506.2 Hz, 1H), 8.05 (dd, *J* = 16.6 Hz, *J* = 6.5 Hz, 1H), 7.94 (t, *J* = 5.2 Hz, 1H), 7.91 (d, *J* = 7.6 Hz, 1H), 7.68 (t, *J* = 7.7 Hz, 1H), 7.55 (dt, *J* = 7.3 Hz, *J* = 1.7 Hz, 1H), 7.31 (t, *J* = 7.3 Hz, 1H), 6.95 (d, *J* = 7.5 Hz, 1H), 6.81 (dd, *J* = 16.0 Hz, *J* = 8.0 Hz, 1H); HRMS (EI) calculated for [C₁₂H₁₀NPS]⁺ 231.0272 found 231.281.

7.3 Preformulation:

In order to study the influence of different phosphorus loadings on the flame retardancy of epoxy phenol novolac cured with DICY and fenuron, the resin was first grafted with a known loading of organophosphorus compound. For a given amount of formulation (m_f), the amount of organophosphorus flame retardant (m_{FR}) required for the preformulation step was calculated using this equation:

$$m_{FR} = \frac{m_f \times \%P_{FR}}{\%P_f}$$

where $\%P_{FR}$ is the phosphorus content in the flame retardant and $\%P_f$ is the phosphorus content in the formulation.

The amount of epoxy resin (m_{ep}) was then extrapolated knowing that in a typical formulation for epoxy resin the ratio of epoxy resin to dicydiamide (DICY) to fenuron is 100:6:2.

The epoxy resin (m_{ep}) was degassed in the round bottom flask for 1 h under vacuum while heating at 120 °C using an oil bath. Once degassed, the flame retardant

(m_{FR} , %P_f) and triethanol amine (0.6 g, 1.0 wt %) were charged and the temperature of the oil bath was raised to 140 °C. After 2h at 140 °C, the heat source was removed and the modified epoxy resin allowed to cool 80 °C. The liquid or highly viscous modified resin was then formulated.

7.4 Formulation and Curing:

The formulation and curing of the modified resins was achieved modified published procedure.[Schaefer 2007, Ciesielski 2008]The DICY-cured polymers were obtained by mixing the resin with 6.0 phr DICY (Dyhard 100S) and 2.0 phr 1,1-dimethyl-3-phenyl-urea (Dyhard UR 300), as a curing accelerator, in a Speedmixer DAC 150 SVZ from Hauschild at 3500 rotations per minute for 60 s. The formulation was transferred to an aluminum mold and transferred to an oven at 100 °C. The temperature of the oven was raised at 8 °C/h until the resin was cured. Then, the resins were cured at 130 °C for 1 h and postcured at 200 °C for 2 h. The samples were allowed to cool down slowly to room temperature.

7.5 Cone calorimetry

The cone calorimeter tests were conducted on 100 x 100 x 6 mm³ samples with an irradiation flux of 35 kW/m². In figure 9 the curves of Heat Release Rate of the materials are reported.

7.6 Thermal desorption mass spectroscopy

The TD-MS measurements were carried out in a vacuum chamber coupled to a heatable sample-carrier made of stainless steel, a high-vacuum system from Pfeiffer and a HAL IV RGA 201 from HIDEN Analytics, UK. Powdered samples of the cured resin (1-5 mg) were charged into the sample holder and the system was evacuated (10⁻⁸ hPa). The cured resins were heated from room temperature to 500 °C at a rate of 10 °C/min while the pyrolysis gases were detected with the mass spectrometer.

SCIENTIFIC CONTRIBUTIONS

7.7 Publications

M. Rakotomalala, S. Wagner, T. Zevaco, M. Ciesielski, O. Walter, M. Döring, "Synthesis and reactivity of 6*H*-dibenzo[*c,e*][1,2]oxaphosphinine 6-sulfide, a novel thiophosphacyclic molecule", *Heterocycles*, **2011**, 8 (4), 743-753.

M. Rakotomalala, M. Ciesielski, T. Zevaco, M. Döring, "New Phosphacyclic Molecules and their Application as Flame Retardants for Epoxy Resins", *Phosphorus, Sulfur, Silicon and related elements*, **2011**, 186 (4), 989-996.

Novel Derivatives of 9,10-Dihydro-9-oxa-10-Phosphaphenanthren-10-one, Krems Chemie Chemical Services AG, World Patent WO2011000019

M. Rakotomalala, S. Wagner, M. Döring, "Recent developments in halogen free flame retardants for epoxy resins for electrical and electronic applications", *Materials*, **2010**, 3, 4300-4327.

7.8 Oral Presentations

- Jun. 2011 13th European Meeting on Fire Retardants Polymers, FRPM 11, Alessandria, Italy.
Oral Presentation: "Synthesis and investigation of new heterocyclic phosphorus compound as flame retardant in epoxy resins"
- Jul. 2010 18th International Conference on Phosphorus Chemistry, Wroclaw, Poland,
Oral Presentation: "New heterocyclic phosphorus compounds for flame retardant applications"
- Jul. 2009 12th European Meeting on Fire Retardants Polymers, FRPM 09, Poznan, Poland,
Oral Presentation: "Synthesis and investigation of new heterocyclic phosphorus compound as flame retardant in epoxy resins"

REFERENCE LIST

- (1) Ellis, B. *Chemistry and technology of epoxy resin*; Blackie Academic & Professional: London, UK, 1993.
- (2) May, C. A. *Epoxy Resins, Chemistry and Technology* New York, USA, 1988.
- (3) Pham, H. Q.; Marks, M. J. In *Ullmann's Encyclopedia of Industrial Chemistry*; Wiley-VCH Verlag GmbH & Co. KGaA: 2000.
- (4) Weil, E. D.; Levchik, S. J. *Fire Sci.* **2004**, *22*, 25.
- (5) Woodrow, B.; The Geneva Association (International association for the study of insurance economics): 2010; Vol. Bulletin n°26.
- (6) Stewart, R. <http://www.plastemart.com/upload/Literature/Demand-non-halogenated-flame-retardant-additives-to-grow-on-environmental-issues.asp>. (accessed May 2011)
- (7) Sanapala, R.; Sood, B.; Das, D.; Pecht, M. *Ieee T. Electron. Pa. M.* **2009**, *32*, 272.
- (8) Sanapala, R.; Sood, B.; Das, D.; Pecht, M.; Huang, C. Y.; Tsai, M. Y. In *2008 Emap Conference Proceedings 2008*, p 195.
- (9) Chapman, N. B.; Isaacs, N. S.; Parker, R. E. *J. Chem. Soc.* **1959**, 1925.
- (10) Leisegan, E.; Stephen, A. M. *J. Appl. Polym. Sci.* **1970**, *14*, 1961.
- (11) Mourits, A. P.; Gibson, A. G. *Fire properties of polymer composites* Dordrecht, Netherlands, 2006.
- (12) Bocchini, S.; Camino, G. In *Fire retardancy of polymeric materials*; Wilkie, C. A., Morgan, A. B., Eds.; CRC press: London, 2010, p 77.
- (13) Wang, D. Y.; Liu, Y.; Wang, Y. Z.; Artiles, C. P.; Hull, T. R.; Price, D. *Polym. Degrad. Stabil.* **2007**, *92*, 1592.
- (14) Washington, D. o. E. S. o. Olympia, WA; Vol. 2011.
- (15) Bashkar, B.; Bullet, K. J.; Cunliffer, L. K.; Hull, T. R.; Milness, G. J.; Hunt, B. J.; Joseph, P. *Polym. Degrad. Stabil.* **2007**, *92*, 765.
- (16) *Official Journal of the European Union* **2003**, *37*, 19.
- (17) *Official Journal of the European Union* **2003**, *37*, 24.
- (18) Burreau, S.; Zebuehr, Y.; Broman, D.; Ishaq, R. *Sci. Total. Environ.* **2006**, *366*, 659.
- (19) Coasta, L. G.; Giordano, G. *Neurotoxicity* **2007**, *28*, 1047.
- (20) Defosse, M.; <http://www.plasticstoday.com/articles/plastic-additives-flame-retardants-demand-is-on-fire>. (accessed in May 2011)

- (21) Price, D.; Horrocks, A. R. In *Fire retardancy of polymeric materials*; 2nd Edition ed.; Wilkie, C. A., Morgan, A. B., Eds.; CRC Pres: London, 2010, p 19.
- (22) Camino, G.; Costa, L.; Dicortemiglia, M. P. L. *Polym Degrad Stabil* **1991**, *33*, 131.
- (23) Vogt, J. *Thermochim Acta* **1985**, *85*, 411.
- (24) Bishop, D. P.; Smith, D. A. J. *Appl. Polym. Sci.* **1970**, *14*, 205.
- (25) Patterson-Jones, J. C. J. *Appl. Polym. Sci.* **1975**, *19*, 1539.
- (26) Levchik, S.; Weil, E. D. *Polym. Int.* **2004**, *53*, 1901.
- (27) Schartel, B.; Braun, U.; Balabanovich, A. I.; Artner, J.; Ciesielski, M.; Doring, M.; Perez, R. M.; Sandler, J. K. W.; Altstadt, V. *Eur. Polym. J.* **2008**, *44*, 704.
- (28) Biswas, B.; Kandola, B. K.; Horrocks, A. R.; Price, D. *Polym. Degrad. Stabil.* **2007**, *92*, 765.
- (29) Jimenez, M.; Duquesne, S.; Bourbigot, S. *Thermochim Acta* **2006**, *449*, 16.
- (30) Camino, G.; Costa, L.; Martinasso, G. *Polym. Degrad. Stabil.* **1989**, *23*, 359.
- (31) Levchik, S. V.; Weil, E. D. *J. Fire Sci.* **2006**, *24*, 345.
- (32) Levchik, s. v. W., e. d. In *Advances in Fire Retardant Materials* 2008, p 41.
- (33) Bourbigot, S.; Duquesne, S. *J. Mater. Chem.* **2007**, *17*, 2283.
- (34) Bourbigot, S.; Le Bras, M.; Leeuwendal, R.; Shen, K. K.; Schubert, D. *Polym. Degrad. Stabil.* **1999**, *64*, 419.
- (35) Vannier, A.; Duquesne, S.; Bourbigot, S.; Castrovinci, A.; Camino, G.; Delobel, R. *Polym. Degrad. Stabil.* **2008**, *93*, 818.
- (36) Gerard, C.; Fontaine, G.; Bourbigot, S. *Materials* **2010**, *3*, 4476.
- (37) Katsoulis, C.; Kandare, E.; Kandola, B. K. *Polym. Degrad. Stabil.* **2011**, *96*, 529.
- (38) Liu, W. C.; Varley, R. J.; Simon, G. P. *Polymer* **2007**, *48*, 2345.
- (39) Franchini, E.; Galy, J.; Gerard, J. C.; Tabuani, D.; Medici, A. *Polym. Degrad. Stabil.* **2009**, *94*, 1728.
- (40) Wang, X.; Hu, Y.; Song, L.; Xing, W.; Lu, H. *Journal of Polymer Science Part b- Polymer Physics* **2010**, *48*, 693.
- (41) Camino, G.; Tartaglione, G.; Frache, A.; Manfredi, C.; Costa, G. *Polym. Degrad. Stabil.* **2005**, *90*, 354.
- (42) Bourbigot, S.; Duquesne, S.; Fontaine, G.; Bellayer, S.; Turf, T.; Samyn, F. *Mol. Cryst. Liq. Cryst.* **2008**, *486*, 1367.
- (43) Becker, O.; Cheng, Y. B.; Varley, R. J.; Simon, G. P. *Macromolecules* **2003**, *36*, 1616.
- (44) (EFRA), <http://www.cefic-efra.com/content/Default.asp?PageID=130> (accessed in May 2011)
- (45) Jimenez, M.; Duquesne, S.; Bourbigot, S. *Surf. Coat. Tech.* **2006**, *201*, 979.
- (46) Fontaine, G.; Bourbigot, S. *J. Appl. Polym. Sci.* **2009**, *113*, 3860.

- (47) Hergenrother, P. M.; Thompson, C. M.; Smith, J. G.; Connell, J. W.; Hinkley, J. A.; Lyon, R. E.; Moulton, R. *Polymer* **2005**, *46*, 5012.
- (48) Toldy, A.; Toth, N.; Anna, P.; Marosi, G. *Polym. Degrad. Stabil.* **2006**, *91*, 585.
- (49) Wang, C. S.; Lin, C. H.; Chen, C. Y. *J. Polym. Sci. Pol. Chem.* **1998**, *36*, 3051.
- (50) Worku, A.; Bharadwaj, A.; Thibault, R.; Wilson, M.; Potts, D.; Appl., P. I., Ed.; Dow Global Technologies Inc.: USA, 2010; Vol. WO 2010025165 A1, p 47.
- (51) Braun, U.; Balabanovich, A. I.; Schartel, B.; Knoll, U.; Artner, J.; Ciesielski, M.; Doring, M.; Perez, R.; Sandler, J. K. W.; Altstadt, V.; Hoffmann, T.; Pospiech, D. *Polymer* **2006**, *47*, 8495.
- (52) Sutker, B. J. In *Ullmann's Encyclopedia of Industrial Chemistry*; Wiley-VCH Verlag GmbH & Co. KGaA: 2000.
- (53) Schafer, A.; Seibold, S.; Lohstroh, W.; Walter, O.; Doring, M. *J. Appl. Polym. Sci.* **2007**, *105*, 685.
- (54) Seibold, S.; Schafer, A.; Lohstroh, W.; Walter, O.; Doring, M. *J. Appl. Polym. Sci.* **2008**, *108*, 264.
- (55) Quin, L. D. *A Guide to Organophosphorus Chemistry*; Wiley-Interscience: New-York, USA, 2000.
- (56) Andrews, K. J. M.; Atherton, F. R.; Bergel, F.; Morrison, A. L. *J. Chem. Soc.* **1954**, 1638.
- (57) Binder, H.; Fischer, R. *Chem. Ber.-Recl.* **1974**, *107*, 205.
- (58) Borch, R. F.; Canute, G. W. *J. Med. Chem.* **1991**, *34*, 3044.
- (59) Svava, J.; Weferling, N.; Hofmann, T. *Phosphorus Compounds, Organic*; Wiley-VCH Verlag GmbH & Co. KGaA, 2000.
- (60) Krawiecki, C.; Michalski, J. *J. Chem. Soc.* **1960**, 881.
- (61) Zwierzak, A. *Can. J. Chem.* **1967**, *45*, 2501.
- (62) Reiffenstein, R. J.; Hulbert, W. C.; Roth, S. H. *Annu. Rev. Pharmacol.* **1992**, *32*, 109.
- (63) Cherkasov, R. A.; Kutyrev, G. A.; Pudovik, A. N. *Tetrahedron* **1985**, *41*, 2567.
- (64) Abramov, A. A. *Dokl Akad Nauk Sssr* **1950**, *74*, 1051.
- (65) Wang, C. S.; Shieh, J. Y. *Polymer* **1998**, *39*, 5819.
- (66) Wang, C. S.; Lee, M. C. *Polymer* **2000**, *41*, 3631.
- (67) Atherton, F. R. *Q. Rev. Chem. Soc.* **1949**, *3*, 146.
- (68) Atherton, F. R.; Howard, H. T.; Todd, A. R. *J. Chem. Soc.* **1948**, 1106.
- (69) Atherton, F. R.; Openshaw, H. T.; Todd, A. R. *J. Chem. Soc.* **1945**, 660.
- (70) Atherton, F. R.; Openshaw, H. T.; Todd, A. R. *J. Chem. Soc.* **1945**, 382.
- (71) Atherton, F. R.; Todd, A. R. *J. Chem. Soc.* **1947**, 674.
- (72) Lapp, R. L.; Jacobson, R. A. *Cryst. Struct. Commun.* **1980**, *9*, 65.

- (73) Krishna, J. R.; Krishnaiah, M.; Prasad, G. S.; Reddy, C. S.; Puranik, V. G. *Acta Crystallogr. E* **2007**, *63*, O2407.
- (74) Fernandez, M. D.; Vlaar, C. P.; Fan, H.; Liu, Y. H.; Fronczek, F. R.; Hammer, R. P. *J. Org. Chem.* **1995**, *60*, 7390.
- (75) Koziol, A. E.; Suwinska, K. *Acta Crystallogr. C* **1992**, *48*, 398.
- (76) McConnell, R. L.; Coover, H. W. J. In *Eastman Kodak co USA*, 1960; Vol. US 2952701 19600913.
- (77) Paulik, F. E.; Weis, C. R. In *Monsento Co USA*, 1994; Vol. US 5276066, p 10.
- (78) Gao, L.-P.; Wang, D. Y.; Wang, Y. Z.; Wang, J.-S.; Yang, B. *Polym. Degrad. Stabil.* **2008**, *93*, 1308.
- (79) Buser, A. J. W.; Schutyser, J. A. J. In *Akzo Nobel N. V.* Netherland, 1998; Vol. WO 9807731 A1.
- (80) Weil, E. D.; Fearing, R. B.; Eisenberg, B. J. In *Stauffer Chemical Co USA*, 1973; Vol. US 3746572 A, p 9.
- (81) Diederichs, J.; Ciesielski, M.; Stoess, K.; Doering, M. In *Annual conference on recent advances in flame retardancy of polymeric materials*; BCC Research: Stamford, 2009; Vol. 20th, p 85.
- (82) Bruzik, K.; Stec, W. J. *J. Org. Chem.* **1981**, *46*, 1618.
- (83) Zich, T.; Artner, J.; Mehofer, B.; Doering, M.; Ciesielski, M.; Zwick, G.; Rakotomalala, M.; Austria, Germany, WO 2011000019 .
- (84) Kumaraswamy, S.; Senthil Kumar, K.; Raja, S.; Kumara Swamy, K. C. *Tetrahedron* **2001**, *57*, 8181.
- (85) Balaraman, E.; Kumara Swamy, K. C. *Synthesis* **2004**, *2004*, 3037.
- (86) Swamy, K. C. K.; Kumaraswamy, S.; Raja, S.; Kumar, K. S. *J. Chem. Crystallogr.* **2001**, *31*, 51.
- (87) Mueller, P. G.; Doering, M. private discussion 2011.
- (88) Ciesielski, M.; Schafer, A.; Doring, M. *Polym. Advan. Technol.* **2008**, *19*, 507.
- (89) Schafer, A.; Seibold, S.; Walter, O.; Doring, M. *Polym. Degrad. Stabil.* **2008**, *93*, 557.
- (90) Campbell, I. G. M.; Way, J. K. *J. Chem. Soc.* **1960**, 5034.
- (91) Dewar, M. J. S.; Kubba, V. P. *J. Am. Chem. Soc.* **1960**, *82*, 5685.
- (92) Saito, T.; Ohishi, H. Japan, 1980; Vol. DE3010375 (A1).
- (93) Kolodiazhnyi, O. I.; Prynada, N. *Tetrahedron Lett.* **2000**, *41*, 7997.
- (94) Doak, G. O.; Freedman, L. D. *Chem. Rev.* **1961**, *61*, 31.
- (95) Binder, H.; Fischer, R. *Chem. Ber.-Recl.* **1974**, *107*, 205.
- (96) Schmidpe, A.; Rossknec, H.; Schumann, K. *Z. Naturforsch. B* **1970**, *B 25*, 1182.
- (97) Jenkins, R. N.; Freedman, L. D. *The Journal of Organic Chemistry* **1975**, *40*, 766.

- (98) Wang, T.-S.; Shau, M.-D. *J Appl Polym Sci* **1998**, *70*, 1877.
- (99) Quin, G. S.; Jankowski, S.; Quin, L. D. *Phosphorus Sulfur* **1996**, *115*, 93.
- (100) Morrison, D. C. *J. Am. Chem. Soc.* **1951**, *73*, 5896.
- (101) Dannley, R. L.; Wagner, P. L. *J. Organ.Chem.* **1961**, *26*, 3995.
- (102) Dannley, R. L.; Grava, A. *Can. J. Chem.* **1965**, *43*, 3377.
- (103) Lister, J. H.; Timmis, G. M. *J. Chem. Soc. C: Organic* **1966**, 1242.
- (104) Liu, Y. L. *J. Polym. Sci. Pol. Chem.* **2002**, *40*, 359.
- (105) Gao, F.; Tong, L. F.; Fang, Z. P. *Polym. Degrad. Stabil.* **2006**, *91*, 1295.
- (106) Camino, G.; Costa, L. *Polym. Degrad. Stabil.* **1988**, *20*, 271.
- (107) Fenimore, C. P.; Jones, G. W. *Combust. Flame* **1964**, *8*, 133.
- (108) Granzow, A.; Cannelongo, J. F. *J. Appl. Polym. Sci.* **1976**, *20*, 689.
- (109) Bourbigot, S.; Duquesne, S. In *Fire retardancy of polymeric materials*; Wilkie, C. A., Morgan, A. B., Eds.; CRC presss: London, 2010, p 129.
- (110) Levchik, S. V.; Camino, G.; Costa, L.; Luda, M. P. *Polym. Degrad. Stabil.* **1996**, *54*, 317.
- (111) Gao, M.; Yang, S. S. *J. Appl. Polym. Sci.* **2010**, *115*, 2346.
- (112) Samyn, F.; Bourbigot, S.; Jama, C.; Bellayer, S. *Polym. Degrad. Stabil.* **2008**, *93*, 2019.
- (113) Hartwig, A.; Putz, D.; Schartel, B.; Bartholmai, M.; Wendschuh-Josties, M. *Macromol. Chem. Phys.* **2003**, *204*, 2247.
- (114) Schartel, B.; Knoll, U.; Hartwig, A.; Putz, D. *Polym. Advan. Technol.* **2006**, *17*, 281.
- (115) Manias, E.; Polizos, G.; Nakajima, H.; Heidecker, M. J. In *Flame retardant polymer nanocomposie*; Morgan, A. B., Wilkie, C. A., Eds.; Wiley: New York, 2007, p 31.
- (116) Garea, S. A.; Iovu, H.; Bulearca, A. *Polym. Test* **2008**, *27*, 100.
- (117) Wang, W. S.; Chen, H. S.; Wu, Y. W.; Tsai, T. Y.; Chen-Yang, Y. W. *Polymer* **2008**, *49*, 4826.
- (118) Kaya, E.; Tanoglu, M.; Okur, S. *J. Appl. Polym. Sci.* **2008**, *109*, 834.
- (119) Rakotomalala, M.; Wagner, S.; Zevaco, T.; Ciesielski, M.; Walter, O.; Doring, M. *Heterocycles* **2011**, *83*, 743.

LIST OF FIGURES

Figure 1-1: Synthesis of diglycidyl ether of bisphenol A from epichlorohydrin. ³	2
Figure 1-3: Commonly used epoxy resins for EE applications.	3
Figure 1-4: Newly formed bonds during curing of epoxy resins using: (a) amine or (b) phenol-novolac.	4
Figure 1-5: Regularly used hardeners for epoxy resins.	4
Figure 1-6: Structure of tetrabromobisphenol A.....	5
Figure 1-7: Predicted world flame retardant demand (in 1000 metric tonnes) for 2014 by The Freedomia Group Inc.....	6
Figure 1-8: Overview of the publications dealing with flame retardancy (Sci Finder).....	6
Figure 1-9: Commercially available organophosphorus flame retardants for EE application.....	12
Figure 2-1: Schematic representation of the apparatus set-up for UL 94 vertical test. a) sample; b) bunsen burner; c) cotton.....	15
Figure 2-2: Schematic representation of the set-up apparatus for the oxygen index test. a) flame source; b) sample. ⁵²	16
Figure 2-3: Schematic representation of the apparatus set up for cone calorimetric measurements. ⁵²	17
Figure 3-1: Synthesis of DOPO from 2-hydroxy biphenyl.	18
Figure 3-2: Mechanism of formation of phosphonic acid derivatives via a) Michaelis-Becker reaction and b) Arbusov reaction.	19
Figure 3-3: ¹ H NMR spectra of a) 9,10-dihydro-9-oxa-10-phosphaphenanthrene-10-oxide (1) and b) 6 <i>H</i> -dibenzo[<i>c,e</i>][1,2]oxaphosphinine 6-sulfide (4) in CDCl ₃ . * emphasize the doublets corresponding to the P-H bond.....	20
Figure 3-4: H,H-gCOSY of 6 <i>H</i> -dibenzo[<i>c,e</i>][1,2]oxaphosphinine 6-sulfide (4) in CDCl ₃	21
Figure 3-5: View of the molecular structure of (4) in the crystal, aromatic H atoms and solvent molecules omitted due to reasons of clarity. Selected bond lengths [pm]: (7) S1-P 190.94 (4), O1-P 161.77 (5), P-H1 138.03 (3).....	21
Figure 3-6: Synthesis of compounds (5) from (4).	22
Figure 3-7: View of the molecular structure of (7), (8) and (9) in the crystal, H atoms and solvent molecules omitted due to reasons of clarity. Selected bond lengths [pm] and torsion angles [°]: (7) S1-P 191.15(4), O2-P 158.57(4), S1-P-O2-C13 37.72; (8) S1-P 193.65(6), N1-P 162.06(4), S1 P-N1-C13 10.07; (9) S1-P 191.96(6), N1-P 163.71(4), S1-P-N1-C13 20.40.....	24
Figure 3-8: Synthesis of DDPS-OH (11) from DDPO (10).	25
Figure 3-9: Synthesis of DDPS (13) from DDP-Cl (12).....	26
Figure 3-10: Reactivity of DDPS with benzoquinone.....	27

Figure 3-11: Heterocyclic phosphorus substrates investigated as HFFR in epoxy resins.	28
Figure 3-12: ¹ H-NMR spectrum of DAP-Cl in CDCl ₃	29
Figure 3-13: ¹ H, ¹ H-gCOSY of DAPO (a) and its tautomer (b).....	30
Figure 3-14: ¹ H-NMR spectra of the two isolated tautomers of DAPO (16). The asterics specify the signal corresponding to the P-H bond.	31
Figure 3-15: Equilibrium between the two tautomeric forms of DAPO.....	31
Figure 3-16: Reaction of DAPO with benzaldehyde in toluene.....	32
Figure 3-17: Reaction of DAPO with benzaldehyde in ethanol.....	33
Figure 3-18: Suggested mechanism for the formation of compound 19.	33
Figure 3-19: Oxidation of DOPO to form DOPO-OH.	33
Figure 3-20: Synthesis of DAPO-OH (21) by oxidation of DAPO (16).....	34
Figure 3-21: Synthesis of DAPO-OH from DAPO-Cl.	35
Figure 3-22: Oxidation of DAPO with sodium hydroxide.....	36
Figure 3-23: Synthesis of DAPS-OH from DAPO.	37
Figure 3-24: Synthesis of DAPS (26) from DAP-Cl (17).....	37
Figure 3-25: ¹ H-NMR spectra of DAPS (top) and DOPS (bottom) measured in CDCl ₃	38
Figure 3-26: Summary of the heterocyclic organophosphorus compounds.....	39
Figure 4-1: Chemical addition of Phosphorus molecules to DEN 438.	40
Figure 4-2: Curing condition of chemically modified DEN438 with DICY (middle) and Fenuron (right).....	41
Figure 4-3: Influence of phosphaphenanthrene derivatives on the glass transition temperature of DEN 438 cured with DICY and Fenuron.....	44
Figure 4-4: Influence of DDP derivatives on the glass transition temperature of DEN 438 cured with DICY fenuron.	45
Figure 4-5: TGA traces of DEN 438 cured with DICY and Fenuron containing phosphaphenanthrene derivatives DOPS, DOPO and DAPO.	46
Figure 4-6: Plot of OI and NI vs. phosphorus content for DOPO and DOPS modified DEN438 measured in oxygen atmosphere (solid lines) and nitrous oxide atmosphere (dashed lines).....	50
Figure 4-7: Plot of OI vs. phosphorus content for DDPO and DDPS-modified DEN 438 measured in oxygen atmosphere (solid line) and nitrous oxide atmosphere (dashed line).....	52
Figure 4-8: Plot of Oxygen content vs. Self quenching time of virgin, DOPO-modified and DOPS-modified DEN 438 measured in oxygen atmosphere. Points with black contour line correspond to specimens burned more than 5 cm.	54
Figure 4-9: Plot of Oxygen content vs. Self-quenching time of virgin, DDPO-modified and DDPS-modified DEN 438 measured in oxygen atmosphere. Points with black contour line correspond to specimens burned more than 5 cm.	55
Figure 4-10: Burning rate of DEN 438 resin modified with oxaphosphaphenanthrene derivatives DOPO and DOPS.	57
Figure 4-11: Burning rate of DEN 438 resin modified with dioxophosphorinane derivatives DDPO and DDPS.	57

Figure 4-12: Thermal desorption mass spectrum of the DEN 438 cured resins preformulated with DOPO (top-left), DOPS (top-right), DOPO-OH (bottom left) and DOPS-OH (bottom-right). The abundance of PO (blue), PO ₂ /PS (red), HPO (green), POS (yellow) are plotted as a function of temperature.....	59
Figure 5-1: Idealised Heat Release Rate (HRR) of for the combustion of DEN 438 (black) with DOPO (blue), nanoclay (light green), or DOPO and nanoclay (dashed dark green).	63
Figure 5-2: Thermal gravimetric curves in air of cured DEN 438 (black); with DOPO (1 %P) (red); with Cloisite 30B (red); with DOPO and Cloisite 30B (blue). The vertical blue line emphasises the temperature at which 50% of the initial weight is lost.	65
Figure 5-3: Thermal gravimetric curves in N ₂ of cured DEN 438 (black); with DOPO (1 %P) (red); with Cloisite 30B (red); with DOPO and Cloisite 30B (blue). The vertical lines emphasises the temperature at which 95% of the initial weight is lost.....	65
Figure 5-4: Heat release rate (HRR) for of the DEN 438 samples.	68

LIST OF TABLES

Table 2-1: Definition of UL 94 Vertical test classifications.	15
Table 4-1: Overview of the composition of DEN 438 resin chemically modified with DOPO, DAPO and DOPS.	41
Table 4-2: Overview of the composition of DEN 438 resin chemically modified with DOPO-OH, DAPS-OH and DOPS-OH.	42
Table 4-3: Overview of the composition of DEN 438 resin chemically modified with DDPO, DDPS and DDPS-OH.	42
Table 4-4: Tg of DEN438 modified with DOPO, DAPO or DOPS and cured with DICY / Fenuron (neat DEN 438 182 °C).	43
Table 4-5: Tg of DEN438 modified with DOPO-OH, DAPS-OH or DOPS-OH and cured with DICY / Fenuron (neat DEN 438 182 °C).	44
Table 4-6: Tg of DEN438® modified with DDPO, DDPS, DDPS-OH and cured with DICY / Fenuron (neat DEN 438 182 °C).	45
Table 4-7: UL-94 V rating of the oxide derivatives: DOPO, DAPO and DDPO.	47
Table 4-8: UL-94 V rating of the sulfide derivatives: DOPS and DDPS.	48
Table 4-9: UL-94 –V ratings for the thionic acid DOPS-OH, DAPS-OH and DDPS-OH.	48
Table 4-10: Summary of the Oxygen Index test for oxa-phosphaphenanthrene derivatives DOPO and DOPS in DEN 438 resin cured with DICY and Fenuron.	49
Table 4-11: Summary of the Oxygen Index test for dimethyldioxophosphorinane derivatives DDPO and DDPS in DEN 438 resin cured with DICY and Fenuron.	51
Table 5-1: Summary of formulations investigated.	63
Table 5-2: Summary of UL-94, Tg measured using differential scanning calorimetry and TGA data.	64
Table 5-3: LOI and combustion rates.	66
Table 5-4: LNI and combustion rates.	66
Table 5-5: Summary of the cone calorimetric measurements.	67

I hereby declare that I was the sole author of this dissertation and that I have not made use of any sources or help apart from those cited.

Muriel Rakotomalala

May , 31st 2011